EVALUATION OF SELF-CONSOLIDATING CONCRETE FOR BRIDGE STRUCTURE APPLICATIONS

A Master's Thesis
Presented to
The Academic Faculty

By

Alen Horta

In Partial Fulfillment
Of the Requirements for the Degree
Master of Science in Civil Engineering

Georgia Institute of Technology
August, 2005

Evaluation of Self-Consolidating Concrete for Bridge Structure Applications

Approved by:

Dr. Lawrence F. Kahn, Chair
School of Civil & Environmental Engineering
Georgia Institute of Technology

Dr. Kimberly E. Kurtis
School of Civil & Environmental Engineering
Georgia Institute of Technology

Dr. James S. Lai
School of Civil & Environmental Engineering
Georgia Institute of Technology

Date Approved: June 17, 2005

ACKNOWLEDGMENTS

The research presented in this report was sponsored by the Georgia Department of Transportation under Georgia DOT Task Order No. 02-07, Research Project No. 2042. During the course of this research project, the research team at Georgia Tech received valuable support and guidance from Georgia DOT professionals including Mr. Paul Liles, and Mr. Myron Banks. Their support and guidance are greatly acknowledged. Tindall Corporation and Standard Concrete Products helped fabricating the walls and girders. Holcim, and Sika Chemical Corporation generously donated time, knowledge, and materials for this project.

The opinions and conclusions expressed herein are those of the authors and do not represent the opinions, conclusions, policies, standards or specifications of the Georgia Department of Transportation or of the other sponsoring and cooperating organizations.

The following students helped in the experimental investigation: Robert Haines, Richard Jennings, Mauricio Lopez, Javier Silva, Ford Burgher, and Catherine Prince. Expert advice was received from Mr. John Howell of Standard Concrete Products, Mr. Gary Knight of Holcim; Mr. Bruce Strickland and Mr. Ralph Hodgins of Sika Corporation; their assistance was greatly appreciated.

TABLE OF CONTENTS

LIST OF TABLES

LIST OF FIGURES

LIST OF SYMBOLS

d - creep constant depending on member shape and size

E – modulus of elasticity

f – shrinkage constant depending on member shape and size

f_c' – compressive strength of concrete

f_r – modulus of rupture

h – relative humidity for shrinkage calculations

H_1 – total depth of apparatus minus filling head depth, U-box and L-box

H_2 – final depth, U-box and L-box

H_d – filling head depth, U-box and L-box

H_f – final depth, U-box and L-box

k – creep and shrinkage coefficient parameters (AASHTO-LRFD)

K – ultimate shrinkage base value

s – slump (in)

S – specimen area (in^2)

t – age of concrete (days) for creep and shrinkage calculations

t_0 – age at the beginning of drying for shrinkage calculations

t' – age of concrete at loading (days) for creep calculations

V – specimen volume (in^3)

w_c – unit weight of concrete

w/cm – water-to-cementitious materials ratio

α - shrinkage constant depending on member shape and size, or air content

$(\varepsilon_{sh})_t$ – shrinkage strain after "t-t_0" days under drying

$(\varepsilon_{sh})_u$ – ultimate shrinkage strain

γ - creep and shrinkage coefficient parameters (ACI-209)

$ø_t$ – creep coefficient at age "t" loaded at t′

$ø_u$ – ultimate creep coefficient

ψ - creep constant depending on member shape and size, fine aggregate-to-total aggregate ratio

SUMMARY

Self-consolidating concrete (SCC) is a relatively new type of concrete that is highly flowable and non-segregating, does not require vibration when cast, is capable of flowing through narrow openings or extremely congested reinforcement, and provides a void-free surface. The goal of this research was to determine whether precast prestressed bridge elements with congested reinforcement, including girders, end-walls and diaphragms, could be cast using SCC without vibration and yet comply with all parameters of strength, no honeycombing, and void-free surface finish. A qualitative and quantitative evaluation of the surface finish, and homogeneity of the concrete throughout the specimens was performed in order to assess the performance of plant-mixed SCC. Strength, creep, shrinkage and chloride permeability of the SCC field mixes were investigated.

Eight planar 6-in. thick, 6-ft deep and 6-ft wide wall sections and eight sections of 72-in. deep and 13-ft long bulb-tee girders were fabricated in two precast plants. The wall panels used three different SCC mixes, while four different mixes were used for the BT-72 girders. The w/cm of the mixes varied from 0.30 to 0.38. The main differences among the SCC mixes were the maximum size aggregate and the combinations of coarse and fine aggregate used. Cores were taken at different locations on each of the walls and girders to assess the distribution of compressive strength of the SCC. The specimens were sawn vertically at different location, and the aggregate distribution of each sawn surface section was quantified to assess segregation of the SCC mixes throughout the depth and length of the elements.

Good quality SCC mixes were produced for the walls and the BT-72 girder sections. The good mixes completely filled the walls and girders without the need of internal or external vibration, and those mixes resulted in a superior surface finish and a homogenous distribution of the aggregate throughout the section. The 28-day strengths of the SCC mixes varied from 8,600 psi (57 MPa) to 13,700 psi (94 MPa).

SCC test results with slump flow between 22 and 29 inches, U-flow with depth ratio greater than 85% and L-box result with depth ratio greater than 85% were necessary for assuring a good quality mix. Yet, such test results were not sufficient for predicting a mix's performance in congested sections. Only construction of muck-up sample sections showed the true self-consolidating performance of a mix.

Good quality SCC mixes used a blend of coarse and fine aggregates, which included a blend of #7 (1/2-in., 13 mm) stone and #89 (3/8-in., 9 mm) stone, and also a blend of fine aggregates including natural and manufactured sand. Further, a cementitious content of 900 lb/yd^3 (534 kg/m^3) was required.

The modulus of elasticity of SCC mixes ranged between 65% and 76% of what is predicted by AASHTO Standard (2002) for conventional concrete mixes. Also, the observed modulus of rupture was 60% higher than that given by the AASHTO Standard (2002). New expressions that better accommodate the experimental results were proposed for both the modulus of elasticity and modulus of rupture of SCC.

Both ACI 209 (1997) and AASHTO-LRFD (2004) models for creep coefficient and drying shrinkage can be use to calculate prestress losses in elements using SCC. The long-term prestress losses are expected to be no greater than those found for conventional concrete. The field-mixed SCC mixes showed chloride permeability in the Moderate level, between 2,000 and 4,000 Coulombs at 56 days.

CHAPTER 1

INTRODUCTION

1.1 – Purpose and Objectives

The purpose of this research project was to develop self-consolidating concrete (SCC) for bridge structure applications including precast prestressed bridge girders, and end-walls and diaphragms. The specific objectives of the field investigation phase of this research were:

a) to determine the homogeneity of *in situ* properties of SCC in girders and end-walls;
b) to study the flowability and mechanical properties of SCC mixes produced in precast concrete plants; and
c) to study long-term creep and shrinkage, plus chloride permeability of the field mixed SCC

1.2 – Definitions

1.2.1 – Self-Consolidating Concrete

Self-consolidating concrete (SCC) describes concrete that is highly flowable and non-segregating and that does not require vibration when cast, yet is capable of flowing through narrow openings or extremely congested reinforcement and of providing a void-free surface. SCC is also known as self-compacting concrete, self-leveling concrete, and high-fluidity concrete.

1.2.2 – Workability

Workability measures the easiness of fresh concrete to be placed and to flow around reinforcement without blockage. Workability combines all features of fresh concrete to assess the self-compacting ability of a concrete (EFNARC, 2002).

1.2.3 – Blockage

Blockage is the interlocking of the aggregate particles impeding the flow of the fresh concrete through a specified opening (EFNARC, 2002).

1.2.4 – Flowability

Flowability is the capacity of the fresh concrete to flow under its own weight, both horizontally and vertically and through narrow spaces or congested reinforcement without honeycombing or entrapping air (TR-6-03, 2003).

1.2.5 – Segregation Resistance

Segregation resistance is the ability of fresh concrete to remain homogenous in composition during and after placement, without separation of individual components. Segregation resistance is also referred as stability (TR-6-03, 2003).

1.3 – Scope

This research included the fabrication of eight, 6-ft by 6-ft by 6-in. thick end-wall panels and eight, 13-ft long precast prestressed concrete BT-72 girders using different SCC mixes. The homogeneity of the concrete within each specimen was tested. Mechanical and long-term properties of the different SCC mixtures were also studied. All specimens were fabricated at precast/prestressed concrete plants in metro Atlanta, Georgia, using locally available materials.

1.4 – Need for Research

At present, precast bridge structural elements are being rejected due to the presence of honeycombing and multiple air voids in their surface finish. Further, current practice for constructing precast bridge girders requires two to three workers to internally vibrate the girder and the same number of workers to "rub" the girder surface to produce a smooth finish. Use of SCC is claimed to diminish the occurrence of honeycombing, to result in an improved surface finish that requires no rubbing, and to avoid the use of internal vibration. Such improved quality and reduced construction labor may result in reduced cost. However, despite these potential benefits, the Georgia Department of Transportation (GDOT) material specifications currently do not allow the use of SCC. Thus, research is needed to determine whether a structure with congested reinforcement can be cast using SCC, achieve good consolidation and a smooth surface finish without vibration, and yet attain the required strength, workability, and finish.

1.5 – Report Organization

Chapter 1 introduces self-consolidating concrete and asserts the purpose and main objectives of the research. Chapter 2 gives a brief background on SCC, previous research on SCC characteristics, testing methods, and mechanical and material properties. Chapter 3 describes the experimental program and results obtained in casting of SCC end-wall panels. Chapter 4 discusses the experiments and results obtained during casting 13-ft long sections of SCC bridge girders. Long-term properties of the SCC mixtures used in Chapters 3 and 4 are presented and discussed in Chapter 5. Chapter 6 discusses and compares all of the results obtained in this field investigation along with the findings from the previously performed laboratory investigation (Ramage et al., 2004). Finally, Chapter 7 provides the conclusions and recommendations for further research and field application of SCC.

CHAPTER 2

BACKGROUND

2.1 – Use and Advantages of SCC

The concept of SCC was first proposed by Professor Hajime Okamura of Kochi University of Technology, Japan, in 1986 as a solution to concrete's durability concerns. Inadequate consolidation of the concrete and unskilled labor were the main causes for poor durability performances of Japanese structures. The development of a concrete that self-consolidates would eliminate from the construction process the factors driving the poor durability performance of the concrete (Vachon, 2002).

In the last decade, SCC has become very popular in structural applications in Japan and Europe, and just recently in the United States. Housing and tunneling as well as bridge construction for the Swedish National Road Administration were the main areas of use for SCC. In the Netherlands and Germany, the precast industry is mainly driving the development of SCC. In the United States, the precast industry is also leading SCC technology implementation. Double tee girders, piles and reduced size slabs constitute the main applications for SCC in North America. An Axim survey found that 30 percent of PCI members are using SCC at a daily rate equivalent to about 5,000 yd^3 (Marsh, 2002). Furthermore, several state departments of transportation in the United States are already involved in the study of SCC (Vachon, 2002).

One of the practical advantages of SCC over conventional concrete is its lower viscosity and, thus, its greater flow rate when pumped. As a consequence, the pumping pressure is lower, reducing wear and tear on pumps and the need for cranes to deliver

concrete in buckets at the job site (Khayat et al., 1999). This also reduces significantly the construction period and the amount of personal necessary to accomplish the same amount of work. The construction of the Akashi-Kaikyo Bridge (Figure 2-1), considered the longest span suspension bridge in the world, is a good example of SCC application. The casting of the two bridge anchorages consumed a total of 380,000 yd^3 (290,000 m^3) of SCC that allowed reducing the anchorage construction period by 20 percent (Ouchi, 2003).

Figure 2-1. The Akashi-Kaikyo Bridge, Japan, with a detail of a SCC anchorage

SCC gives designers and contractors a solution for using concrete in special problems, like casting of complicated shapes of elements, heavily congestion of reinforcement, or casting of areas with difficult access. In all these cases, the use of conventional concrete compromises the durability of the structure due to poor consolidation.

SCC is also called a "healthy" and "silent" concrete as it does not requires external or internal vibration during and after pouring to achieve proper consolidation. Mechanical vibration is a noisy and demanding task for the members of the casting team. The reduction or total elimination of this assignment diminishes the environmental impact for both those who are involved in the construction process and the surrounding neighbors (Walraven, 2002).

A complicated aspect of SCC production is that each mix must be specially designed based on available materials, required performance specifications and production practices. Nearly every aspect of a production process must be evaluated to fully capitalize on the advantages associated with the use of SCC (Neuwald, 2004).

2.2 – Testing Methods

The main reason why government agencies are reluctant to allow the use of SCC is the current lack of standards for it. However, some considerations about mix design and quality control tests are covered in a recent publication by Precast/Prestressed Concrete Institute (PCI) in their "Interim Guidelines for the Use of Self-Consolidating Concrete" (TR-6-03, 2003). Also, the American Concrete Institute (ACI) and the

American Society for Testing Materials (ASTM) Committee C09.47 on Concrete and Concrete Aggregates are involved in the development of quality control standards.

Three functional requirements are internationally recognized as the main characteristics of SCC in fresh state (Petersson et al., 2003):

1) Filling ability. This is the ability of the concrete to flow under its own weight both horizontally and vertically upwards without honeycombing around any shape.

2) Passing ability. This is the ability of the concrete to flow freely through dense reinforcement without blocking.

3) Resistance to segregation This is the ability of SCC to maintain a homogenous mix during and after placement, without separation of aggregate from the paste, or water from solids.

Several methods have been created to assess each of these characteristics of SCC. However, the close interdependence of the SCC properties in fresh state makes it impossible for any method to test and evaluate these properties individually. Some methods give a more limited evaluation than others; therefore, they must all be conducted and defined separately (Ferraris et al., 2000).

2.2.1 Slump FlowTest

The slump flow method is the oldest and most widely used test in concrete technology (Mindess et al., 2003). The simplicity of the procedure and apparatus used makes it suitable for every-day practice and field application. Mainly the test measures the fluidity or filling ability of the concrete paste.

To determine the slump flow, an Abrams cone is placed on a non-absorptive surface and filled with fresh concrete without any tampering, as seen in Figure 2-2. The cone is lifted and the concrete flows out under its own weight. Two perpendicular measurements of what appears to be the maximum diameter are taken across the spread of concrete and the average is reported (Figure 2-3). The final flow time, from cone removing to flowing completion is recorded, as well as the T_{20} flow time, which is the time needed by the paste to spread up to 20 in. (50 mm). Slump flow spread diameter values of 20 to 26 in. (500 to 650 mm) are considered satisfactory according to Sonebi and Bartos (2001). Khayat (1999) distinguishes between regular SCC and highly viscous SCC and sets a flow value of at least 22.5 in. (570 mm) with a time of 5 and 15 seconds, respectively. The Brite-Euram research suggested that a T_{20} of of 3-7 seconds is acceptable for civil engineering applications, and 2-5 seconds for housing applications (EFNARC, 2002). Constantiner and Daczko (2002) recommend acceptable values of slump flow that depends on the specific application of the SCC, varying from less than 22 in. to greater than 26 in.

It has been argued that the free and unrestrained flow in the test does not reflect the real conditions of pouring the concrete in construction practice (Ramsburg, 2003).

Nevertheless, the test at least can be used to asses the consistency of concrete from batch to batch (EFNARC, 2002).

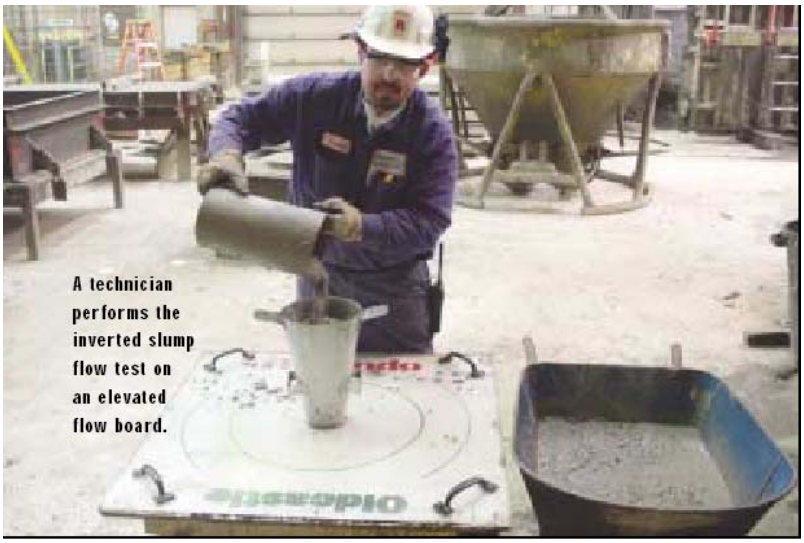

Figure 2-2. Pouring of fresh concrete in inverted cone for slump flow test (Ramsburg, 2003)

Figure 2-3. Measurements of slump flow spread diameter

2.2.2 – J-Ring Test

The J-Ring is used in conjunction with the slump flow test, the V-funnel test or any other apparatus that provides a discharge of concrete. These combinations test the flowing ability and, with the contribution of the J-Ring, the passing ability of the concrete.

The J-Ring equipment consists of a rectangular section 1 1/8 x 1 in. (30 x 25 mm) open steel ring, drilled with holes to accept threaded sections of reinforcing bars. It is possible to use different size bars with variable spacing in accordance with normal reinforcement considerations. PCI gives some recommendations for the rebar spacing that can be used in the test based on the maximum nominal size of aggregate used (Table 2-1). The diameter of the ring of vertical bars is 12 inches, and the height is four inches. When the J-Ring is used with the slump flow test, the spread diameter is measured as usual to assess flow characteristics, the difference in height between the concrete inside and that just outside the J-Ring is measured, as seen in Figure 2-4. The diameter spread results are compared with those obtained without the use of the J-ring apparatus.

Table 2-1. Recommended number of bars in J-ring based on the maximum nominal coarse aggregate size and size of rebar (TR-6-03, 2003)

Maximum nominal size of aggregate	**Spacing center to center of the rebar [rebar diameter 16 mm ≅ 5/8 in.]**	**Clear spacing between the outer side of rebar**	**No. of rebars**
8 mm ≅ 1/4”	30 mm ≅ 1 1/8”	14 mm ≅ 1/2”	31
10 mm ≅ 3/8”	35 mm ≅ 1 3/8”	19 mm ≅ 3/4”	27
20 mm ≅ 3/4”	55 mm ≅ 2 1/8”	39 mm ≅ 1 1/2”	17

Figure 2-4. J-Ring test in conjunction with slump flow (Vachon, 2002)

EFNARC gives no specific number for acceptance of J-Ring test; the technician must visually assess the blocking or segregation of the mix based on the difference in height of the concrete inside and outside the bars: the higher the difference in heights, the greater the blockage in the mix. Vachon (2002) proposed that the difference of spread diameter with and without the use of the J-ring should be less than 2 in. (50 mm), otherwise the mixture is considered no longer acceptable.

2.2.3 – L-box Test

The L-Box test allows measurement of the filling ability, passing ability, and resistance to segregation of SCC mixes (Sonebi and Bartos, 2001). The vertical part of the box is filled with fresh concrete and left at rest for 60 seconds to allow any internal

segregation to occur. The gate is opened, and the concrete flows out into the horizontal part of the box. Normally, one or two layers of rebars are located at the opening to produce a narrower flow (Figure 2-5).

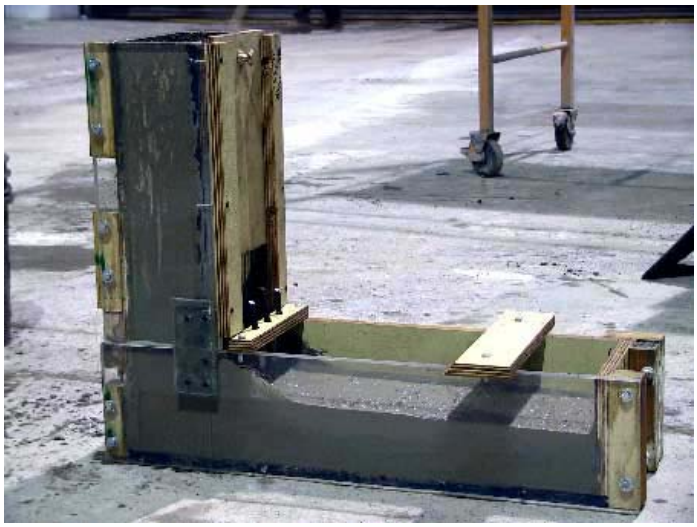

Figure 2-5. L-box test (Neuwald, 2004)

The parameters measured in the L-box test are the descent of sample head (H_d), which indicate the blocking ability of fresh concrete; the final depth of the concrete at the opposite end of the apparatus (H_f), which indicates the filling ability; and the flowing times to a particular flow distance, which indicate the deforming velocity. Flow distances recommended by Khayat et al. (2000) are 8 and 16 in. (200 and 400 mm) from the gate of the apparatus. Van et al. (1998), concluded that if the filling head drop (H_d) is greater than 19.5 in. (490 mm), that is, H_1 is less than 4.5 in, blocking behavior is considered satisfactory; if the concrete can fill all corners without honeycombing and the final depth (H_f) is greater than 3.25 in. (83 mm), the deformability is satisfactory. EFNARC (2002)

guidelines assess the blocking ability of the mix by a blocking ratio (H_2/H_1), where H_1 is the final concrete level at the vertical end, and H_2 is the same as H_d (Figure 2-6). Skarendahl and Petterson (2000) consider a blocking ratio between 0.80 and 0.85 as acceptable. The EFNARC (2002) guidelines set the range of acceptance to be within 0.80 and 1.0.

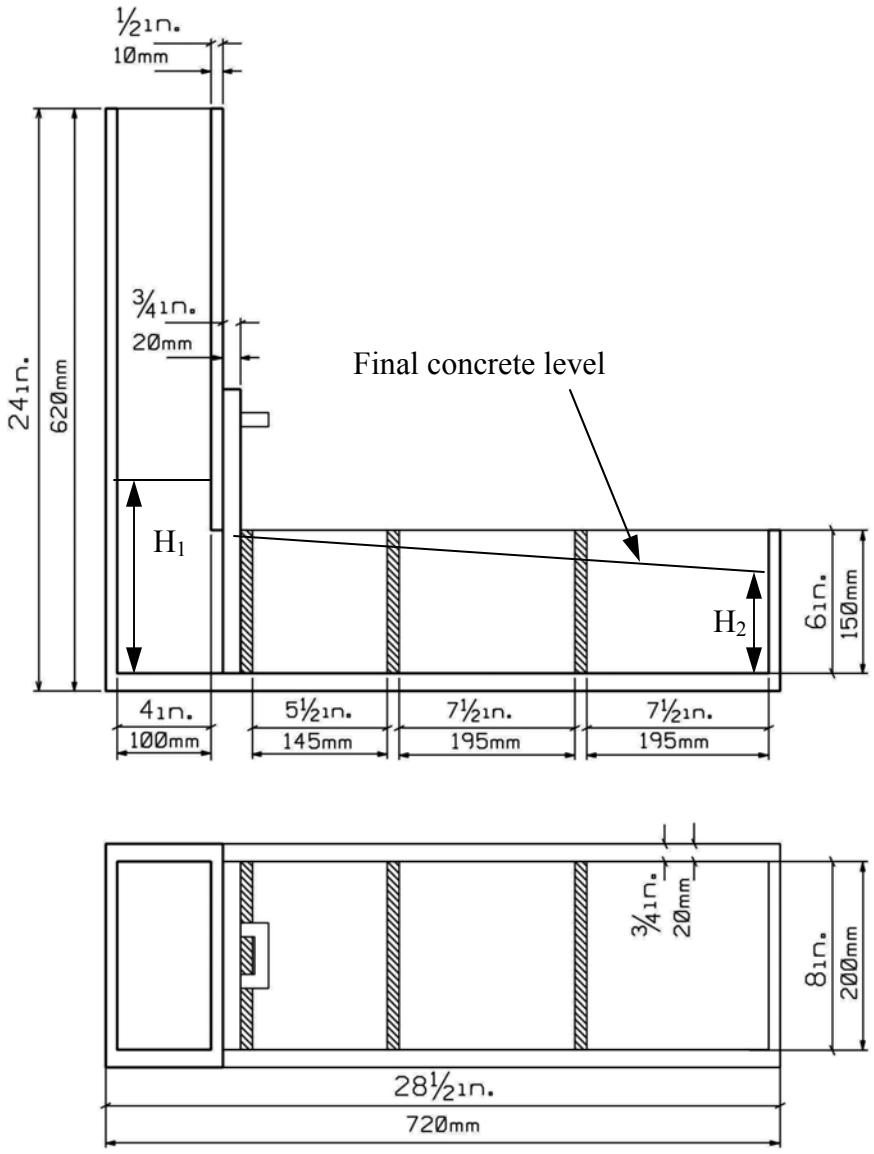

Figure 2-6. Plan and section drawings of the L-box apparatus with dimensions (Ramage et al., 2004). Concrete heights measured in L-box test are included.

2.2.4 – U-Flow Test

The U-flow test measures the filling ability, and blocking ability of SCC. It is considered by Ouchi (2003) as the most appropriate for determining the self-consolidating abilities of a concrete mix. The U-box apparatus consist is two chambers separated by a gate and row of vertical reinforcing bars (Figure 2-7). One of the chambers is filled with concrete and allowed to rest for one minute. When the gate is open the concrete flows through the rebars at the gate and upward into the other chamber. The final height of concrete at both chambers is measured, as shown in Figure 2-8. The maximum height percentage is the ratio of the filling height to the final height of the concrete in the first chamber (H_2/H_1).

Figure 2-7. U-flow apparatus with three #5 bars (Ramage et al., 2004)

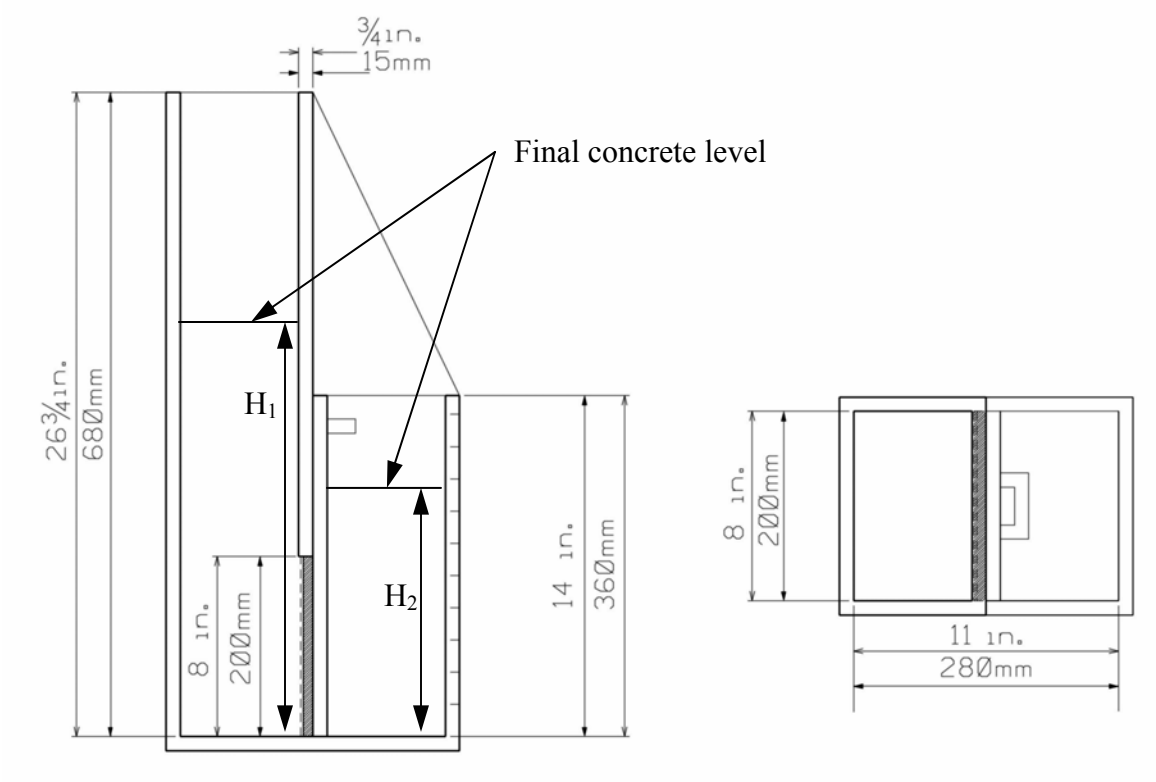

Figure 2-8. Cross section and plan view of U-flow apparatus with dimensions (Ramage et al., 2004). Concrete heights measured in U-flow test are included.

Ferraris et al. (2000) considered 70% of the maximum height as the arbitrary point for determining the acceptance of the mix design as SCC. However, other tests suggest that 60% is adequate (Bui et al., 2002). Saak et al. (2001) set an empirical level of 88%. Ramage et al. (2004) observed that SCC mixes with good stability showed 85% passing in the U-flow test.

2.2.5 – V-funnel Test

The V-funnel is used to evaluate the filling capacity of a concrete, and the capacity to pass through narrow spaces without blocking the flow (Figure 2-9). The funnel is filled with about 12 L (0.42 ft^3) of concrete and then released through the bottom (Griffin et al., 2002). The time that it takes the concrete to completely exit the funnel is measured, which gives an indication of the viscosity of the mix (Vachon, 2002).

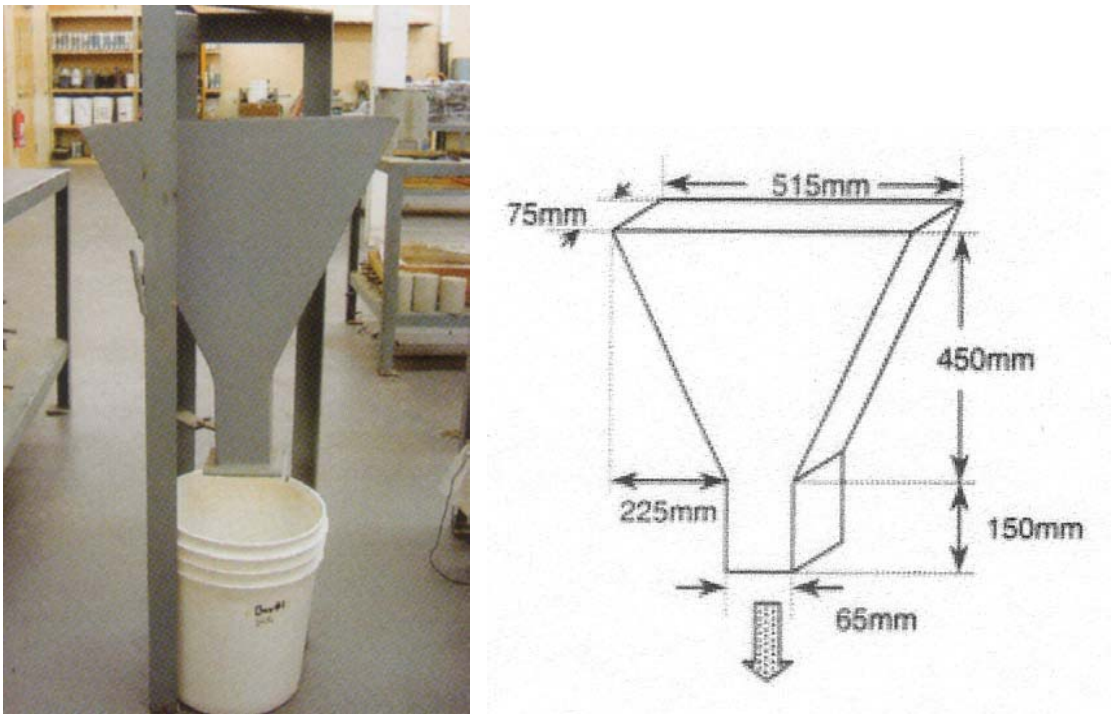

(a) (b)

Figure 2-9. (a) V-funnel apparatus (Euclid, 2003), and (b) V-funnel dimensions (Dietz and Ma, 2000)

A higher exit time is an indication of low flowability due to higher internal friction or high viscosity of the paste. However, a short exit time is an indication of low viscosity and, as a consequence, poor stability of the mix. Poppe and Schutter (2001) recommended 8 to 12 seconds as acceptable for exit time of the concrete from the V-

funnel. Ferraris et al. (2000) suggested that times under 20 seconds are considered adequate.

2.2.6 – Visual Stability Index

The resistance to segregation of SCC can be visually evaluated in a lesser or greater degree in almost every test mentioned above. PCI (TR-6-03, 2003) included a Visual Stability Index (VSI) test to help quantify the stability of SCC mixes. The VSI test is recommended to be implemented with the slump flow test; although, the parameters evaluated in the VSI test can be found as well in the L-flow test, U-flow test and in general every test that allows the observation of a significant volume of SCC. The range of values for the VSI is 0 through 3, with zero being a highly stable mix, and 3 designates a highly unstable mix. Table 2-2 presents the different criteria for VSI numbers proposed by PCI (TR-6-03, 2003) and Master Builders (2003).

Table 2-2. Combined visual stability index of TR-6-03 (2003) and Master Builders (2003)

Rating	**Number**	**Criteria**
Highly Stable	0	No evidence of slump segregation
	0.5	Very slight evidence of bleed and air popping
Stable	1	No mortar halo
		No aggregate pile-up
		Slight bleed and air popping
	1.5	Just noticeable mortar halo and aggregate pile-up
Unstable	2	Slight mortar halo, less than 0.4 in. (10mm)
		Slight aggregate pile-up
		Noticeable bleed
Highly Unstable	3	Large mortar halo greater than 0.4 in. (10mm)

The parameters for determining the VSI number of a given mix are mortar halos, bleed, air bubbles, and aggregate pile-up. Mortar halos result from the segregation of the paste from the concrete due to too much water or coarse aggregate in a mix. An unstable mix may contain a mortar halo less than 0.4 in. (10 mm); larger halos result in highly unstable concrete mixes. Slight bleed and few air bubbles surfacing are allowed for stable mixes, but not highly stable. Aggregate pile-ups occur in unstable mixes only (Master Builders, 2003). Figure 2-10 illustrates different cases of VSI numbers based on the degree of bleeding of the spread for various slump flow tests.

a) VSI=0 Optimum stability

(b) VSI=1 Slight bleed

(c) VSI=2 Slight mortar halo

(d) VSI=3 High segregation

Figure 2-10. Visual stability index examples for various slump flow tests (Ramage et al., 2004)

2.2.7 – Resistance to Segregation Test

ASTM Committee C09.47 and PCI (TR-6-03, 2003) have suggested the GTM Screen Stability test to quantify the resistance to segregation of a mix. The test, developed by a French contractor, has found great acceptance in the American community; as it is considered simple and effective to assess segregation resistance in SCC mixtures. Despite its apparent success, it has received criticism from others as taking too much time for its use in the field (Skarendahl and Petersson, 2000).

The test consists of taking a sample of fresh concrete of about 0.375 ft^3 (10 L) and after one minute that allows any internal settlement to occur, half the sample is poured through a ¼- inch sieve and is allowed to sit for two minutes. Then, the mortar that passed through the sieve is weighted and the value obtained is expressed as a percentage of the original sample on the sieve (TR-6-03, 2003).

The percentage of mortar passed through the sieve its call the segregation ratio. Observations have shown that when the segregation ratio stays in between 5 and 15% of the weight of the sample, the resistance to segregation ability is considered acceptable. Values of segregation ratio below five percent suggest excessive resistance in the mixture, which will affect the surface finish. In the other hand, values over 15 % suggest excessive segregation, thus poor stability of the mix (EFNARC).

Another method of determining the stability and self-healing ability of fresh SCC is the "S" groove test. Gary Knight of Holcim (2004) proposed this test to take place one minute after the slump flow test was completed. Using a finger or a tamping rod, an “S” is drawn into the concrete on the slump flow board. If the mix is stable, the concrete will rapidly fill the ‘S’ groove and the stability of the concrete is good, as seen in Figure 2-11;

otherwise a layer of paste or bleed will fill in the groove essentially showing the segregation of the coarse aggregate within the mix (Figure 2-12).

Figure 2-11. Resistance to segregation of concrete paste. Excellent self-healing ability (Ramage et al., 2004)

Figure 2-12. Resistance to segregation of concrete paste. Poor self-healing ability (Ramage et al., 2004)

2.3 – Mechanical and Material Properties

2.3.1 – Compressive Strength

Testing of compressive strength of SCC cylinders has been carried out following the same procedures as those described in ASTM C39. Takenaka et al. (2001) and Ramage et al. (2004) concluded that there was no significant improvement in the compressive strength of SCC samples prepared following the rodding procedures in ASTM C39 and samples prepared with fewer rodding or no rodding at all. Preparation of the control cylinders in two lifts, each lift rodded only five times has provided effective consolidation in SCC samples according to Khayat et al. (2000) and Ramage et al. (2004).

The compressive strengths of SCC mixes are comparable to those of conventional vibrated concrete made with similar mix proportions and water/cement ratio (Ouchi et al., 2003). Ambroise and Pera (2001) stated that SCC can develop similar strength and greater durability than conventional concrete. SCC exhibits the typical relation between w/cm versus strength found in conventional concrete.

2.3.2 – Elastic Modulus of Elasticity

The modulus of elasticity of SCC mixtures is always in the same order than those of conventional concrete mixes of similar w/cm according to Attiogbe et al. (2002). Persson (2000) observed that the modulus of elasticity of both sealed samples and air dried samples of SCC mixes was about 80% of that in normal weight conventional concrete mixtures (Figure 2-13). These lower values of modulus of elasticity have been

attributed to the higher percentage of paste content in SCC mixes. Ramage et al. (2004) found that this value was about 70% of what is proposed by ACI 318 (2002) for normal weight concrete mixes.

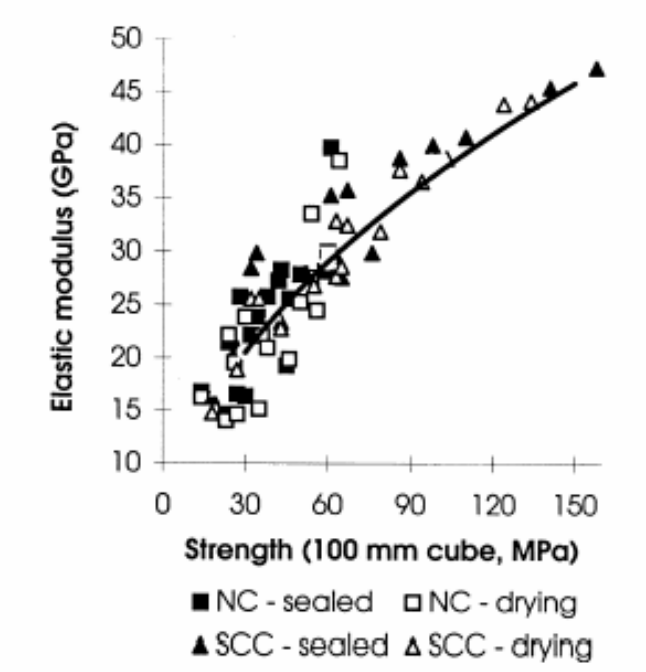

Figure 2-13. Elastic modulus of elasticity of SCC samples and conventional concrete mixtures (Persson, 2000)

2.3.3 – Modulus of Rupture

Griffin et al. (2002) observed that the equation given by ACI 318 (2002) provides a conservative prediction based on the 28-day compressive strength of SCC mixes. However, Sonebi et al. (2003) showed that SCC beams had similar cracking moments as that of conventional concrete beams of the same dimensions, reinforcement and strength. Also, the experimental cracking moments of the beams were close to the values predicted by CEB-FIP model Code 1990.

2.4 – Long Term and Durability Properties

2.4.1 – Shrinkage

Long-term shrinkage is a primary concern that specifiers have with the use of SCC in prestressed applications. Initial studies have indicated that drying shrinkage for SCC is very close to that of conventional concrete. Turcry et al. (2002) concluded that SCC and conventional concrete specimens developed similar drying shrinkage of about 350 με at 150 days (Figure 2-14). Both Persson (2000) and Attiogbe et al. (2002) found similar results for drying shrinkage of SCC and conventional concrete mixes after one and half year of testing. On the other hand, Raghavan et al. (2002) reported drying shrinkage of SCC mixes 25% lower than shrinkage found in conventional concrete mixes. Nevertheless, the Raghavan et al. (2002) do not specify after what period of time these values were recorded.

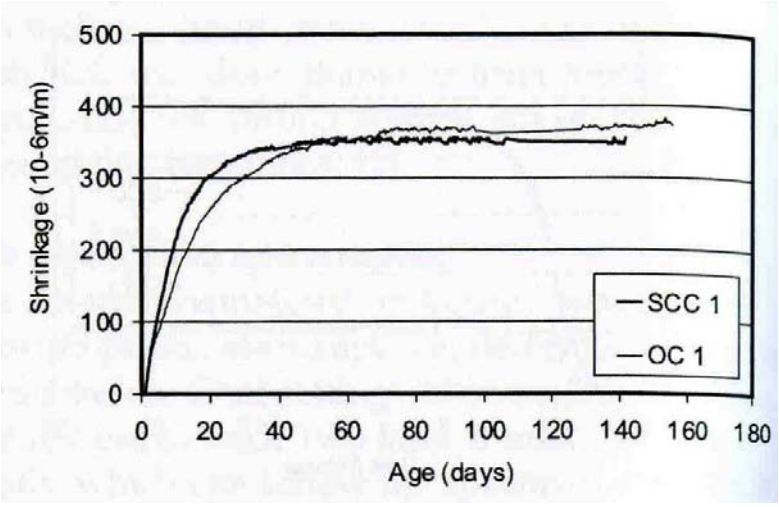

Figure 2-14. Drying shrinkage of SCC versus conventional concrete (OC) mixes (Turcry et al., 2002)

Significant differences have been found in plastic shrinkage during the first 24 hours when comparing SCC to conventional concrete, which may be attributed to self-desiccation (Neuwald, 2004). Turcry et al. concluded that the plastic shrinkage of SCC is about four times larger than regular control mixes of equivalent strength. SCC mixes showed 1,250 με shrinkage at 24 hours, compared with 300 με registered by a conventional concrete mix (Figure 2-15). Initial plastic shrinkage can be reduced by moist-curing products. Providing a continuous water source to the concrete as it cures will help ensure that the capillary pores are filled and the hydration reaction continues to take place. Increasing coarse aggregate contents will also reduce plastic shrinkage, but again this may affect the fresh properties of the SCC mix (Neuwald, 2004).

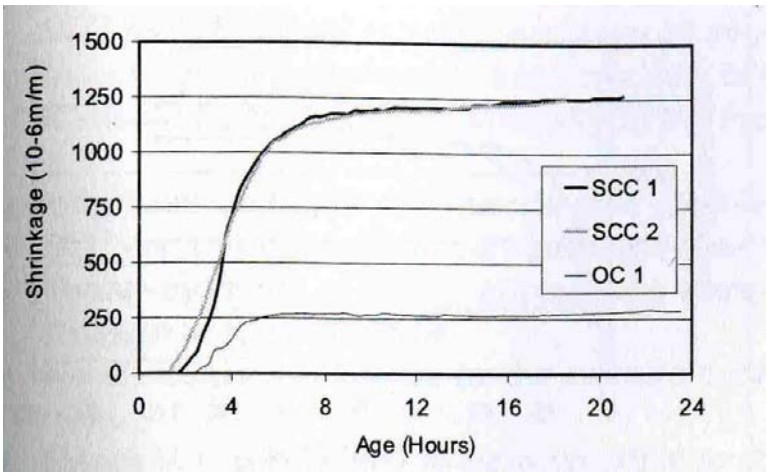

Figure 2-15. Plastic shrinkage of SCC versus conventional concrete (OC) mixes (Turcry et al., 2002)

.

2.4.2 – Creep

Raghavan et al. (2002) observed that even when the initial elastic strain is greater for SCC mixes compared with that of conventional concrete, the final creep strain is lower for SCC mixes. Persson (2000) concluded that the creep coefficient of mature SCC coincided well with that of conventional concrete when the strength at loading is held constant. Also, the creep coefficient decreases when the compressive strength of the SCC mixtures increases at the same rate found for conventional concrete mixes.

Attiogbe et al. (2002) stated that the specific creep coefficient of air cured specimens of SCC was slightly greater than that in conventional concrete mixes. However, for steam-cured specimens the specific creep of SCC and conventional concrete mixes was about the same, as shown in Figure 2-16.

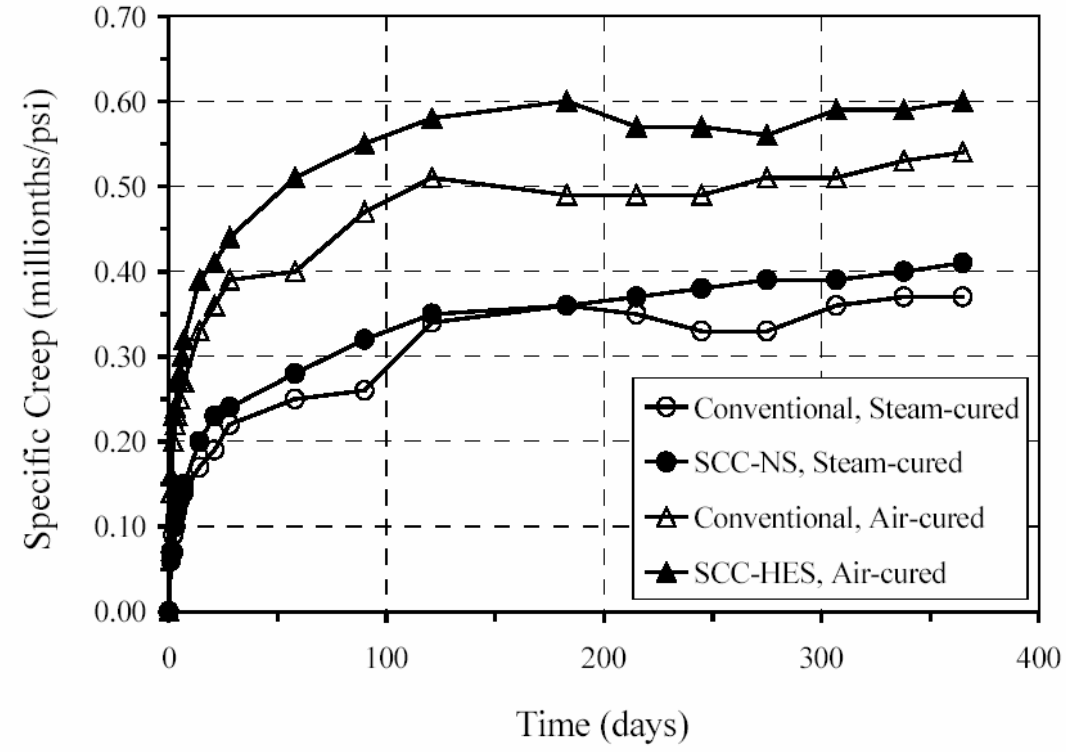

Figure 2-16. Specific creep of SCC versus conventional concrete mixes (Attiogbe et al., 2002)

2.4.3 – Chloride Permeability

Attiogbe et al. (2002) reported that the early-age porosity of SCC seems to be lower than that of conventional concrete, indicating the potential for an enhanced long-term durability of SCC compared with the conventional concrete. This can be attributed to the apparent improvement in the microstructure of SCC due to the use of a greater percent of finer material and supplementary cementitious materials (SCMs) and the reduced w/cm of the mixture (Westerholm et al., 2002). Also, the use of SCMs in SCC increases the resistance against chloride intrusion when compared with conventional concrete and SCC mixes without SCMs.

A rapid chloride permeability test performed by Hughes (2002) in SCC mixes with w/cm of 0.38 and according to ASTM 1202 showed that all mixes had a chloride permeability in the Low range, between 1,000 and 2,000 Coulombs. Ozyildirim and Lane (2003) reported permeability values for SCC mixes with w/cm of 0.36 and 0.41 between 780 and 1,625 Coulombs at 28 days, which corresponded with Very low and Low permeability levels, respectively. Raghavan et al. (2002) found the chloride permeability of SCC mixes to be about 1,100 and 1,500 Columbs after 28 days, compared to average 4,000 Coulombs for conventional concrete.

CHAPTER 3

SELF-CONSOLIDATED CONCRETE END-WALL PANELS

3.1 – Introduction

Diaphragms and end-walls in bridge structures are typical examples of deep and narrow elements were consolidation of concrete proves to be difficult. The research presented in this chapter describes a field evaluation of the performance of SCC in these types of elements.

In this phase of the experimental program, eight planar 6-in. thick, 6-ft deep and 6-ft wide wall sections were fabricated. These wall panels were cast from the top, creating a narrow space of only 6-in. wide for the concrete to flow through. The SCC mixes used for casting the end-wall panels were recommended by Ramage et al. (2004) in Task 1 of this research project. All panels were fabricated at the Tindall Corporation plant in Conley, Georgia.

The wall panels' cross-section, 6-ft deep and 6-in. thick, not only created a narrow opening for the concrete to flow through, but also matched the web width of a bulb-tee girders' cross-section. That way the results of this phase of the experiment would be a good approximation of what we could expect in the casting of actual bulb-tee members (Chapter 4).

3.2 – Material Properties

All the materials used for this research were common to the concrete used by the precast/prestress industry in Georgia. The material were supplied by local quarries or provided by Tindall Corp.

3.2.1 –Cementitious Materials

Type I cement provided by Tindall Corporation, was used for all wall panels. The oxide analysis and Bogue potential composition of the cement is summarized in Table 3-1 as provided by the Tindall plant. The Blaine fineness for this cement was 380 m^2/kg.

Table 3-1. Chemical composition and fineness of Type I cement

Oxide Analysis	**% by Weight**
SiO_2	20.60%
Al_2O_3	5.70%
Fe_2O_3	3.00%
CaO	65.00%
MgO	2.20%
SO_3	2.80%
Loss on Ignition	1.00%
Na_2O	0.09%
K_2O	0.35%
Insoluble Residue	0.24%
Equivalent Alkalis	0.30%

Fineness	
Blaine Fineness	380 m^2/kg
45um sieve, retained	6.20%

Bogue Potential Composition	
C_3S	60.1%
C_2S	14.0%
C_3A	9.4%
C_4AF	9.3%

Two different supplementary cementitious materials were used in combination with Type I cement: Class F fly ash and ground granulated blast furnace slag. These mineral admixtures enhance the workability of the mixes as well as their strength (Sonebi et al., 2001). The fly ash was donated by Boral Material Technologies Incorporated, and it conformed to ASTM C618 specifications. The specific gravity of the fly ash was 2.35. The ground granulated blast furnace slag, simply termed slag, was donated by Holcim, United States. The Blaine fineness reported for the slag was 588 m^2/kg with a specific gravity of 2.84.

3.2.2 –Aggregates

3.2.2.1 –Fine Aggregates

Two different types of fine aggregates were used: natural sand and manufactured sand. Natural sand alone was considered too smooth and would not form as cohesive a mix as the manufactured sand. However, using only manufactured sand negatively affected the workability of the mixes due to the angularity of the particles (Ramage et al., 2004). Thus, a blend of manufactured and natural sand was used.

Figure 3-1 illustrates the gradation of the natural and manufactured sand used and how it compared with ASTM C33 specifications. Natural sand failed to meet the ASTM requirements only for sieve #16; nevertheless this did not seem to affect its expected performance of the SCC mixes. The main material properties of both sands are summarized in Table 3-2.

Table 3-2. Material properties of Fine Aggregates used in SCC wall panels

Properties	Manufactured Sand	Natural Sand
Specific gravity	2.653	2.639
Bulk density (lb/ft^3)	165.55	164.67
Absorption capacity	0.422%	0.401%
Fineness	2.90	2.35

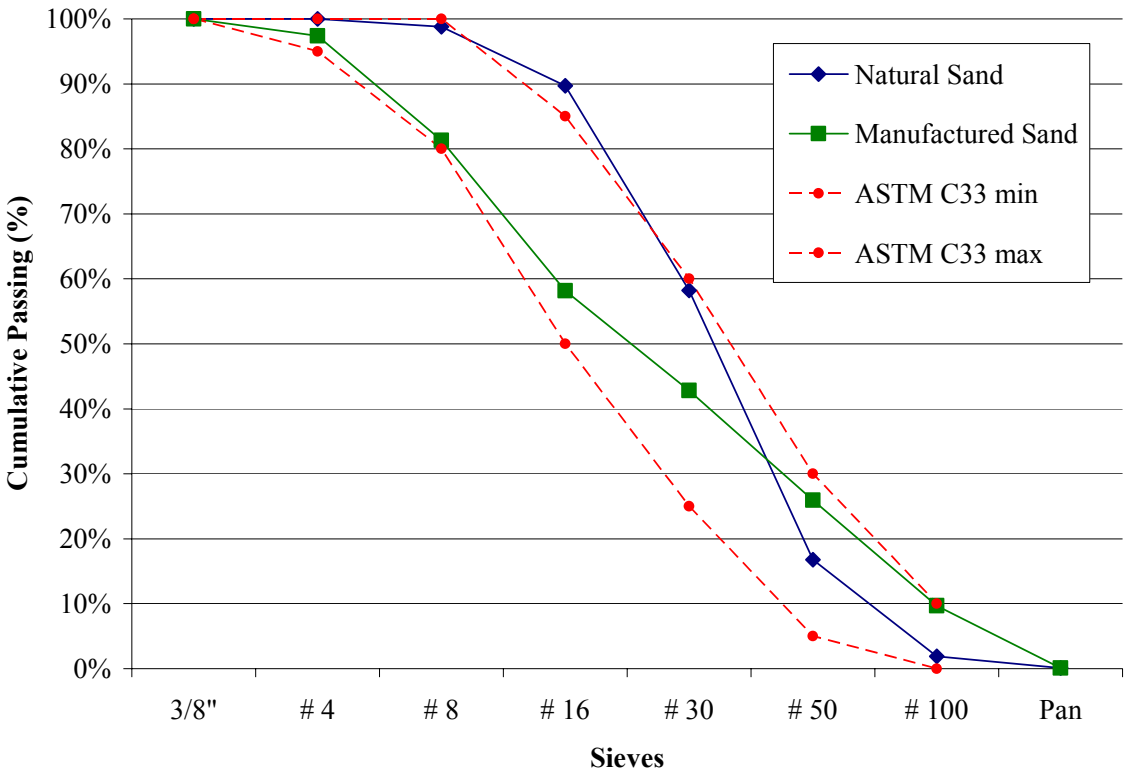

Figure 3-1. Gradation curves for fine aggregates showing ASTM C33 specifications

3.2.2.2 –Coarse Aggregates

The #7 (13 mm) and #89 (9 mm) coarse aggregate was supplied by Forrest Park Quarry owned by Florida Rock Industries, Inc.; the #67 (19 mm) stone was provided by Tindall Corp. All the coarse aggregates used were crushed granitic gneiss. Material properties of all coarse aggregates were determined according to ASTM C127; these

properties are presented in Table 3-3. Three sieve analysis tests were performed for each size stone, and the average gradation results are illustrated in Figures 3-2 to 3-4. Every chart is accompanied by the gradation specifications given by ASTM C33 for each size aggregate.

Table 3-3. Material properties of coarse aggregates used in SCC wall panels

Aggregate	**#89**	**#7**	**#67**
Maximum Size Aggregate	3/8 in. (9 mm)	1/2 in. (13 mm)	3/4 in. (19 mm)
Specific Gravity	2.650	2.650	2.643
Specific Density	167.5 lb/ft^3	167.5 lb/ft^3	165.3 lb/ft^3
Dry Rodded Unit Weight	92.3 lb/ft^3	92.1 lb/ft^3	95.9 lb/ft^3
Absorption	0.64%	0.64%	0.51%

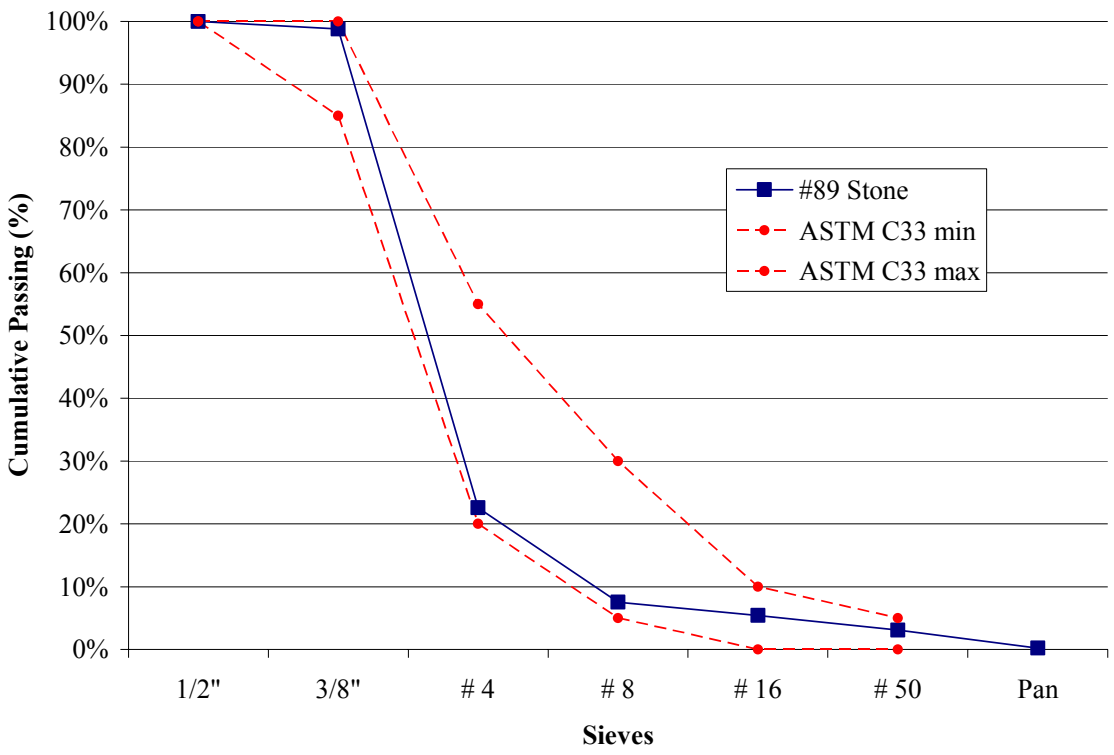

Figure 3-2. Gradation of #89 stone showing ASTM C33 specifications

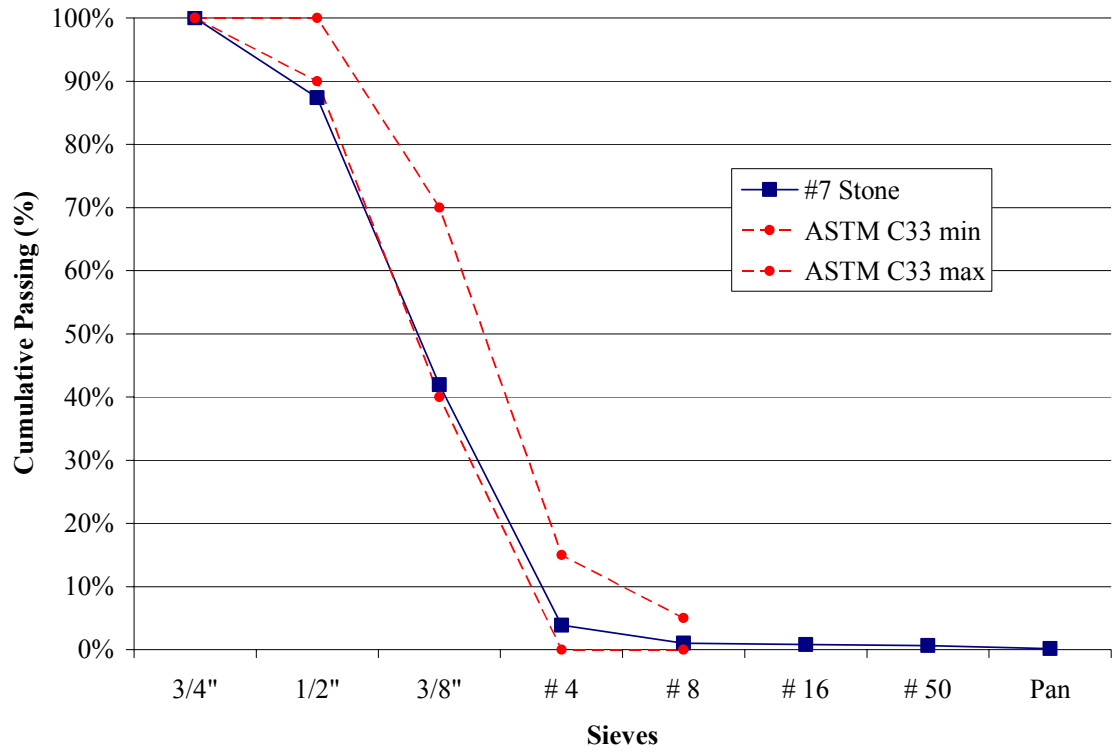

Figure 3-3. Gradation of #7 stone showing ASTM C33 specifications

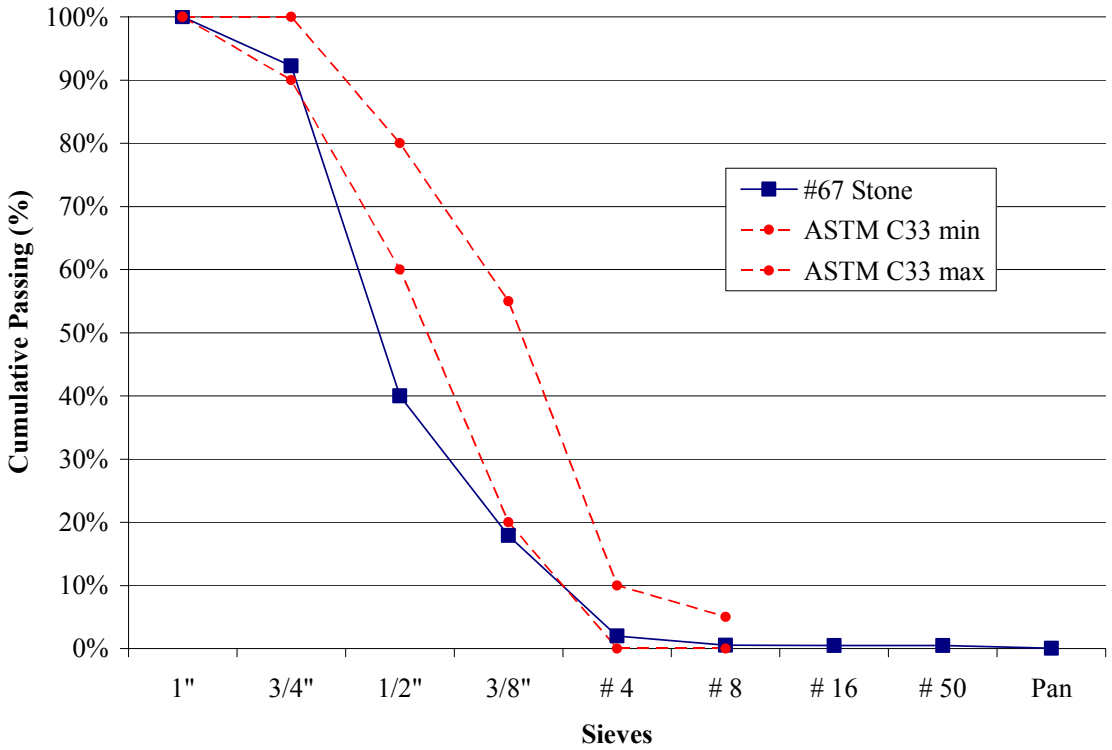

Figure 3-4. Gradation of #67 stone showing ASTM C33 specifications

The #67 stone presented a higher percentage of large aggregate than the #7 stone, including ¾-in. to 1-in. particles. The #7 stone was used in combination with #89 stone. The #67 stone was not combined with any other coarse aggregate, as this was the common practice of the Tindall plant.

3.2.3 –Chemical Admixtures

The two chemical admixtures used in casting the wall panels were high range water reducer (HRWR) agents and an air-entraining agent (AEA). The HRWR agents used were each polycarboxylate-polymer based materials but were made by different manufacturers as given below.

Sika ViscoCrete® 6100 is a HRWR and superplasticizer designed for conventional precast/prestress applications, and for SCC. It meets the requirements for ASTM C494 types A and F, and AASHTO M194 types A and F. The recommended dosage rate is 3 to 12 fl. oz/cwt (195 to 780 mL/100 kg) of cementitious materials; dosages greater than 12 fl.oz/cwt are allowed when silica fume is specified among the cementitious materials (Sika Construction).

Grace ADVA®Cast 540 is a HRWR formulated to achieved high early compressive strength for precast/prestress applications as well as SCC applications. It complies with ASTM C494 Type F and ASTM C1017 requirements. The dosage rates of this admixture range from 5 to 20 fl.oz/cwt (325 to 1300 mL/100kg) of cementitious materials (Grace).

Grace DARAVAIR 1000 is a liquid air-entraining admixture based on a high-grade saponified rosin formulation. It provides freeze-thaw resistance and finishability

performance for all types of concrete. It complies with ASTM C260 specifications for air-entraining admixtures. The recommended dosage rates are from 0.5 to 3 fl. oz/cwt (30 to 200 mL/100kg) of cementitious materials or as to give the specified air contents (Grace).

3.3 –Mix Proportioning

Two of the SCC mixes used for the casting of the wall panels were proportioned according to previous research and the results obtained by the Task 1 report of this research project (Table 3-4). The proportions of all SCC mixes used for the end wall research are summarized in Table 3-5. Mix 1 (S-Slag/Ash, 7-S/F-BL) incorporated 20% slag and 9% fly ash replacements, by mass of cementitious materials. Mix 2 (G-Slag, 7-S-BL) contained 24% slag replacement. These ternary and binary binders were found by Khayat et al. (2000) and Ramage et al. (2004) to enhance the stability of fresh SCC as well as strength. Type I cement was used in both cases. The mixes recommended by Ramage et al. (2004) were not used directly because their supplementary cementitious material (SCM) contents far exceeded the current Georgia DOT maximum of 20% cement replacement.

The different nomenclatures for the mixes represent the following: (1) the mix casting order; (2) the A-B represents the use of Sika (S) or Grace (G) admixtures, and the SCMs used, either a SCM blend (Slag/Ash) or a single SCM (Slag); (3) the C-D-F represents the maximum size aggregate, #7 stone (7) or #67 stone (67), the SCMs used, either a SCM blend (S/F) or a single SCM (S), and the blend of fine aggregates, natural and manufactured sand (BL).

Two different design strength mixes were tested for the wall panels. Mix S-Slag/Ash (7-S/F-BL) was designed with a water-cementitious materials ratio (w/cm) of 0.30 and target strength of 9,000 psi (62 MPa) at 28 days, while mix G-Slag (7-S-BL) had a w/cm of 0.37 and target strength of 7,000 psi (48 MPa) at 28 days. Also, two different polycarboxilate-based HRWR agents were tested. Sika ViscoCrete® 6100 was added to S-Slag/Ash mix, while Grace ADVA® Cast540 was used in G-Slag mix. Both these mixes proposed a blend of natural and manufactured sand as fine aggregate, as well as a blend of #7 (13 mm) stone and #89 (9 mm) stone as coarse aggregate. These blends achieve a more uniform gradation of aggregates, which provides better performance of self-consolidating abilities (Ramage et al., 2004).

A third SCC mix was included in this study at the request of Tindall Corp. Their plant at Conley, Georgia uses this "Tindall" mix for casting of jail cell elements with acceptable performance according to Mr. Charlie Boswell. The Tindall mix (67-N) used Type I cement as well, but did not incorporate any supplementary cementitious materials, a w/cm of 0.38 and ADVA® Cast 540 HRWR. This was the only mix that incorporated AEA. This Tindall mix only used a single coarse aggregate, #67 (19 mm) stone, and natural sand as fine aggregate. Tindall considered their mix much more economical than the S-Slag/Ash (7-S/F-BL) and G-Slag (7-S-BL) mixes.

Table 3-4. Mix proportions recommended by Task 1 report (Ramage et al.,2004)

Mix Components	**S-TA-1**	**G-TA-1**
Cementitious, lb/yd^3 [kg/m^3]		
Cement Type I	640 [380]	524 [311]
Slag	180 [107]	401 [238]
Fly Ash, Class F	80 [47]	-
Silica fume	-	31 [18]
Total Powder	*900 [534]*	*956 [567]*
Water, lb/yd^3 [kg/m^3]	283 [168]	366 [217]
w/cm	*0.31*	*0.38*
Coarse Aggregate, lb/yd^3 [kg/m^3]		
# 67 stone	-	-
# 7 stone	928 [551]	916 [543]
# 89 stone	500 [297]	494 [293]
Total Coarse	*1428 [848]*	*1410 [836]*
Fine Aggregate, lb/yd^3 [kg/m^3]		
Natural sand	538 [319]	589 [349]
Manuf. Sand	360 [214]	589 [349]
Total Fine	*898 [533]*	*1178 [698]*
Total Aggregates	*2326 [1381]*	*2588 [1534]*
Admixtures, fl oz./cwt [mL/100 kg]		
HRWR (ViscoCrete® 6100)	7.1 [463]	-
HRWR (ADVA® Cast540)	-	8.4 [548]

Table 3-5. Mix proportions for SCC used in End-Wall Panels

Mix Components	Mix 1 S-Slag/Ash 7-S/F-BL	Mix 2 G-Slag 7-S-BL	Mix 3 Tindall 67-N
Cementitious, lb/cy [kg/m^3]			
Cement Type I	720 [427]	730 [433]	750 [445]
Slag	200 [119]	225 [133]	-
Fly Ash, Class F	90 [53]	-	-
Total Powder	*1010 [599]*	*955 [567]*	*750 [445]*
Water, lb/yd^3 [kg/m^3]	306 [182]	350 [208]	288 [171]
w/cm	*0.30*	*0.37*	*0.38*
Coarse Aggregate, lb/cy [kg/m^3]			
# 67 stone	-	-	1465 [870]
# 7 stone	1030 [611]	910 [540]	-
# 89 stone	555 [329]	485 [288]	-
Total Coarse	*1585 [940]*	*1395 [828]*	*1465 [870]*
Fine Aggregate, lb/cy [kg/m^3]			
Natural sand	615 [365]	600 [356]	1331 [790]
Manuf. Sand	395 [234]	580 [344]	-
Total Fine	*1010 [599]*	*1180 [700]*	*1131 [790]*
Total Aggregates	*2595 [1540]*	*2575 [1528]*	*2796 [1660]*
Admixtures, fl oz./cwt [mL/100 kg]			
HRWR	7.1 [463]	6.9 [450]	5.5 [360]
Air-entrainer (Daravair 1000)	-	-	0.4 [26]

3.4 –Wall Design

3.4.1 – Wooden Form Panels

Plywood sheets and wood studs were used for building wall forms. Side and end forms were ¾-in. plywood sheets, with vertical 2x4-in. studs spaced 18 in. on-center and horizontal 2x4-in. wales spaced at 18 in. The sides were connected by ¼-in. threaded rod ties located at every joint between studs and wales.

All form panels were assembled at Georgia Tech Laboratory and delivered to Tindall Corp. plant in preparation for casting of the walls. As shown in Figure 3-5 the forms were aligned and braced against each other with short 2x4-in. studs at the top, middle and bottom. The final form panel was then braced to the ground with diagonal braces.

Figure 3-5. Layout of wooden forms for SCC end-wall panels at Tindall plant

The interiors of all forms were coated with water-sealant paint to protect the wood and to avoid the absorption of batch water from the concrete. An additional layer of debonder oil was sprayed over the painted to facilitate the demolding of the formwork.

3.4.2 –Wall Reinforcement

As shown in Figure. 3-6, the walls reinforcement consisted in vertical ½-in. (13 mm) prestressing strand spaced at 9 in. (230 mm) on-center each face, and horizontal #4 (13M) bars at the top and bottom spaced at 6 in. (150 mm) on-center. Towards the center of the wall, the horizontal bar spacing was 11 in. (280 mm) on-center. Each wall panel was provided with a #4 (13 M) pick-up bar at both ends to help with the lifting and transportation of the panels. In some cases #4 bars were replace by ½ -in. unstressed prestressing strands.

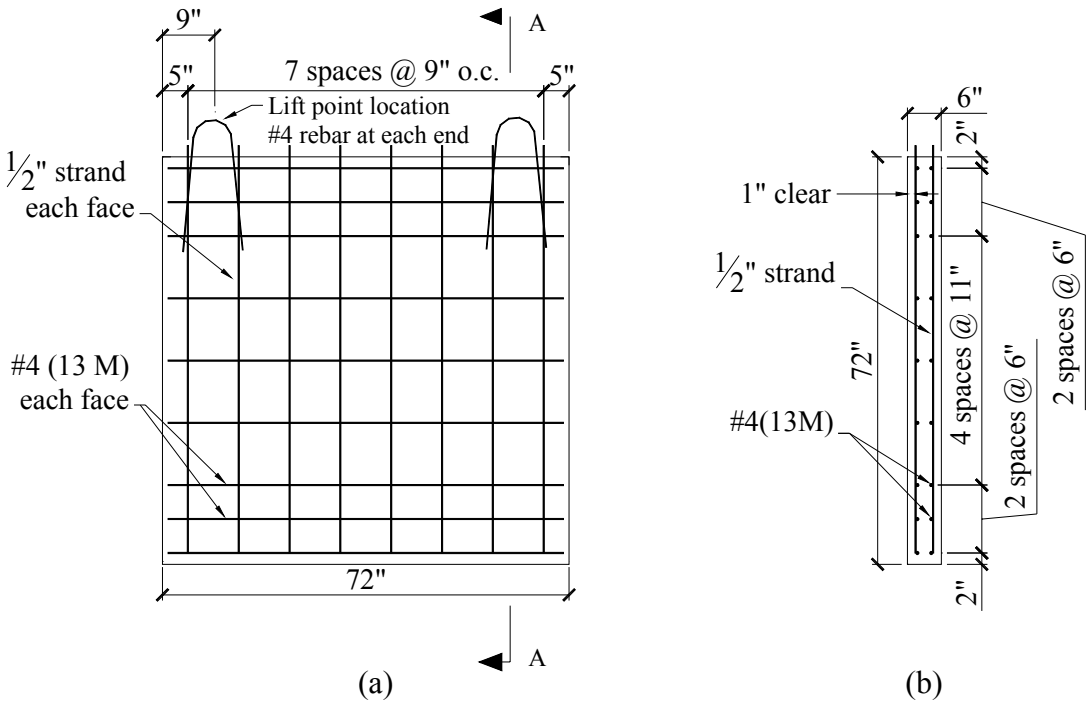

Figure 3-6. Rebar detailing of wall panels (a) elevation view, and (b) Section A-A

Each layer of rebar cages were tied up and slid into the formwork. The 1-in. (25 mm) cover of the vertical reinforcement was achieved by the use of spacing chairs placed against the plywood sheets, as shown in Figure 3-7.

(a) (b)

Figure 3-7. Reinforcement of wall panels (a) spacing chairs, and (b) 1/2-in. (13 mm) strands

3.5 –Casting of SCC Wall Panels

All concrete mixes were prepared at the Tindall batching plant. The batching sequence consisted of introducing the fines and coarse aggregates, allowing them to mingle. The cementitious materials and mix water were then added and mixed until a 2-in. slump was apparent. At this point the HRWR agent was added, and the concrete was agitated for another minute. Finally, the fresh concrete was tested for consistency and air content prior to casting of the walls.

With exception of the slag and fly ash, materials were introduced in the mixer by use of the batching plant bins. As shown in Figure 3-8, the slag and fly ash were delivered to the batching plant in 55-gal. barrels and added manually to the mixer.

Figure 3-8. Lifting of the slag and fly ash barrels to the batching plant

3.5.1 –Testing of Fresh Concrete

The slump flow test, the L-box test and U-flow test were performed to asses the self-flowing ability of the fresh concrete. Visual observations were noted for any blockage, excess or air, bleeding of water or lack of filling ability. Table 3-6 summarizes the results obtained on each of these tests for all the mixes tested.

Table 3-6. Fresh State Testing Results

Mix	Aggregates		w/cm	HRWR		Slump Flow		VSI Index		VSI Notes			U-Flow	L-Flow			
	Coarse	Fine		fl.oz/yd^3	fl.oz/cwt	T_{20}	D	F	H	B	A	P	% Max	H_d (in)	H_{S1} (in)	H_{S2} (in)	H_f (in)
S-Slag/Ash	#7, #89	Blend Sands	0.30	72	7.1	2	34	1	1	x			100	20	4	4	4
G-Slag	#7, #89	Blend Sands	0.37	66	6.9	2	26	0	0				100	20	4	3	3
Tindall	#67	Nat Sand	0.38			-	18	1.5	1.5			1	50	13	5	3.5	2.5

*Notes:

T_{20}: Time (sec)
F: Fresh State
H: Hardened State
B: Bleed on slump flow
A: excessive air in the mix
P: Aggregate pile-up (in)
Nat: Natural sand

D: mean diameter (inches)
%Max: Height percent of maximum
H_d: filling head drop
H_{S1}: depth at 6 inches away from gate
H_{S2}:depth at 13 inches away from gate
H_f: final depth

Both S-Slag/Ash and G-Slag mixes exhibited excellent self-consolidating abilities. Although the diameter of the S-Slag/Ash mix in the slump flow test went over the recommended upper limit of 28 in., no signs of excessive bleeding or aggregate segregation were apparent. It should be noted that the Tindall mix did not perform as well as the first two mixes. The slump diameter obtained by this mix was only 18 in. (458 mm), never achieving the 20-in. (510 mm) mark. Its U-flow test only achieved 50% passing of the concrete.

3.5.2 – Placement of SCC Mixes

One batch of 3.5 yd^3 (2.7 m^3) was produce for every mix. As the walls were fairly small in volume, every batch allowed the placement of 4 wall panels at a time. Only one wall was cast for Tindall mix. A Tucker-built truck delivered the fresh concrete from the batching plant to the wall forms, only 100 yards away. Placement of the concrete was

conducted from one end of every wall, a single casting point located 20 in. (510 mm) away from the end of the wall. The concrete spread readily away from the discharge point into the entire length of the elements.

As shown in Figure 3-9, a special wooden funnel was used to help place the concrete into the 6-in. width. This constituted another test for the concrete itself, as the width of the funnel opening was 4.5 in. (114 mm). All mixes, except Tindall mix, flowed well through the funnel and inside the wall's reinforcement. The Tindall mix needed the aid of a spud vibrator inserted in the funnel to allow the concrete to flow through it.

Figure 3-9. Placement of SCC mixes in wall panels

After the forms were completely filled, the top surface slopes were around 6% for all mixes except for the Tindall mix. The top surface of the wall cast with Tindall mix was too irregular to define a single slope. Figure 3-10 shows the leveling of the top surface of the walls.

Figure 3-10. Surface slope after casting of SCC wall panels.

Half of the walls cast with a given mix were externally vibrated, the other half were not. The vibration was limited to 5 sec.; a spud vibrator was pushed against the side of the wooden forms at different levels of the walls when all concrete was in place. Figure 3-11 shows the spud vibrator and external vibration.

Figure 3-11. Vibration process in SCC wall panels

Finally, all wall panels were covered with a tarp to allow for curing of the concrete and to limit moisture loss. This tarp was kept in place until the day of demolding the formwork, about one week after placement.

3.5.3 – Demolding of Formwork

Although the compressive strength of concrete cylinders samples at 3 days was already greater than 70% of the target strength of the mixes at 28 days, it was decided to wait an entire week to allow for a further hydration of the cement before the forms were removed. As shown in Figure 3-12 and Figure 3-13, the surfaces of most walls were clean and smooth. The surface finish of the wall panels mirrored the surface of the plywood sheets from the formwork. The white patches on the concrete surface were the white primer paint that was applied to the forms.

Figure 3-12. Demolding of formwork in SCC wall panels

Figure 3-13. Smooth surface finish in SCC wall panels

The wall panels were stacked and kept at the Tindall plant for two more weeks to allow concrete to gain strength. After that period, they were transported to the Georgia Tech Laboratory.

3.6 –Testing for Homogeneity of SCC Wall Panels

In order to asses the quality of the SCC mixes used in casting the end-wall panels, three different tests were develop: (1) a surface-finish evaluation, which quantified voids and air bubbles present in given areas of the walls, (2) a compressive strength analysis of core samples taken at different positions in the walls, and (3) an aggregate distribution estimation of different cross sections of the walls. These three variables gave quantitative measurements of the general homogeneity of the mixes, going beyond the simple visual analysis.

3.6.1 – Surface Finish Evaluation

A visual inspection of the SCC wall panels gave an idea of the quality of their surface finishes. The walls cast with mixes S-Slag/Ash (Mix 1, 7-S/F-BL) and G-Slag (Mix 2, 7-S-BL) displayed an excellent surface finish. Only a close and detailed observation of the walls revealed minor flaws in the panels' surfaces. These flaws consisted of entrained-air bubbles that were always smaller than 3/8 inches in diameter.

As seen in Figure 3-14, no apparent differences were observed in a visual inspection of two different wall panels cast with a same given mix. Furthermore, no apparent differences were observed between vibrated and non-vibrated wall panels of the same mix.

(a) (b)

Figure 3-14. Visual comparison of surface finish of two walls from a same mix S-Slag/Ash (Mix 1) (a) non-vibrated wall, and (b) vibrated wall

No apparent differences were observed either in a visual comparison of the surface of walls from the S-Slag/Ash (Mix 1) and G-Slag (Mix 2) mixes. Figure 3-15 depicts a comparison of a wall cast with S-Slag/Ash mix with one cast using G-Slag.

(a) (b)

Figure 3-15. Visual comparison of surface finish of two walls from different mixes (a) S-Slag/Ash (Mix 1), and (b) G-Slag (Mix 2)

The wall cast with the Tindall mix exhibited a poor concrete consolidation and honeycombing. As seen in Figure 3-16, Tindall mix aggregates got trapped among the wall's reinforcement, thus blocking the flow of the paste. The surface is characterized by multiple voids that often would span the entire thickness of the wall. Only the concrete at bottom area of the wall showed a more adequate consolidation, but this is attributed to the consolidation provided by the self-weight of the concrete from the upper layers.

Figure 3-16. Surface finish of wall panel cast using Tindall mix

In a quantitative approach to analyzing the surface finish of the walls, 1-ft by 1-ft areas were drawn on the surface of all walls at three locations: top, center and bottom. The top position was located at the near end of the wall, the end where the concrete was placed. The center square was drawn at the geometric center of the walls. Finally, the bottom position was located at the far end, the opposite end to the casting point. Figure 3-17 locates the different positions of these areas within a wall. The locations of these points were chosen as they followed the critical path of the concrete when poured inside the walls. The number of air bubbles that fell inside every square area was registered and organized by diameter sizes. The smallest size diameter registered was 1/8 in. and the largest was 3/8 in. Air bubbles smaller than 1/8-in. diameter were considered impractical to be analyzed. No air bubbles larger than 3/8-in. diameter were found on the surface finish of the S-Slag/Ash and G-Slag walls.

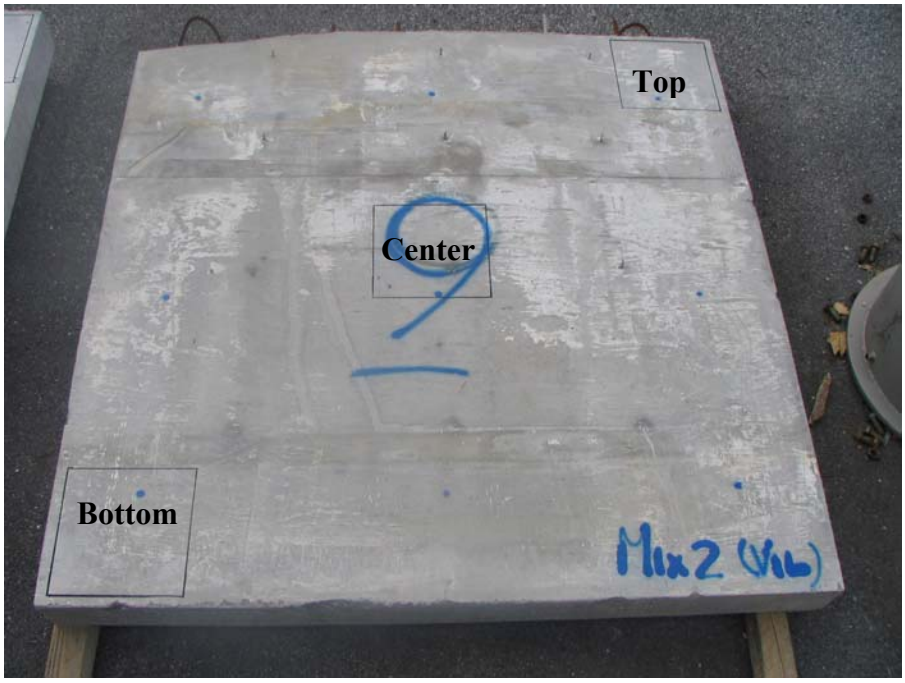

Figure 3-17. Areas for surface-finish study

Figures 3-18 and 3-19 sort the data obtained in this analysis for mix S-Slag/Ash and G-Slag, respectively. The y-axis depicts the number of air bubbles found for each given diameter of the voids, represented in the x-axis. Vibrated and non-vibrated walls of a same mix are shown in a single chart for comparison. Both S-Slag/Ash and G-Slag mixes displayed a reduced number of air bubbles in all locations. The general trend on both mixes was that the larger the air-bubble size, the fewer the number of occurrences. The higher number of bubbles was found to be 1/8-inch in diameter. The maximum area fraction of air bubbles to surface of the walls was 0.42% for mix S-Slag/Ash and 0.34% for mix G-Slag; each ratio was much lower than the 2% maximum requirement for properly consolidated concrete (Walker, 1992).

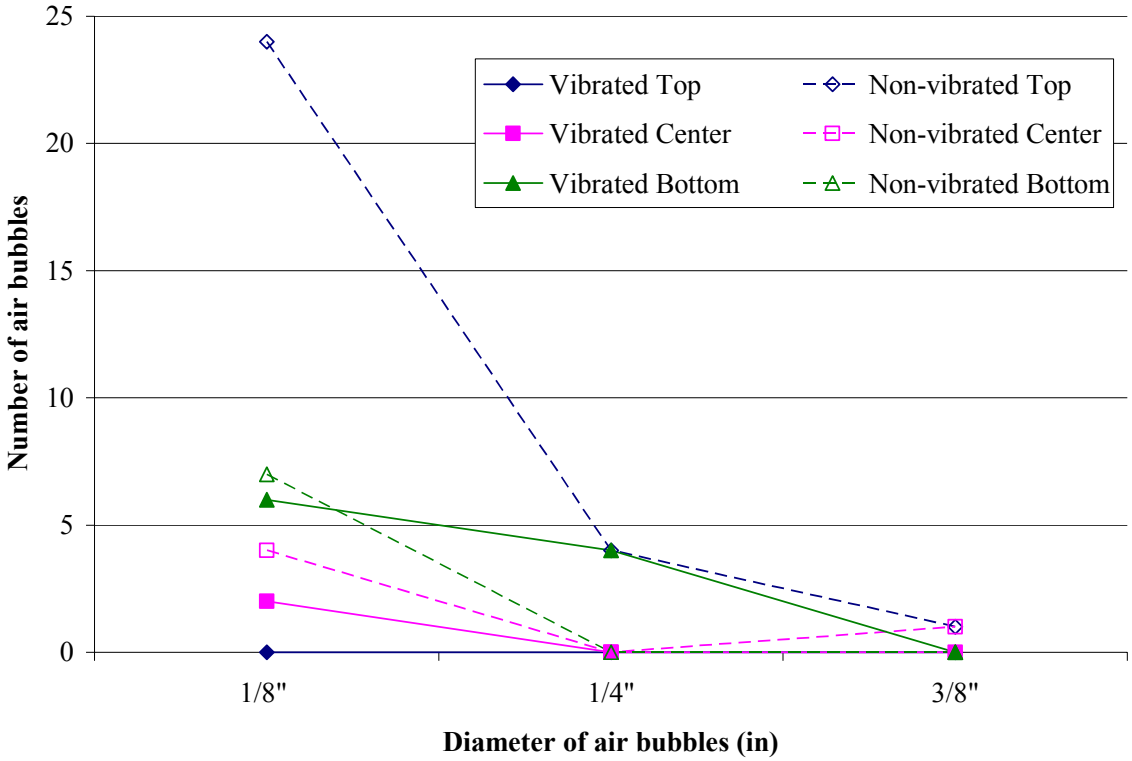

Figure 3-18. Air bubbles in SCC wall panels. Mix S-Slag/Ash (Mix 1, 7-S/F-BL)

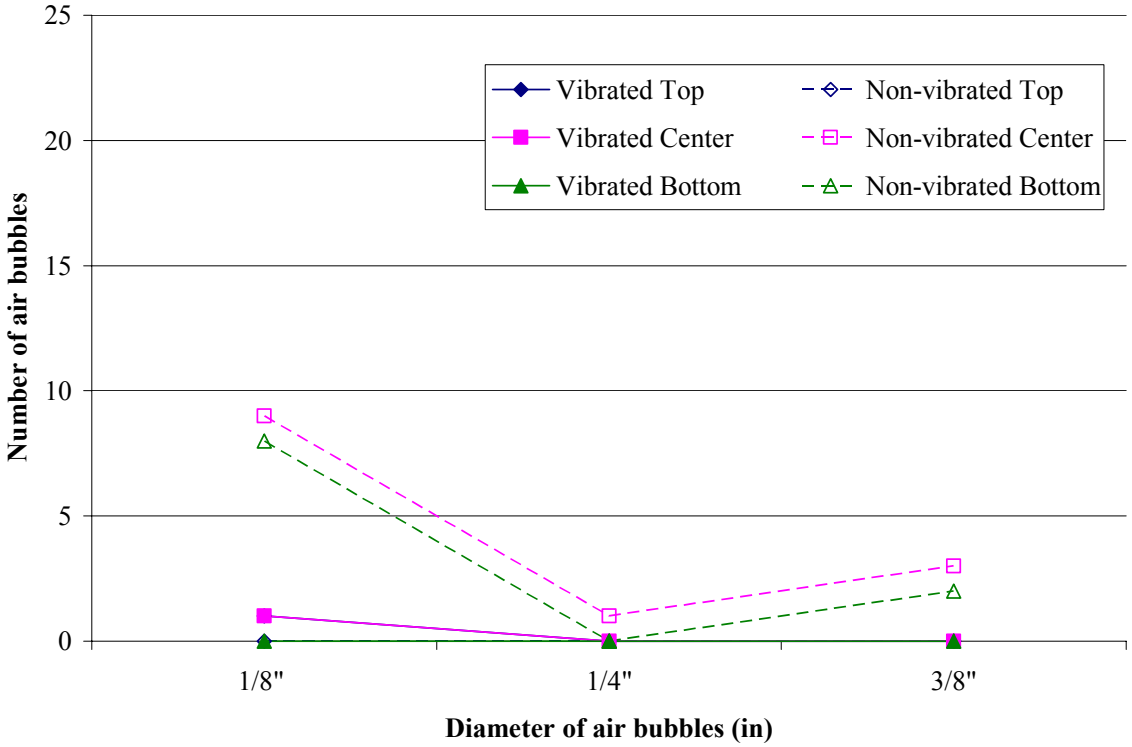

Figure 3-19. Air bubbles in SCC wall panels. Mix G-Slag (Mix 2, 7-S-BL)

Non-vibrated walls displayed a higher number of bubbles than vibrated ones in all given locations. This difference was more noticeable in the areas close to the ends of the wall. As seen in Figure 3-6, the wall reinforcement was more closely spaced at the top and bottom than towards the center of the walls. This, and the boundary conditions created by the end surfaces of the walls where air is more likely to be trapped, are proposed to explain the greater number of air bubbles around these areas.

The S-Slag/Ash mix displayed a more uniform distribution of air voids than G-Slag mix. Vibrated and non-vibrated walls of the S-Slag/Ash mix showed similar results at all areas, except for 1/8-in. bubbles at the top section of the non-vibrated walls. Nevertheless, considering the size of this bubbles and the reduced percentage that the void to surface fraction represents, this inconsistency can be neglected.

The G-Slag mix showed a greater difference between vibrated and non-vibrated walls. But, within a single wall the air-bubble distribution was consistent throughout the surface of the walls. This was true for both vibrated and non-vibrated walls.

In general, the as-cast surface finish of all walls, except the wall cast with Tindall mix, displayed a superior quality to that obtained using conventional concrete. The quantitative analysis of the walls' surface finish corroborated the visual inspection conclusion about the homogeneity of the SCC used for both mixes S-Slag/Ash and G-Slag. Mix G-Slag showed the best surface finish in non-vibrated walls, with the lowest area fraction of air bubbles to surface of the wall.

3.6.2 –Compressive Strength of Cores Samples

To evaluate the in-place properties of the SCC mixes, 3-in. diameter cores were taken at nine locations on each wall. The cores were drilled and tested 56 days after casting of the walls. Figure 3-20 depicts the distribution of the cores. Each position of the cores characterized the compressive strength of a given area of the walls. A single core was taken at each position as the dimensions of the walls and location of the reinforcement did not permitted otherwise. The cores were taken at three different heights of the wall. Three cores were taken at each height. Near end corresponded to the end of the wall close to the casting point; far end corresponded to the opposite end.

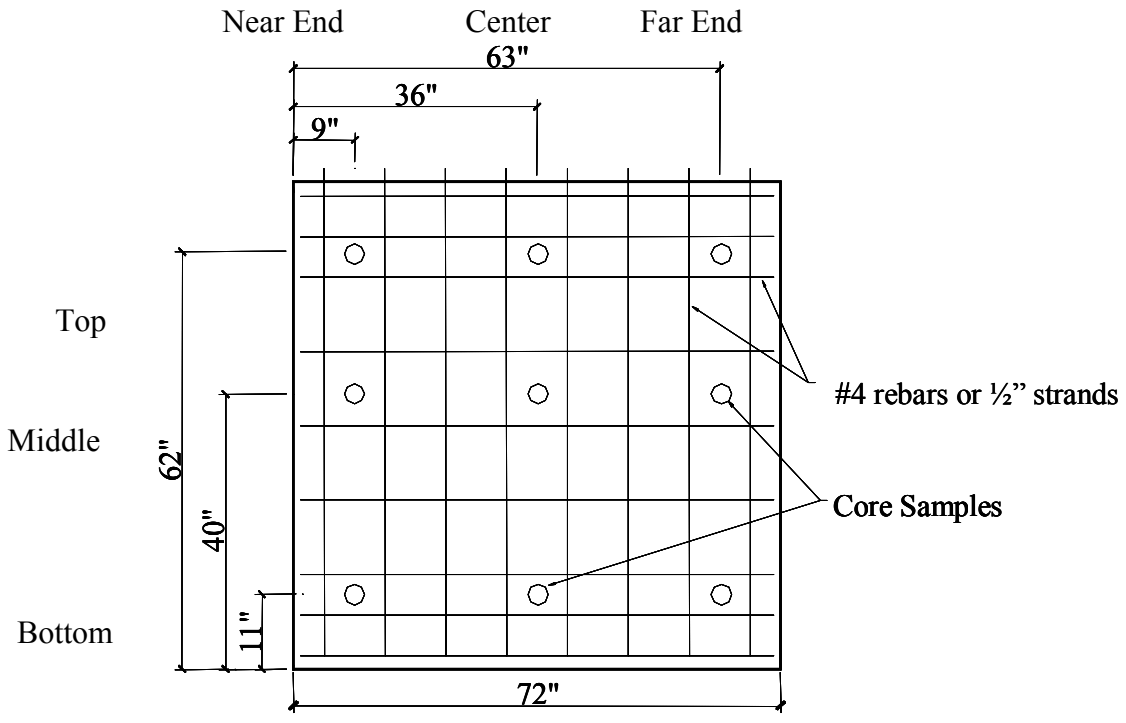

Figure 3-20. Distribution of cores along SCC wall panels

The surface of the cores emulated the surface finish of the walls. Figure 3-21 shows a comparison between cores taken from the wall using Tindall mix and a wall using G-Slag mix. Tindall mix cores presented multiple voids and signs of poor consolidation, as opposed to G-Slag mix cores that offered a smooth and void-free surface.

(a)

(b)

Figure 3-21. Comparison of surfaces in core samples (a) Tindall mix, and (b) G-Slag mix

The compressive strengths obtained from the cores for each wall are presented in Figure 3-22. The cores taken from walls using S-Slag/Ash mix showed a higher compressive strength than those using G-Slag, which corresponded with their w/cm and the results obtained with the control cylinders discussed later in this Chapter. The coefficients of variation (COV) values of the strength of the cores taken from these two mixes were less than 5%, indicating an excellent reproducibility of the test results. The mean compressive strength for both vibrated and non-vibrated walls using S-Slag/Ash mix was 10,950 psi (76 MPa). The mean strength for walls using G-Slag mix was 8,600 psi (59 MPa). The 56-day control cylinder strength were 11,600 psi and 8,600 psi, respectively. Table 3-7 summarizes mean values and COV obtained for the compressive strength from all wall panels. The thickness of all walls was 6 in., making the L/D ratio of the cores equal to 2, with no need to trim the length of the cores. In order to compare the compressive strength of the cores with those of the control cylinders, the values obtained from the cores where reduced by 2% to adjust them for equivalent 4x8 in. cylinder strength (Mehta and Monteiro, 1996). The compressive strength values presented here are already adjusted.

Table 3-7. Adjusted mean compressive strength of 3 x 6 in. cores at 56 days of SCC wall panels

Mix	Wall	Mean (psi)	COV
S-Slag/Ash	Vib	11,000	5.1%
	Vib	10,900	4.1%
	Non-vib	10,950	5.0%
G-Slag	Vib	8,900	2.6%
	Vib	8,100	2.5%
	Non-vib	8,350	2.1%
	Non-vib	9,000	4.3%
Tindall	Vib	6,650	45.6%

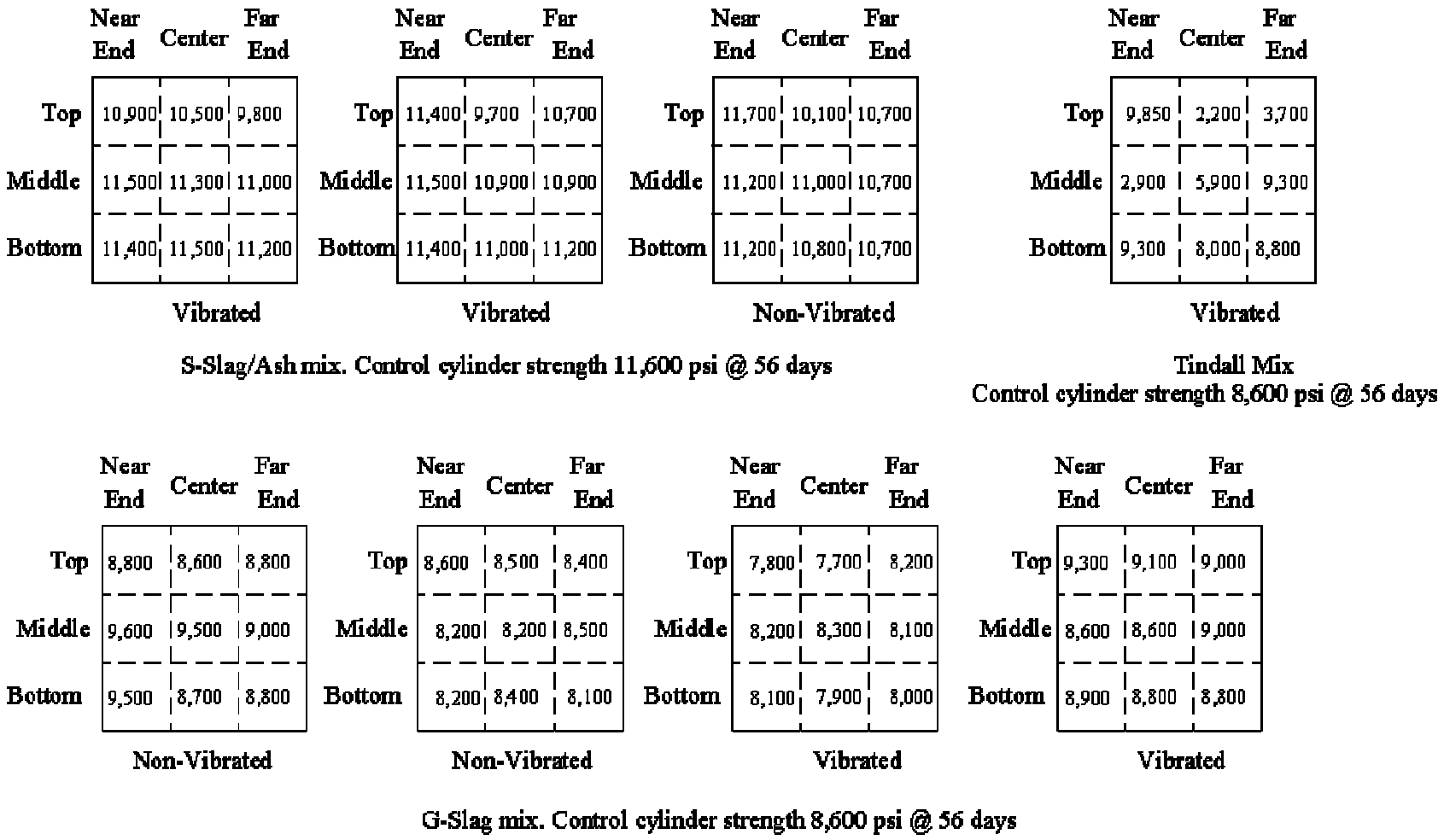

Figure 3-22. Distribution of core compressive strength at 56 days (psi) for SCC wall panels

As before, Tindall mix did not performed as well as the other two mixes. The cores' compressive strengths were random and in general lower than those from the control cylinders. The COV for Tindall mix was 45.7%, which clearly demonstrated an irregular consolidation of the concrete.

An analysis of variance (ANOVA) of the in-place compressive strength of the walls was also performed to establish the significant factors affecting this variable. The analyzed factors were vibration method, horizontal location of the core sample relative to the point of casting, and vertical location of the cores samples.

The ANOVA for G-Slag mix showed that none of the variables included in the study were significant factors in the experimental results. An initial analysis for S-Slag/Ash mix showed that the height of the cores samples was statistically significant. Cores at the top of the walls seemed to have lower compressive strength than those at the bottom. However, it was found that S-Slag/Ash concrete had been contaminated with light-weight aggregate, which had floated toward the top area of the walls. This lightweight aggregate affected the compressive strength of the cores taken at the top of the walls.

Figure 3-23 illustrates the presence of lightweight aggregate in a core from the top area of a wall. Dropping these values from ANOVA, the height of the cores was no longer a significant factor in the compressive strength of mix S-Slag/Ash. The horizontal location and whether the wall was vibrated or not were determined not to be statistically significant.

Figure 3-23. Lightweight aggregate in core samples of S-Slag/Ash mix

The fact that the vibration did not represent a statistically significant factor to differentiate the cores data showed that no improvements in the strength of the concrete were obtained in those walls where vibration was applied. The homogeneity of the mixes was corroborated by ANOVA illustrating the uniformity of the concrete at all locations of the walls.

3.6.3 – Aggregate Distribution throughout Cross Sections

All wall panels were sawn vertically in order to analyze the distribution of aggregates throughout their cross-sections. If the reinforcement inside the walls had produced blockage of the aggregates during casting, a different ratio of aggregate to paste would be noticeable in the cross-sections of the wall panels. Two cuts along the height of the walls were performed, each cut approximately 1 ft away from the end of the walls. Figure 3-24 illustrates the sawing of the panels. The cut closer to the casting point defined the "near end" surface; the cut at the opposite end was labeled "far end" surface.

Figure 3-24. Sawing of SCC wall panels

The different sections were labeled and then stacked in order to expose each cross-section and to perform a visual evaluation of the aggregate distribution. As seen in Figure 3-25, the sections were stacked in such fashion that the near end surface would be right on top of the far end surface, facilitating a visual comparison between the two.

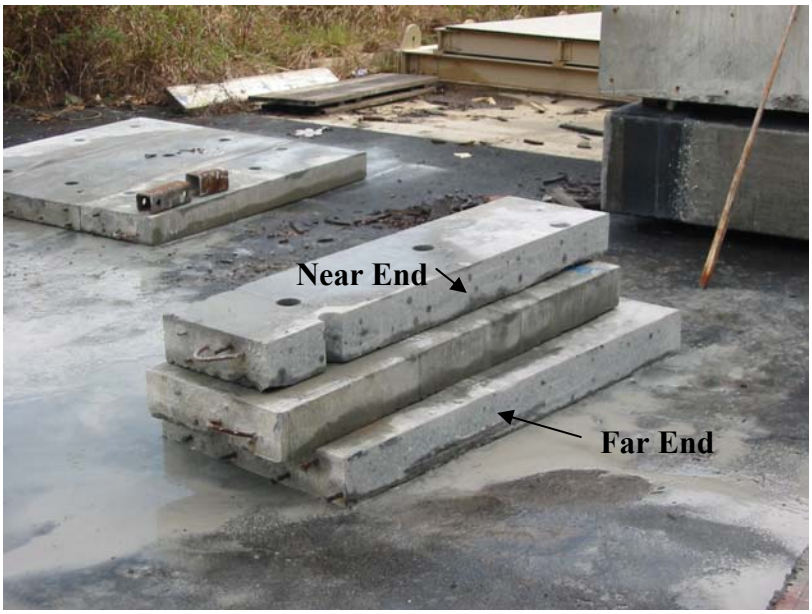

Figure 3-25. Stacking of cross sections for aggregate distribution analysis

When looking at the walls cast with S-Slag/Ash and G-Slag mixes, an even distribution of the aggregates was noticed for all sections inspected. No major variations were found between top and bottom areas of the cross-sections or between near and far end surfaces. Figure 3-26 illustrates a near end and far end section of a wall using the G-Slag mix. Bleeding is evidenced by voids (water pockets) beneath reinforcement, generally considered for horizontal bars with more than 12-in. of concrete beneath the bar. It should be noticed that no such voids were found around the reinforcement at any level, indicating that there was excellent consolidation and that there was no bleeding. This tight packing of the SCC around reinforcement has been noted in the literature and proven to shorten the transfer and development lengths of prestressing strands (Burgueño, 2004).

(a)

(b)

Figure 3-26. Comparison of cross-sections of wall using G-Slag mix (Mix 2, 7-S-BL) (a) near end and, (b) far end. Top of each section is toward the left

As shown before with the cores samples, the interior surface of the Tindall mix wall did not displayed a good consolidation. Figure 3-27 offers a comparison of the near end and far end cross sections of this wall. The near end surface presented a large concentration of small, entrapped air bubbles, but in general the concrete did not presented major flaws as the consolidation energy due to placement was the highest at the near end. The far end surface, on the other hand, was characterized by large air voids and loose aggregate without surrounding paste, both clear signs of poor consolidation. Air-pockets beneath horizontal reinforcement were found all along the cross-section. Cross sections showed that the coarse aggregate had separated from the paste in the transit of concrete through the wall.

(a)

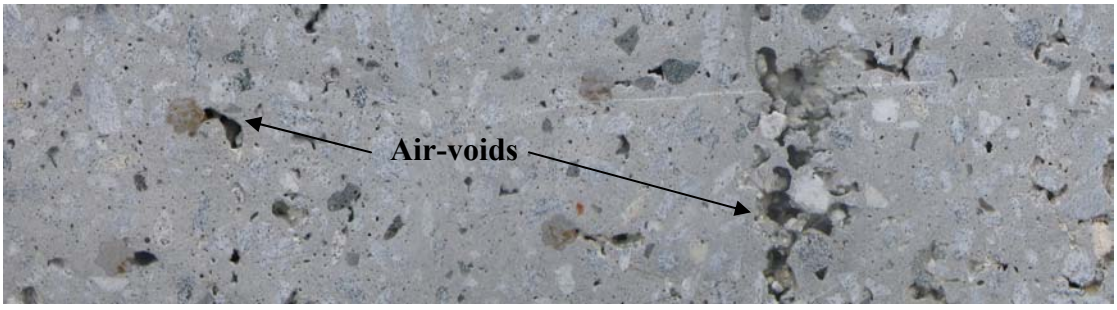

(b)

Figure 3-27. Comparison of cross-sections of wall using Tindall mix (a) near end and, (b) far end. Top of each section is toward the left

In order to apply a Digital Image Analysis (DIA) method, every wall cross-section was divided in three 2-ft long regions and labeled top, middle and bottom. Figure 3-29 presents the results obtained from the DIA of the walls. Appendix A discusses the software and methodology used for the DIA method. The aggregate percentage found in walls using S-Slag/Ash mix was higher than that in walls using G-Slag mix, which corresponded with the theoretical values of coarse aggregate to concrete ratio (CA/concrete) of these mixes, 32.0% and 28.5% for S-Slag/Ash and G-Slag mixes, respectively. The COV values of the percentage of aggregates within a single wall were less than 3.1%, much lower than the 6% allowed under ASTM C94 for uniformity of the concrete. The mean percentage of aggregate for vibrated and non-vibrated walls using S-Slag/Ash mix was 30.2% and 31.0%, respectively. These values for walls using G-Slag mix were 27.5% and 27.6% for vibrated and non-vibrated walls, respectively. Table 3-8 summarizes the statistical results of the values obtained.

Table 3-8. Percentage of coarse aggregate-to-concrete ratios by volume for SCC walls

Mix	Wall	Mean	COV	Theoretical
S-Slag/Ash	Vib	30.4%	2.2%	32.0%
	Vib	30.0%	1.8%	
	Non-vib	31.0%	1.9%	
G-Slag	Vib	27.5%	2.5%	28.5%
	Vib	27.8%	2.2%	
	Non-vib	27.3%	3.1%	
	Non-vib	27.7%	2.4%	
Tindall	Vib	34.0%	12.3%	32.2%

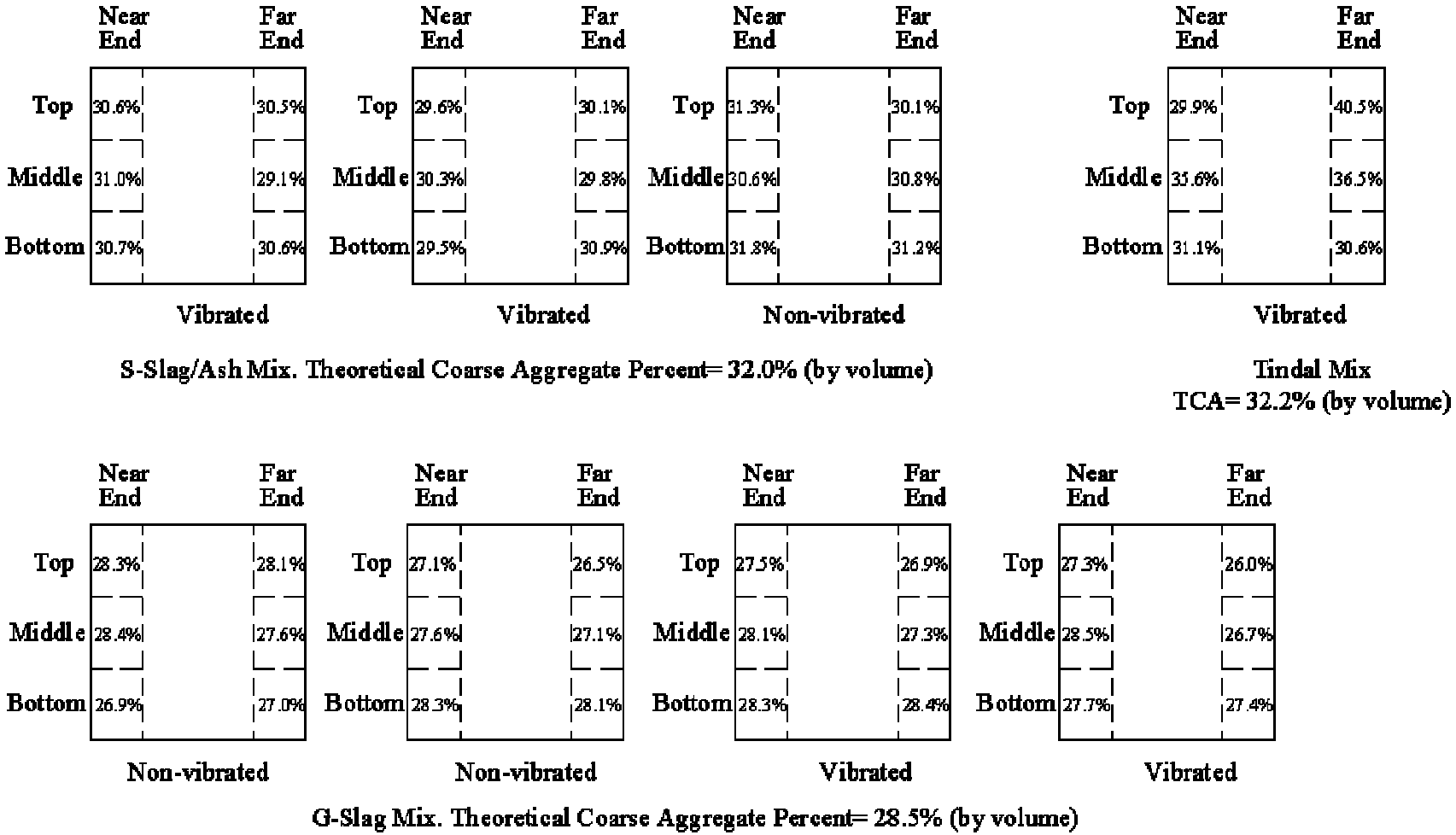

Figure 3-28. Aggregate distribution in SCC Wall Panels

The results obtained for the Tindall mix showed a large variation of the coarse aggregate within the wall. The COV of this mix was 12.3%. In some cases the percentage of aggregates present at a given region was higher than the theoretical CA/concrete ratio. This was an indication of aggregate segregation; the aggregate would separate from the paste creating large voids around loose stones. The top region of the far end surface was the critical case of aggregate segregation with a CA/concrete of 40.5%.

The results obtained with the DIA corresponded with the visual inspection of the cross-section of the walls. No significant aggregate segregation was found in any of the surfaces analyzed except for the wall with the Tindall mix. The DIA proved to be an accurate method to determine the percentage of aggregate present at a given section, as the results obtained are close to the theoretical values expected. The maximum difference between theoretical and in-place values was 2.5%; a value about equal to the COV.

3.7 –Mechanical and Material Properties of SCC Wall Panels

Several control cylinders were cast during placement of the walls. The cylinders were filled using pails instead of typical scoops as the fluidity of the concrete made the use of scoops too unmanageable. The casting was conducted in two lifts each rodded lightly five times with a standard ½-in. (10 mm) diameter steel rod, following a technique developed by Takenaka et al. (2001).

All control cylinders were left at the job site covered with wet burlap for 24 hours. The next day they were transported to the Georgia Tech Structures Laboratory, demolded and stored in a fog room where they were kept until testing as shown in Figure 3-30. The fog room held a constant temperature of 73°F (23°C) and 100% humidity.

Figure 3-29. Shelves of concrete cylinders located in the fog room

3.7.1 –Compressive Strength of Control Cylinders

Compression test were conducted using 4 x 8 in. (100 x 200 mm) cylinders at 3, 7, 28, 56 and 90 days according to ASTM C39 specifications. Three cylinders were tested at each time period for every mix. Figure 3-31 illustrates the mean compressive strength obtained for the mixes used in the wall panels at different ages.

All mixes developed high strength at early ages. Mix S-Slag/Ash had a design strength of 9,000 psi (62 MPa), and the design strength for both G-Slag and Tindall mixes was 7,000 psi (48 MPa) at 28 days. These mixes developed 89%, 100% and 71% of their desired compressive strength after 3 days, respectively. At 28 days all mixes had surpassed their design strengths.

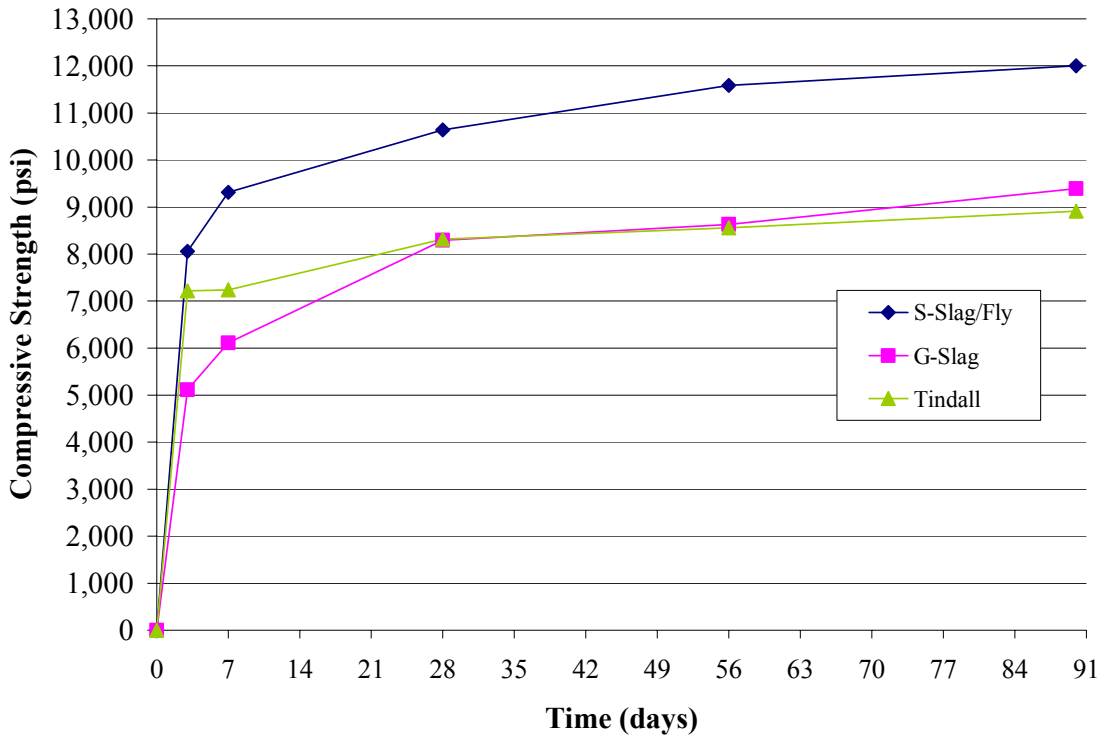

Figure 3-30. Compressive strength of SCC wall panel control cylinders

A comparison of the mean compressive strength of the control cylinders and core samples showed no significant differences between them, except for the Tindall mix. Table 3-9 summarizes the values obtained at each test. These results indicated a similar degree of hydration between the cylinders kept in the fog room and the wall panels. A bigger difference was found in Tindall mix as the cores taken from the wall did not consolidated as well as the concrete in the control cylinders.

Table 3-9. Comparison of strength of core samples at 56 days versus control cylinders of SCC wall panels*

Mix	Control (psi)	Cores (psi)	Difference
S-Slag/Ash	11,600	11,000	5.2%
G-Slag	8,600	8,600	0.0%
Tindall	8,600	6,650	22.7%

*3 x 6 in. core strength were adjusted to equivalent 4 x 8 in. cylinder strength by multiplying the strength by a factor of 0.98

A set of 30 4 x 8 in. control cylinders were tested in order to determine the required average compressive strength (f_{cr}') of G-Slag mix. This mix was selected due to its high stability in fresh state and yet excellent self-consolidating abilities, as demonstrated in section 3.5.1. According to ACI 318-02 specifications, for the specified compressive strength of 7,000 psi (48 MPa) and the standard deviation found in the cylinders set, G-Slag mix required a mean strength, f_{cr}' of 7,690 psi (53 MPa) at 28 days. The G-Slag mix at 28 days had a mean compressive strength of 8,300 psi (57 MPa) with a standard deviation of 516 psi and a COV of 5.7%. If the 8,300 psi were considered f_{cr}', the mix would satisfy a design strength, f_c' of 7,600 psi.

3.7.2 –Modulus of Elasticity

The static modulus of elasticity test was conducted using 6 x 12 in. (150 x 300 mm) cylinders at 28 days, according to ASTM C469 specifications. The average modulus of elasticity and Poisson ratio of three tested cylinders for each SCC mix is presented in Table 3-10. A comparison between the theoretical value given by ACI 318 (Equation 3-1) for conventional concrete, ACI 363 (Equation 3-2) for high strength concrete and the experimental results is also shown in this table.

$$E = 33 * w_c^{1.5} \sqrt{f_c'} \qquad \text{Equation 3-1}$$

$$E = \left(\frac{w_c}{145}\right)^{1.5} * (40{,}000\sqrt{f_c'} + 1 * 10^6) \qquad \text{Equation 3-2}$$

Where

E: Modulus of elasticity (psi);

w_c: unit weight of concrete (lb/ft^3)

f_c': compressive strength of concrete (psi)

Ramage et al. (2004) found that workable SCC mixes had an elastic modulus of about 70% of that given by the ACI 318 expression. The SCC mixes used in this study displayed a modulus of elasticity of about 65% of what Equation 3-1 predicted for conventional concrete and 70% of Equation 3-2 for high strength concrete. The Poisson ratio found in SCC mixes ranged between 0.23 and 0.29. These values are higher than those normally found in conventional concrete, which ranged between 0.15 and 0.20.

Table 3-10. Comparison of Modulus of Elasticity for SCC versus conventional concrete

Mix	f_c' (psi)	E_{SCC} (ksi)	$E_{ACI\ 318}$ (ksi)	$E_{ACI\ 363}$ (ksi)	$E_{SCC}/E_{ACI\ 318}$	$E_{SCC}/E_{ACI\ 363}$	Poisson (ν)
S-Slag/Ash	10,641	3,728	5,880	5,286	63.4%	70.5%	0.29
G-Slag	8,294	3,389	5,191	4,788	65.3%	70.8%	0.29
Tindall	8,313	3,318	5,197	4,792	63.9%	69.2%	0.23

The values found for modulus of elasticity in all SCC mixes were proportional to their respective compressive strengths. The S-Slag/Ash mix which had the highest compression strength value also achieved the highest modulus. The G-Slag and Tindall mixes that had similar compressive strength values also presented comparable modulus results. Figure 3-32 illustrates the modulus of elasticity of the SCC mixes as function of the 28-day compressive strength, and compares the experimental values with the values given by Equations 3-1 and 3-2.

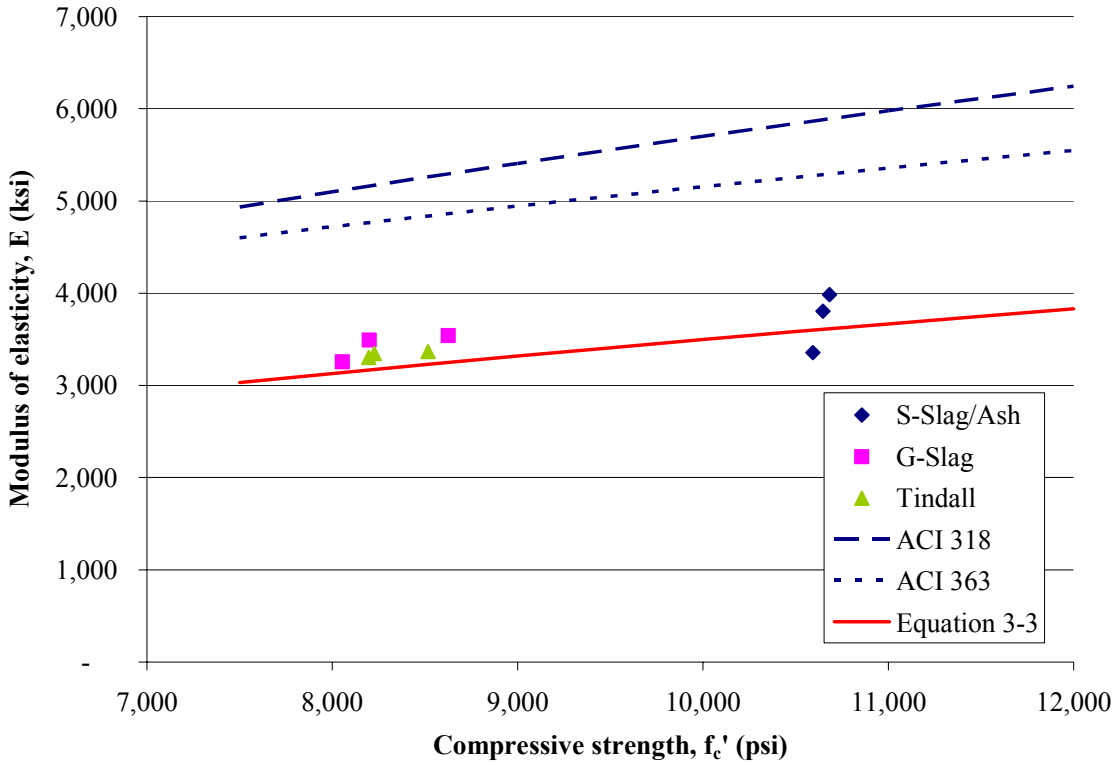

Figure 3-31. Experimental and predicted SCC modulus of elasticity versus 28-day compressive strength

A more conservative expression for the modulus of elasticity of SCC mixes to account for the performance of all tested cylinders is given in Equation 3-3. This expression is based on the mean modulus of elasticity of the SCC mixes with a 95% confidence limit (p=0.05). The mean value for the modulus of elasticity to the square root of compressive strength ratio of all mixes was 37,291 psi/psi, the standard deviation was equal to 1,158 psi/psi and the COV equal to 3.1%. Nevertheless, the number of samples tested was still reduced and further investigation is required to properly assess the results presented here.

$$E = 34{,}975\sqrt{f_c'} \qquad \text{Equation 3-3}$$

Where

E: modulus of elasticity (psi);

f_c': compressive strength of concrete (psi)

3.7.3 –Modulus of Rupture of SCC Wall Panels

The standard tests for the flexural strength of concrete (modulus of rupture, f_r) were conducted using 4 x 4 x 16 in. (100 x 100 x 400 mm) beams according to ASTM C78 specifications. The specimens were covered with wet burlap the first 24 hours, demolded and stored in a fog room the next day and kept in constant temperature and humidity for 28 days until testing. The test set up used for SCC beam samples is illustrated in Figure 3-33. Figure 3-34 depicts the typical failure mode of the samples tested.

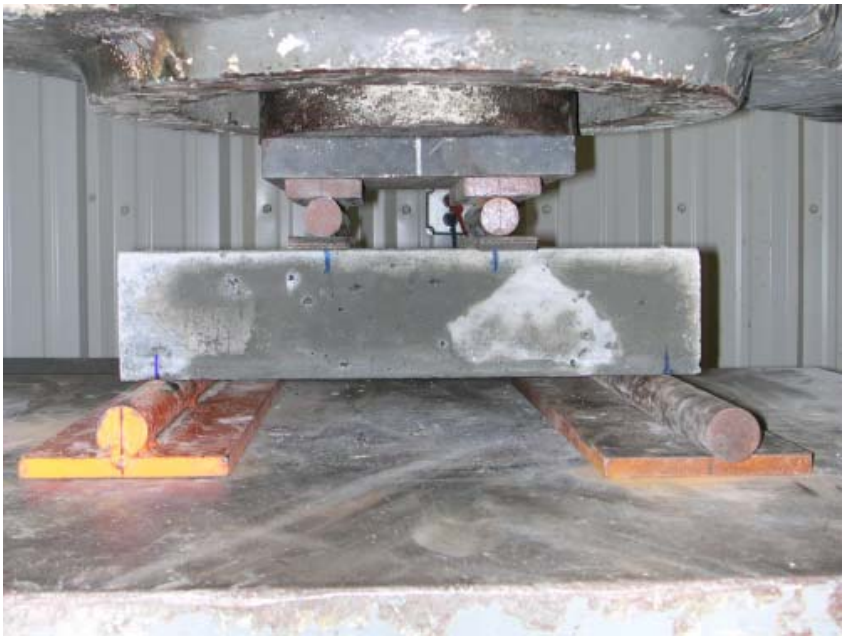

Figure 3-32. Modulus of Rupture test set up

Figure 3-33. Flexural failure of sample in Modulus of Rupture test

Three beam specimens were tested for every mix. The average of the modulus of rupture obtained for all mixes are presented in Table 3-11. The results were compared with the predicted modulus of rupture given by ACI 318 as $7.5\sqrt{f_c'}$ for conventional concrete. All SCC mixes displayed a higher modulus than that given by ACI. In general a 60% increase in the modulus of rupture values was observed for the SCC mixes.

Table 3-11. Comparison of Modulus of Rupture of SCC versus conventional concrete

Mix	f_c', psi [MPa]	$f_{r\ ACI\ 318}$, psi [Mpa]	$f_{r\ SCC}$, psi [Mpa]	$f_{r\ SCC}/f_{r\ ACI\ 318}$
S-Slag/Ash	10,641 [73]	774 [5.3]	1,263 [8.7]	163.3%
G-Slag	8,294 [57]	683 [4.7]	1,229 [8.5]	180.0%
Tindall	8,313 [57]	684 [4.7]	1,102 [7.6]	161.2%

When comparing the relationship between modulus of rupture and the compressive strength of the SCC mixes a direct correlation was found. The SCC with the highest strength also achieved the highest modulus of rupture. Figure 3-35 illustrates the variation of the modulus of rupture to square root of compressive strength ($f_r/\sqrt{f_c'}$) ratio for all tested specimens. On this chart a new expression was proposed to define the modulus of rupture for SCC mixes based on a 95% confidence limit (p=0.05) (Equation 3-4). The mean value for $f_r/\sqrt{f_c'}$ ratio was 12.6 psi/psi, with a standard deviation of 0.86 psi/psi and a COV of 6.8%.

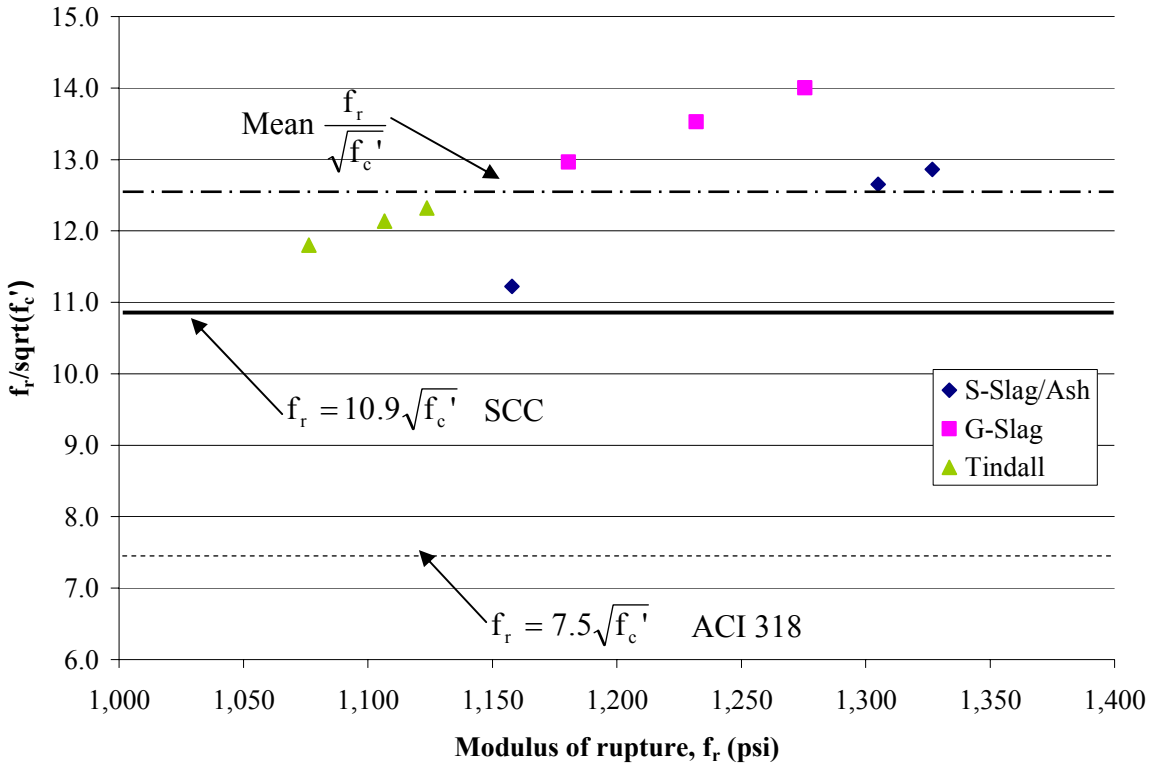

Figure 3-34. Comparison of Modulus of Rupture to the square root of compressive strength ratio of SCC versus conventional concrete

The expression given for SCC mixes accommodates the results obtained in this study. Nevertheless, given the limited number of test completed for this research and the scattering of the data, further investigation is recommended in order to better asses this subject.

$$f_r = 10.9\sqrt{f_c'} \qquad \text{Equation 3-4}$$

Where

f_r: modulus of rupture (psi)

f_c': compressive strength of concrete (psi)

CHAPTER 4

SELF-CONSOLIDATING CONCRETE GIRDERS

4.1 – Introduction

Precast prestressed concrete bridge girders may be rejected due to the presence of air-voids caused by poor consolidation of concrete. The rather narrow cross section geometry and highly congested reinforcement of these elements make the placement of concrete and internal vibration difficult. Air-voids can lead to weakened sections and can accelerate corrosion of reinforcing steel. Furthermore, concrete girders often require a significant amount of surface preparation in order to achieve a satisfactory appearance.

Bulb-tee concrete girders, 72-in deep were selected for testing of SCC due to their slender web, heavily reinforced bottom flanges, and significant height. The top area of the bottom flange of bulb-tee girders is particularly difficult to consolidate, and is frequently the cause for rejection of the girder due to its poor surface finish. This chapter presents a field evaluation of the performance of SCC in bulb-tee girders.

Eight sections of 72-in. deep and 13-ft long bulb-tee beams were fabricated at the Standard Concrete Products (SCP) plant in Atlanta, Georgia. Four different SCC mixes were used for the beams. In addition, a series of trial batches were made both at Georgia Tech Laboratory and at the SCP plant.

4.2 – Material Properties

All materials used in the research were available to local precast/prestressed plants in Georgia. The SCP plant at Atlanta provided all the materials for the trial batches and placement of the girder sections, including the concrete constituents and steel reinforcement.

4.2.1 – Cementitious Materials

Type III cement provided by Lafarge North America, was the cement used for all girders. The oxide analysis and Bogue potential composition of the cement is summarized in Table 4-1 as provided by Lafarge. This cement complied with ASTM C150 Type III and AASHTO M85 Type III specifications. The Blaine fineness for this cement was 592 m^2/kg.

Table 4-1. Chemical composition and fineness of Type III cement

Oxide Analysis	% by Weight
SiO_2	20.50%
Al_2O_3	4.70%
Fe_2O_3	3.00%
CaO	63.60%
MgO	2.80%
SO_3	3.40%
Loss on Ignition	1.40%
Na_2O	0.03%
K_2O	0.33%
Insoluble Residue	0.09%
Equivalent Alkalis	0.25%

Fineness	
Blaine Fineness	592 m^2/kg
45μm sieve, retained	0.1%

Bogue Potential Composition	
C_3S	57.6%
C_2S	15.4%
C_3A	7.4%
C_4AF	9.1%

The only supplementary cementitious material used in combination with Type III cement was Class C fly ash. The fly ash was provided by Holcim, United States, and it conformed to ASTM C618 specifications. The specific gravity of the fly ash was 2.69.

4.2.2 – Aggregates

4.2.2.1 – Fine Aggregates

Two types of fine aggregates were used in the SCC mixes: natural sand and manufactured sand. Some mixes used a blend of the two types of sands, while others used either all natural or all manufactured sand as fine aggregates. Section 4.3 discusses the proportioning of different SCC mixes.

Gradation of the natural and manufactured sands is illustrated in Figure 4-1, as well as the ASTM C33 specifications for gradation of fine aggregates. Natural sand showed a higher passing percent than that specified by ASTM for sieve #16. The same gradation was found for the natural sand used in casting of the wall panels with no apparent detriment in the performance of SCC. Main material properties of both sands are summarized in Table 4-2.

Table 4-2. Material properties of Fine Aggregates used in SCC girders

Properties	Manufactured Sand	Natural Sand
Specific gravity	2.651	2.642
Bulk density (lb/ft^3)	165.42	164.83
Absorption capacity	0.76%	0.23%
Fineness Modulus	2.73	2.30

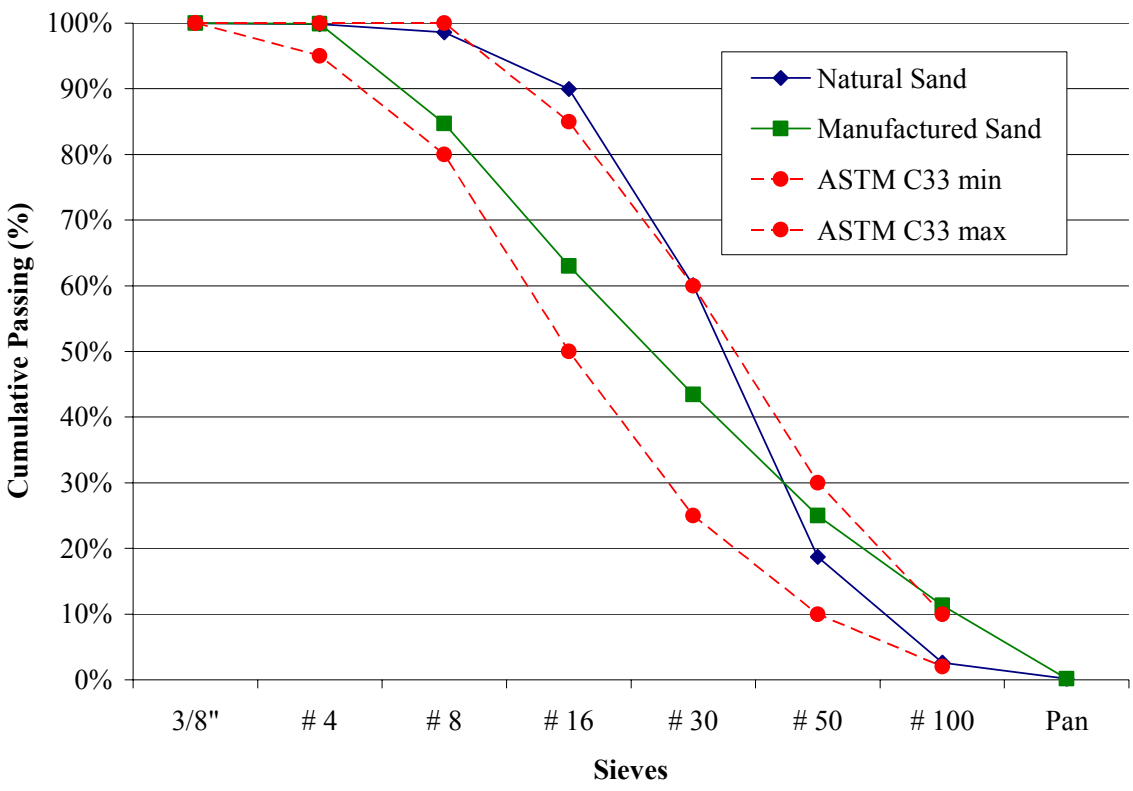

Figure 4-1. Gradation curves for Fine Aggregates and ASTM C33 specifications

4.2.2.2 – Coarse Aggregates

The coarse aggregate was supplied by Lithia Springs Quarry owned by Vulcan Materials Company. All the coarse aggregates used were crushed granite-gneiss. The material properties of all coarse aggregates were determined according to ASTM C127; these properties are shown in Table 4-3. The averages of three sieve analysis tests for every size stone are presented in Figures 4-2 to 4-4. Every chart is accompanied by the gradation specifications given by ASTM C33 for each size aggregate and the gradation reported by Vulcan Materials. In all cases the gradation measured at Georgia Tech laboratory corresponded to the one given by the Vulcan quarry. The #89 stone did not meet ASTM specification for the #8 sieve. Nevertheless, the passing percentage obtained

for this sieve is similar to the one reported by Vulcan quarry, which did not meet ASTM requirements either.

Table 4-3. Material properties for Coarse aggregates used in SCC girders

Aggregate	**#89**	**#7**	**#67**
Maximum Size Aggregate	3/8 in. (9 mm)	1/2 in. (13 mm)	3/4 in. (19 mm)
Specific Gravity	2.64	2.64	2.64
Bulk Density	167.8 lb/ft^3	167.8 lb/ft^3	167.8 lb/ft^3
Dry Rodded Unit Weight	92.4 lb/ft^3	92.1 lb/ft^3	93.3 lb/ft^3
Absorption	0.76%	0.76%	0.76%
Fineness Modulus	3.70	4.52	4.96

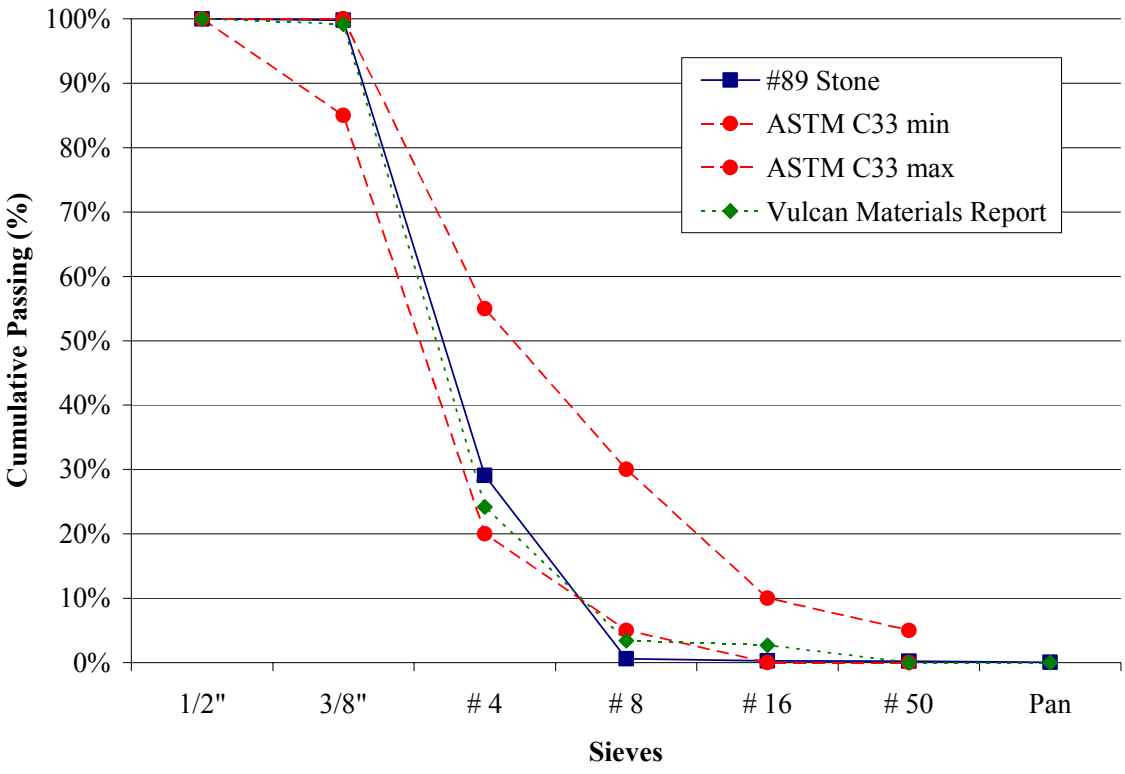

Figure 4-2. Gradation curves for #89 stone and ASTM C33 specifications

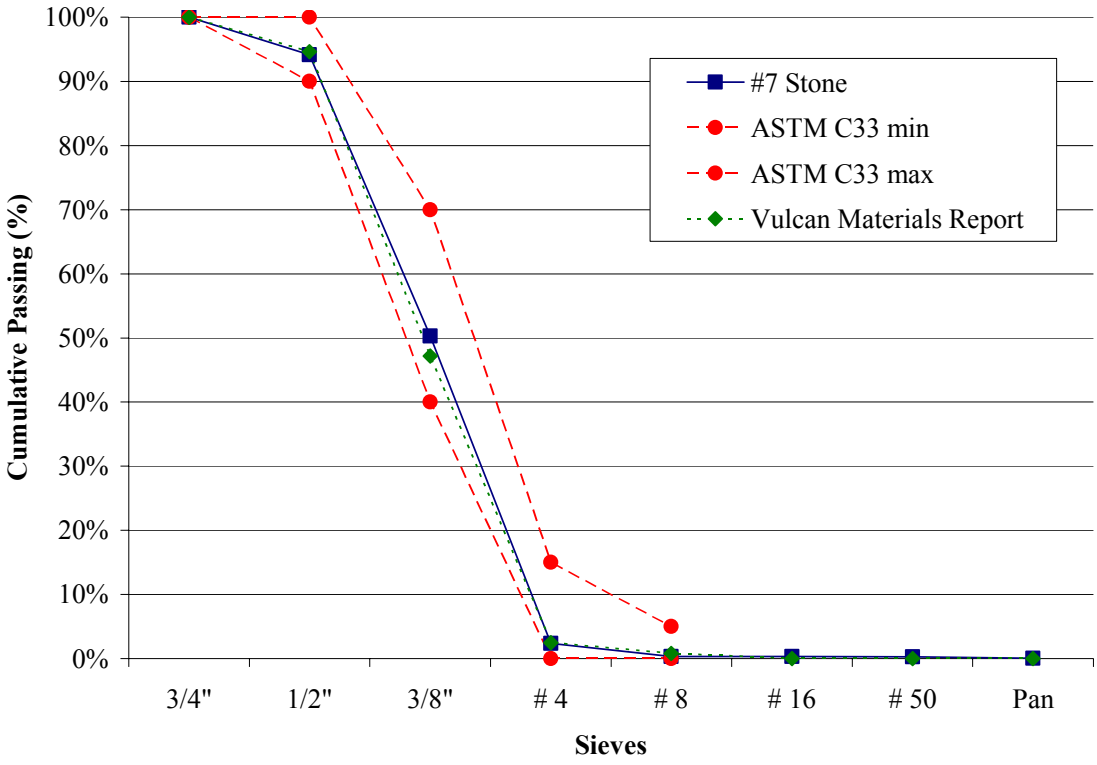

Figure 4-3. Gradation curves for #7 stone and ASTM C33 specifications

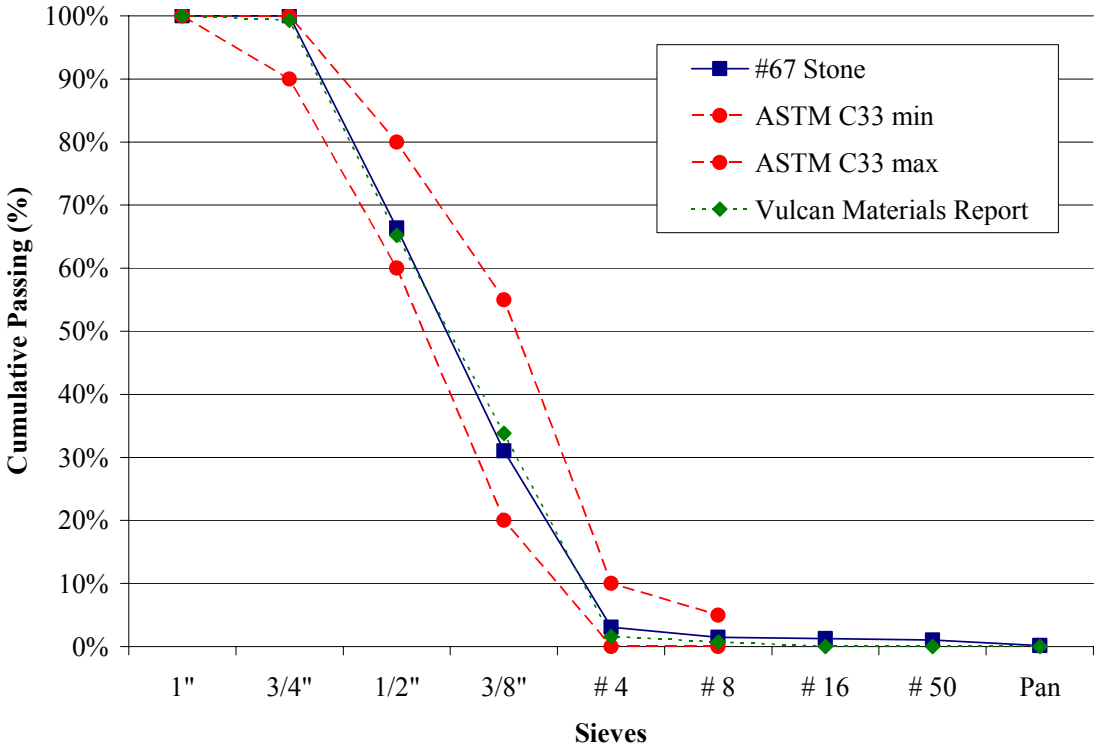

Figure 4-4. Gradation curves for #67 stone and ASTM C33 specifications

The gradation curve of the #67 stone was similar to that for #7 stone. This information suggested that only a small percentage of #6 stone was used in blending of the aggregate for #67 stone. The passing percentage in the ½-in. sieve was the main difference in gradation between #67 and #7 stone. The #67 stone attained 66.4% passing while the #7 stone achieved 94.2% passing. It should be noted that these gradations are different than those given in Chapter 3 for aggregates used in the walls, and are different than those used in the laboratory investigation (Ramage et al., 2004).

4.2.3 – Chemical Admixtures

All the chemical admixtures were supplied by Sika Construction Products Division. Three types of admixtures were used: high range water reducer (HRWR), a low range water reducer (LRWR) and an air-entraining agent (AEA). These admixtures may be added to the mix separately or pre-blended (Kahn and Kurtis, 2000). For the purpose of this research they were always added separately.

Sika ViscoCrete® 6100 was also used for casting of the SCC wall panels. Section 3.2.3 details the manufacturer specifications for this HRWR agent. Ramage et al. (2004) observed that this particular HRWR would overdose SCC mixes when used in dosages over 7 fl.oz/cwt (456 mL/100 kg). For casting of the SCC girders dosage of ViscoCrete was kept at 6 fl.oz/cwt (391 mL/100 kg).

Sika Plastiment is a water-reducing and retarding agent based on a sodium salt of organic acid mix. It meets the requirements for ASTM C494 Type B and D and AASHTO M194 Type B and D. Plastiment is said to control the hydration heat and to

produce superior surface finish. The recommended dosage rates are 2 to 4 fl.oz/cwt (130 to 260 mL/100 kg) of cementitious materials (Sika Construction).

Sika AEA-14 is an aqueous solution of organic materials. It complies with ASTM C260 for air-entraining admixtures. This admixture provides stable and predictable air content in concrete. Dosage rates of this admixture ranging between 1 to 3 fl.oz/cwt (65 to 195 mL/100kg) of cementitious materials entrain 4 to 6 percent of air in concrete (Sika Construction).

4.3 –Mix Proportioning

Five SCC mixes were proposed for casting of the girders. The mixes proportions were based on recommendations by Mr. John Howell of SCP, Atlanta, and the results obtained with casting of the wall panels (Chapter 3). All mixes used Type III cement as in common practice at SCP, and incorporated 17% Class C fly ash replacement by mass of cementitious materials. The total amount of cementitious material was proposed to be kept constant at 900 lb/cy (534 kg/m^3). The w/cm was designed to be a constant 0.32 for all SCC mixes.

The main difference between the mixes was the type of aggregates that they used. The #67 (19 mm) stone and #7 (13 mm) stone were used interchangeably as the maximum size aggregate. In four cases they were blended with #89 (9 mm) stone to produce a more uniform gradation of the coarse aggregate. The fine aggregate used was either natural sand or manufactured sand or a blend of these two sands. In all cases the coarse to fine aggregate ratio was proposed to be kept constant, as well as the aggregate to concrete ratio. Table 4-4 summarizes the proposed SCC mixes. Proportions of Mix 4

were the closest to that used for casting the wall panels, using a blend of #7 and #89 stones and a blend of sands.

Table 4-4. Proposed mix designs for SCC girders

Mix Components	Mix 1	Mix 2	Mix 3	Mix 4	Mix 5
Cementitious (lb/yd^3)					
Cement Type III	750	750	750	750	750
Fly Ash, Class C	150	150	150	150	150
Total Powder	*900*	*900*	*900*	*900*	*900*
Water (lb/yd^3)	288	288	288	288	288
w/cm	*0.32*	*0.32*	*0.32*	*0.32*	*0.32*
Coarse aggregate (lb/yd^3)					
# 67 stone	-	1100	1100	-	1400
# 7 stone	1100	-	-	1100	-
# 89 stone	300	300	300	300	-
Total Coarse	*1400*	*1400*	*1400*	*1400*	*1400*
Fine aggregate (lb/yd^3)					
Natural sand	1296	-	200	200	-
Manufactured sand	-	1296	1096	1096	1291
Total Fine	*1296*	*1296*	*1296*	*1296*	*1291*
Total Aggregates	*2696*	*2696*	*2696*	*2696*	*2691*
Admixtures (fl oz./cwt)					
HRWR (ViscoCrete 6100)	5.6	5.6	5.6	5.6	5.6

Prior to casting the BT-72 sections, a series of trial batches were performed both at the Georgia Tech Structures Laboratory and at the SCP plant, in order to assess the performance of these SCC mixes for both fresh and hardened state. All the mixes were evaluated using the testing methods discussed in previous sections. The fresh state tests included the slump flow test, the U-flow test, and the L-box test, as well as determining

their VSI. As for hardened state tests, multiple cylinders were tested for compressive strength and hardened VSI evaluation.

4.3.1 –Laboratory Mixes

All laboratory mixes were performed at Georgia Tech Structures laboratory. All aggregates were provided by SCP plant, and kept exposed at the laboratory yard as to simulate the conditions at the precast plant.

4.3.1.1 –Mix Procedure

The proportions of all aggregates were based on saturated surface dry (SDD) conditions. A rapid moisture content test was performed prior to every batch and the constituents' proportions were adjusted accordingly. For the moisture content test, a bail with 2 lb (0.9 kg) of aggregate was heated in a heating plate allowing water to evaporate. The bail was weighted every 15 minutes and achieved total evaporation when no further change in weight of the sample was apparent. The difference between initial and final weight represented the moisture content of the aggregate. The measurements of all ingredients were taken to the nearest 0.1 lb (0.05 kg), except for water and the chemical admixtures, which were measured to the nearest 0.001 lb (0.005 kg) and 0.03 fl oz. (1mL), respectively.

Using a 4 ft^3 double shear pan mixer, up to 2 ft^3 (0.057 m^3) of SCC was produced in every batch (Figure 4-5). The mixer was initially sprayed with water in order to avoid any absorption of the batch water by the pan. The fine aggregate was added first to allow the blend of the natural and manufacture sand if needed, and to bring them both to a state of similar moisture content. The coarse aggregate was then added to the mix, and allowed blending with the fine aggregate for one minute. The cement and fly ash were then added simultaneously with the mix water and mixed for another minute. If a 2-in. slump was not achieved with the initial mix water, additional water was added to accomplish this purpose. At this point, the chemical admixture was added. A target amount of 5.6 fl.oz/cwt (365 mL/100kg) was initially considered as the maximum amount of HRWR agent to be used with these mixes. Two thirds (2/3) of that amount was first added to mix. Additional HRWR were added until self-flowing capability of concrete was apparent. The maximum mix time allowed was 7 minutes.

Figure 4-5. Pan mixer at the Georgia Tech laboratory

As every mix required different amounts of water to achieve the point of self-flowing ability, their w/cm varied from the proposed values. The minimum and maximum w/cm achieved were 0.35 and 0.39, respectively. Mixes 2A and 3A were variations of Mixes 2 and 3, respectively, which were mixed with additional water and different dosages of HRWR accordingly. Table 4-5 summarizes the mixes tested at the laboratory. The HRWR dosages used varied from 4.6 to 6.0 fl.oz/cwt (300 to 390 mL/100kg). Previous research identified 7 fl.oz/cwt (456 mL/100kg) as the maximum dosage rate for Sika ViscoCrete® 6100 before causing superplastizer overdose in SCC mixes (Ramage et al., 2004).

Table 4-5. Mix proportions for SCC tested at Georgia Tech laboratory

Mix Components	**Mix 1**	**Mix 4**	**Mix 2**	**Mix 2a**	**Mix 3**	**Mix 3a**
Cementitious (lb/yd^3)						
Cement Type III	766	766	766	752	764	760
Fly Ash, Class C	153	153	153	150	152	152
Total Powder	*919*	*919*	*919*	*902*	*916*	*912*
Water (lb/yd^3)	339	322	322	355	331	339
w/cm	*0.37*	*0.35*	*0.35*	*0.39*	*0.36*	*0.37*
Coarse aggregate (lb/yd^3)						
# 67 stone	-	-	1123	1100	1120	1113
# 7 stone	1124	1124	-	-	-	-
# 89 stone	307	311	307	300	306	302
Total Coarse	*1431*	*1435*	*1430*	*1400*	*1426*	*1415*
Fine aggregate (lb/yd^3)						
Natural sand	1320	201	-	-	203	202
Manufactured sand	-	1160	1363	1340	1148	1145
Total Fine	*1320*	*1361*	*1363*	*1340*	*1351*	*1347*
Total Aggregates	*2751*	*2796*	*2793*	*2740*	*2777*	*2762*
Admixtures (fl oz./cwt)						
HRWR (ViscoCrete 6100)	5.1	5.3	5.3	6.0	5.7	4.6

4.3.1.2 –Testing of Laboratory Mixes

Mixes 1 and 4 performed the best in the laboratory trials. As shown in Table 4-6, both recorded a maximum diameter in the slump flow test of around 25 in. (610 mm) and reached the T_{20} mark within 5 seconds. They both also achieved a 100% of maximum surface level in the U-flow test, as well as L-box test. The slight bleeding observed in the slump flow test of Mix 1 was thought to be due to excessive water added during mixing. Nevertheless, this bleeding was only noticed in the slump flow spread. Therefore the VSI of Mix 1 was considered to be 1. Fresh state testing of Mix 4 corroborated previous results obtained in similar mixes, like those used in the wall panels. This mix was considered the one with best results both in fresh state test and in hardened state, with a VSI of 0.

Table 4-6. Fresh state test results for SCC mixes at Georgia Tech laboratory

Mix	w/cm	HRWR		Slump Flow		VSI					U-Flow	L-Flow			
						Index		Notes				H_d	H_{S1}	H_{S2}	H_f
		fl.oz/yd^3	fl.oz/cwt	T_{20}	D	F	H	B	A	P	% Max	(in)	(in)	(in)	(in)
1	0.37	46	5.1	5	24	1	1	x			100	20.0	4.0	3.5	3.5
2	0.35	48	5.3	-	17	3	2			1.5	39	11.5	2.0	1.0	0
2A	0.39	54	6.0	2	25	3	1	xxx	xx		79	19.25	3.0	2.75	2.5
3	0.36	51	5.7	-	15	3	2			2.0	44	8.5	2.0	0	0
3A	0.37	41	4.6	3	25	0.5	1.5				80	20.0	4.0	3.5	3.5
4	0.35	48	5.3	3	25	0	1		x		100	20.0	4.0	3.5	3.5

*Notes:

T_{20}: Time (sec)
F: Fresh State
H: Hardened State
B: Bleed on slump flow
A: excessive air in the mix
P: Aggregate pile-up (in)
D: mean diameter (inches)
%Max: Height percent of maximum
H_d: filling head drop
H_{S1}: depth at 6 inches away from gate
H_{S2}:depth at 13 inches away from gate
H_f: final depth

Mixes 2 and 3 did not perform well in any of the fresh state tests. Although self-flowing capabilities were observed to a certain degree in those mixes, the maximum diameter observed in both mixes slump flow was limited to 17 inches, never reaching the T_{20} mark. No self-healing abilities were achieved by either of the two mixes (Figure 4-6).

Figure 4-6. Poor self-healing abilities of Mix 3

No bleeding was observed in either Mix 2 or Mix 3. However, the slump flow test of these two mixes showed a 2 in. and 1.5 in. piling of the coarse aggregate, respectively. The passing ability of both Mix 2 and 3 was certainly limited, only achieving 39% and 44% passing in the U-box test, respectively. Neither of the two mixes reached the opposite end of the L-box test (Figure 4-7). This poor performance gave both mixes a VSI of 3.

Figure 4-7. Limited passing ability of Mix 2 in L-box and U-flow tests

Mix 2A and 3A performed differently from Mix 2 and 3. Additional water and higher HRWR dosage were used for these mixes. The increase in w/cm produced an excessive amount of bleeding of Mix 2A, which was noticeable in all fresh state tests but especially in the slump flow test (Figure 4-8(a)). The passing ability of mix 2A was considerably better than that for Mix 2 but still fell under the 85% acceptance of the U-box test, achieving only a 79% passing as illustrated in Figure 4-8(b). On the other hand, Mix 3A performed well at the slump flow test, with a spread of 25 inches and T_{20} of 3 seconds. The concrete spread was uniform and without traces of bleeding or mortal halos; a VSI of 0.5 was assigned to mix 3A. Its passing ability, although superior to that in Mix 3, was still below the acceptable performance achieving only 80% passing in the U-box. Nevertheless, the L-box test results of this mix were as good as those obtained in Mixes 1 and 4, with a total level surface. Figure 4-9 illustrates the performance of Mix 3 in all fresh state tests.

(a) (b)

Figure 4-8. Excessive bleeding in Mix 2A (a) slump flow test, and (b) U-flow test

(a) (b)

Figure 4-9. Performance of Mix 3A (a) slump flow test, and (b) U-flow and L-box test

After all performance tests were done, several control cylinders were filled in order to complete compressive strength testing. The Takenaka technique for filling the cylinders was used, as described in section 3.7 (Figure 4-10(a)). Once the cylinders were filled and capped they were placed inside a curing box for 24 hours, as shown in Figure 4-10(b). The cure boxes were used to replicate the curing conditions of precast elements in a plant.

(a) (b)

Figure 4-10. Control cylinders at laboratory (a) filling the cylinders using pails, and (b) inside of a cure box with cylinders of a batch

After 24 hours the cylinders molds were stripped off and the concrete was stored in the fog room until testing. The fog room was kept at a constant temperature of 73°F (23°C) and 100% relative humidity.

Compression tests were conducted using 4 x 8 in. (100 x 200 mm) cylinders at 1, 7, and 28 days. Three cylinders were tested at each time period for every mix, and the average of these values was recorded. Figure 4-11 shows the compressive strength at different ages for all mixes tested.

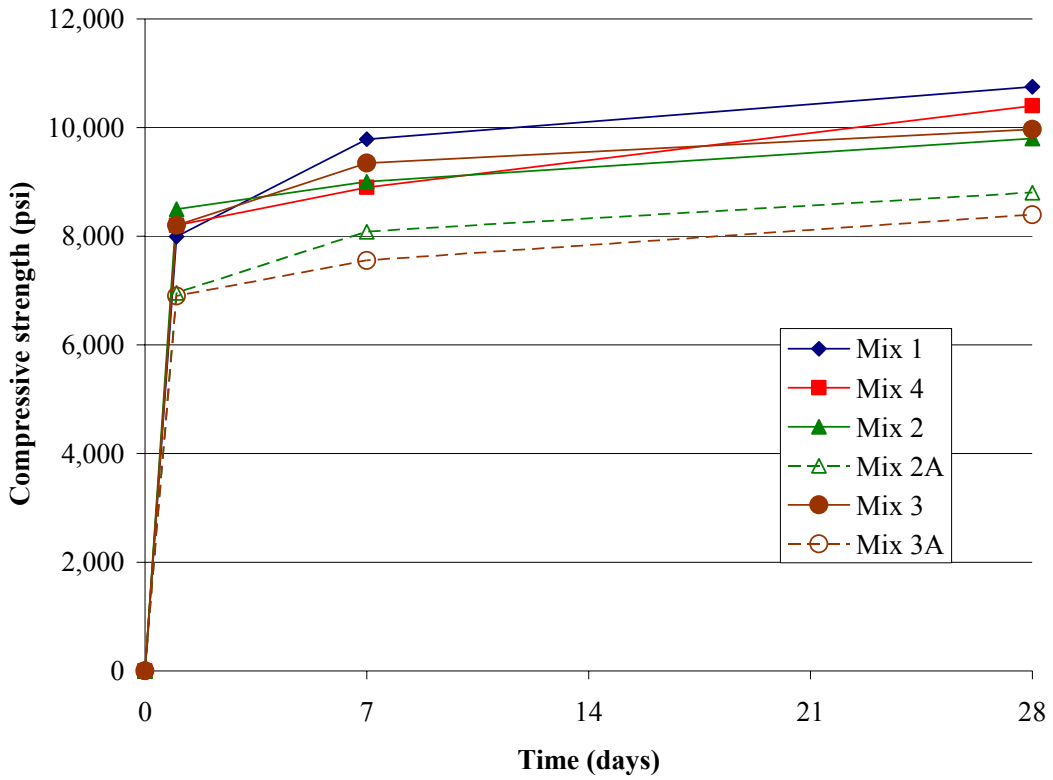

Figure 4-11. Compressive strength of SCC laboratory mixes

The proposed w/cm for all mixes was 0.32 with target strength of 8,000 psi (55 MPa) at 28 days. The addition of extra water to accomplish the required 2-in. slump increased the resulting w/cm in every mix. However, the compressive strength of the mixes was still higher than the target strength at 28 days. Mixes 2A and 3A showed the lowest values for compressive strength at 28 days; Mix 2A with a w/cm of 0.37 achieved 8,800 psi (61 MPa), and Mix 3A with a w/cm of 0.39 showed a compressive strength of 8,400 psi (58 MPa).

Hardened VSI numbers were also given to the mixes to differentiate those that displayed excellent capabilities in fresh state but performed poorly in the compressive strength test or vice versa. Hardened VSI accounts for surface finish, any aggregate

settlement or superplasticizer overdose, as well as other deleterious properties of the hardened concrete. Table 4-6 summarized the hardened VSI numbers for all mixes.

All mixes were characterized by an excessive amount of air entrained bubbles in their surface finish and in the interior of the cylinders. This was the main factor that gave a hardened VSI of 1 to Mixes 1 and 4. Nonetheless, given the reduced size of the bubbles and their uniform distribution, it was thought that the excessive air may have been caused by overexposure of the mixes in the pan, and not due to segregation problems (Figure 4-12).

(a) (b)

Figure 4-12. Surface finish of control cylinders of SCC laboratory mixes (a) Mix 1, and (b) Mix 4

The presence of air bubbles was more critical in Mixes 2 and 3 (Figure 4-12). However, no aggregate segregation or interior voids were apparent in the cylinders. Therefore, the VSI number of both these mixes was 2.

(a) (b)

Figure 4-13. Excessive air in surface finish of SCC laboratory mixes (a) Mix 2, and (b) Mix 3

Control cylinders from Mixes 2A and 3A had a similar surface finish. Nevertheless, the interior of cylinders from Mix 3A showed a larger number of entrapped air-bubbles, which corresponded to the lower compressive strength achieved by this mix when compared with Mix 2A. The VSI numbers for Mixes 2A and 3A were 1 and 1.5, respectively.

(a) (b)

Figure 4-14. Surface finish of SCC laboratory mixes (a) Mix 2A, and (b) Mix 3A

4.3.2 –Trials Mixes

A series of trial batches for the proposed SCC mixes were performed at the SCP plant prior to casting of the girders. The SCC produced was placed in 8-ft long concrete barrier sections. Although the reinforcement of the barriers was minimum and did not offer the same level of rebar congestion as the bulb-tee girders, these trial batches with a full size mixer gave a better idea of the performance of the proposed SCC mixes.

The barriers cast at SCP plant were reinforced with two #4 (13 M) bars along each face of the section and a center #4 bar at the apex. The transverse reinforcement consisted in V-shapes #4 stirrups spaced 12 in. towards the center of the element, and 6 in. spacing at each end. A bent #6 (19 M) bar served as lifting device; it extended to the bottom of each end of the element (Figure 4-15).

Figure 4-15. Reinforcement of concrete barriers inside steel forms

4.3.2.1 – Mix proportions

The SCC mixes used for casting of the concrete barriers were based on the initially proposed mixes presented in section 4.3. The actual mixes placed differed from the original ones as more or less water was needed to achieve the 2-in. slump required during mixing. A fifth mix was proposed for these trial batches in addition to the four mixes showed before. This fifth mix was intended to be more economical to produced than the rest as it only employed #67 stone as coarse aggregate and manufactured sand as fine aggregate. The coarse to fine aggregate ratio and aggregate to concrete ratio of this mix was the same as those in the rest of the mixes tested before in the laboratory. Table 4-7 presents all the mixes used in the trial batches.

In general, less water was needed in the SCP trial batches to produce the initial 2-in. slump during mixing than was needed in the laboratory mixes. The w/cm of these mixes varied between 0.30 and 0.34. The higher efficiency of the full size mixer used at the plant compared with the low energy provided by the laboratory mixer seemed to be the reason for this difference in water requirements.

The trial batches also included a water reducer and an air-entraining agent beside the HRWR agent used in the laboratory mixes. The first two admixtures were used interchangeably, except for Mix 5 where all three admixtures were used.

Table 4-7. Mix proportioning for trial batches at SCP plant

Mix Components	Mix 1	Mix 2	Mix 3	Mix 4	Mix 5
Cementitious (lb/yd^3)					
Cement Type III	746	762	784	773	745
Fly Ash class C	152	151	153	159	150
Total Powder	*898*	*913*	*937*	*932*	*895*
Water (lb/yd^3)	288	282	299	314	265
w/cm	*0.32*	*0.31*	*0.32*	*0.34*	*0.30*
Coarse aggregate (lb/yd^3)					
# 67 stone	-	1150	1278	-	1432
# 7 stone	1231	-	-	1234	-
# 89 stone	183	208	204	210	-
Total Coarse	*1414*	*1358*	*1482*	*1444*	*1432*
Fine aggregate (lb/yd^3)					
Natural sand	1296	1350	1178	208	-
Manufactured sand	-	-	182	1153	1340
Total Fine	*1296*	*1350*	*1360*	*1361*	*1340*
Total Aggregates	*2710*	*2708*	*2842*	*2805*	*2772*
Admixtures (fl oz./cwt)					
HRWR (ViscoCrete 6100)	6.0	6.0	6.0	6.0	6.0
LRWR (Plastiment)	-	-	2.0	2.0	2.0
Air entraining (AEA-14)	0.2	0.2	-	-	0.2

4.3.2.2 –Placement of SCC mixes

One 3 yd^3 (2.3 m^3) batch was produced for every trial mix. Four concrete barrier forms were able to be filled with a single batch. A Tucker built truck transported the concrete from the batching plant to the barrier forms, located 200 yards away. The concrete was placed from a single point at one end of the forms and allowed to flow until completely filled the form. Figure 4-16 illustrates the casting process of the barriers.

Figure 4-16. Placement of SCC trial batches in concrete barriers

After the forms were completely filled the surface slope along the long side of the forms was about 4% in all barriers. No vibration whatsoever was provided to any of the barriers cast. Finally, the top surface was screeded and the forms covered with a thick tarp. After 24 hours the forms were removed and the concrete barriers lifted and stacked in the yard for delivery.

4.3.2.3 –Testing of Trial Batches at SCP plant

Prior to casting of the barriers, the mixes were tested for self-consolidating ability. As with the laboratory mixes, the trial batches were tested using the slump flow test, U-box and L-box tests. Also, a fresh and hardened VSI number was assigned to every mix.

In general all SCC mixes performed very well at all flowing and passing ability tests (Table 4-8). The diameter of the spread in the slump flow test varied between 22 and 28 in. (556 and 712 mm), which fell within the acceptable range of 25 ± 4 in. (635 ± 100 mm) (Hine, 2004). However, the majority of the mixes displayed a diameter spread closer to the upper limit of acceptance. In those mixes a slight bleeding was observed which gave them a fresh state VSI of 0.5 (Figure 4-17). Mix 3 had a VSI of 1 due to the minor bleeding observed; popping air in the surface of the wheel barrel was also noted. All mixes achieved 100% passing through the U-box test and a complete level surface for the L-box test (Figure 4-18).

Table 4-8. Tests results for Trial batches at SCP plant

Mix	w/cm	HRWR		Slump Flow		VSI					U-Flow	L-Flow			
						Index		Notes				H_d	H_{S1}	H_{S2}	H_f
		fl.oz/yd^3	fl.oz/cwt	T_{20}	D	F	H	B	A	P	% Max	(in)	(in)	(in)	(in)
1	0.32	54	6	3	22	0	1		x		100	21	3	3	3
2	0.31	54	6	3	28	0.5	0	x			100	21	3	3	3
3	0.32	54	6	3	27	1	1	x	x		100	21	3	3	3
4	0.34	54	6	2	28	0.5	0.5	x			100	21	3	3	3
5	0.30	54	6	3	27	0.5	0.5	x			100	21	3	3	3

Figure 4-17. Slump flow test for Mix 5. Slight bleeding in the perimeter of the spread

Figure 4-18. L-box test for Mix 5. Excellent passing ability with a complete leveling surface

Mix 5 performed as well as the rest of the mixes, even when this mix only incorporated a single coarse and fine aggregate types and not a blend of either as the rest of the mixes. Previous laboratory testing of mixes similar to Mix 5 did not show as good passing ability, producing blockage of the coarse aggregate at the layer of rebar in either the U-box or L-box (Ramage et al., 2004). The better mixing of the concrete constituents, and especially the HRWR using the full size mixer as opposed to the small laboratory pan mixer seemed to create these differences in performance.

Three 4 x 8 in. control cylinders were filled during the trial batches for compressive strength tests. The cylinders were left exposed as to maintain the same curing conditions of the barrier, which were not steam cured. The next day the cylinders were transported to the Georgia Tech laboratory and stored in the fog room until testing. The 3-day average compressive strength values of the mixes are summarized in Table 4-8. At this early age all mixes displayed a similar compressive strength that ranged between 6,200 and 6,700 psi (43 and 46 MPa). These values represented a strength over 75% of the 8,000 psi target strength.

The surface finish of all cylinders was very similar in all mixes, and no significant differences were observed among them. The surface of the cylinders was in general smooth and air-void free (Figure 4-19). The hardened VSI numbers of the mixes range between 0 and 1. Mix 1 and 3 had a VSI of 1 as the interior of the cylinders displayed a larger number of air bubbles not present in the rest of the mixes. Figure 4-20 shows the interior of a cylinder of Mix 1 after failure in compression.

.

(a) (b)

Figure 4-19. Smooth surface finish of cylinders from Trial batches at SCP plant (a) Mix 4 cylinders, and (b) Mix 5 cylinders

Figure 4-20. Comparison of surface finish and interior of a cylinder from Mix 1. Interior of cylinder displayed a large number of entrapped-air bubbles

The surface finish of the control cylinders corresponded with that in the concrete barriers. A smooth, void-free surface was observed in all barriers cast and no differences were found between barriers from different mixes. Figure 4-21 illustrates the even surface finish of concrete barriers cast at the trial batches.

Figure 4-21. Smooth surface finish in all concrete barriers using SCC mixes

4.3.3 – Mixes used in SCC girders

Based on the results obtained both in the laboratory and at the SCP plant, four final mixes were selected for girder construction: Mix 1, 2, 4 and 5. These four mixes performed satisfactorily in all fresh state tests and showed a good quality surface finish in their control cylinders and barrier sections.

The mix designs were renumbered according to the following scheme: ABC, where A represents the maximum size aggregate (MSA) used for that mix, B is the type of fine aggregate used, and C specifies vibration or non-vibration of the section. Table 4-9 describes the different variations of this scheme. Mix proportions for the selected mixes are summarized in Table 4-10, matching the old designations with the new numbered scheme.

Table 4-9. Numbering scheme for SCC mixes in concrete girders

ABC	Numbering Scheme	Letter	Description
A	Maximum size aggregate	7	MSA #7 stone (13 mm)
		67	MSA #67 stone (19 mm)
B	Fine Aggregate type	M	Manufactured sand
		N	Natural sand
		BL	Blend of manufactured and natural sand
C	Vibration	v	Vibrated section
		blank	Non-vibrated section

The numbering scheme differentiates between vibrated and non-vibrated mixes. However, these mixes are essentially the same regarding the type of aggregates used and their proportions in the mix. Also, the maximum size aggregate of the mixes did not represent the only coarse aggregate used. All mixes used a blend of coarse aggregates except mix 67M that only used #67 stone, as shown in Table 4-10.

For casting of the girders all mixes included the three Sika admixtures previously mentioned: ViscoCrete® 6100 HRWR, Plastiment® LRWR and retarder agent and, AEA-14 air-entraining agent. The HRWR dosage was kept constant for all mixes at 6 fl.oz/cwt (391 mL/100kg). Every mix required different dosages of low range water

reducer and air-entraining agent to help the HRWR achieve self-flowing abilities of the concrete. The Plastiment and AEA-14 dosages range between 1.9 and 2.1 fl. oz/cwt (124 to 137 mL/100kg) and 0.11 to 0.33 fl.oz/cwt (7 to 22 mL/100kg), respectively.

Table 4-10. Mix proportions for SCC girders

	Mix 1		**Mix 2**		**Mix 4**		**Mix 5**	
Mix Components	**7N**	**7Nv**	**67N**	**67Nv**	**7BL**	**7BLv**	**67M**	**67Mv**
Cementitious (lb/yd^3)								
Cement Type III	780	765	780	750	776	754	770	768
Fly Ash class C	166	163	156	146	163	147	153	156
Total Powder	*946*	*928*	*936*	*896*	*939*	*901*	*923*	*924*
Water (lb/yd^3)	297	300	277	293	305	308	294	303
w/cm	*0.31*	*0.32*	*0.30*	*0.33*	*0.32*	*0.34*	*0.32*	*0.33*
Coarse aggregate (lb/yd^3)								
# 67 stone	-	-	1164	1176	-	-	1439	1443
# 7 stone	1254	1250	-	-	1259	1223	-	-
# 89 stone	194	208	215	218	204	182	-	-
Total Coarse	*1448*	*1458*	*1379*	*1394*	*1463*	*1405*	*1439*	*1443*
Fine aggregate (lb/yd^3)								
Natural sand	1210	1280	1339	1320	199	211	-	-
Manufactured sand	-	-	-	-	1139	1155	1357	1206
Total Fine	*1210*	*1280*	*1339*	*1320*	*1338*	*1366*	*1357*	*1206*
Total Aggregates	*2658*	*2738*	*2718*	*2714*	*2801*	*2771*	*2796*	*2649*
Admixtures (fl oz./cwt)								
HRWR (ViscoCrete 6100)	6.0	6.0	6.0	6.0	6.0	6.0	6.0	6.0
LRWR (Plastiment)	2.1	1.9	2.1	1.9	2.1	1.9	2.0	2.0
Air entrainer (AEA-14)	0.15	0.11	0.18	0.18	0.15	0.18	0.18	0.33

4.4 – Formwork and Girders Reinforcement

The BT-72 girders were examples of congested precast bridge members. Both the geometry of these elements and the amount of reinforcement included in them were designed to create a significant challenge for the concrete to properly flow and consolidate. In testing of the SCC mixes, replication of actual casting conditions was very important, including formwork, amount of reinforcement used and its layout across the girders section.

The BT-72 section is commonly used for long span bridges and accommodates a large amount of prestressed reinforcement both in its web and bottom flange. The sections cast were only 13-ft long as to facilitate transportation and later handling for coring and sawing. The top flange of the girders was shortened, making the top and bottom flange the same width so that the section would lay level on its side for saw cutting and coring. Figure 4-22 illustrates the geometry of the BT-72 sections.

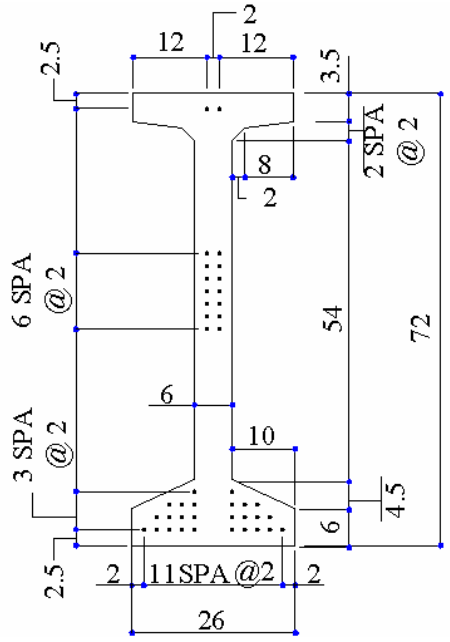

Figure 4-22. Dimensions and strands location of SCC BT-72 beams. Dimensions are in inches

Grade 270 low relaxation 0.6-in. diameter strands were used for all longitudinal reinforcement. The bottom flange included 26 strands and the web accommodated 7 draped strands at each face with 2-in. spacing. Only six strands at the bottom flange and two strands and the top flange were actually prestressed; the rest of the strands were field-tied to the rest of the reinforcement in order to mimic a fully reinforced girder.

The transverse reinforcement varied along the length of the members (Figures 4-23 and 4-24). Stirrups at both ends of the girders were #6 (19 M) bars spaced 3 in. on center. In addition, #3 (10 M) dog house bars confined the bottom flange at 12-in. spacing on center. Towards the center the beams, #5 (16 M) stirrups were spaced 12 in. on center and no dog house bars were needed. Ten #4 (13 M) longitudinal bars were added to the web as shear reinforcement at both ends of the girders.

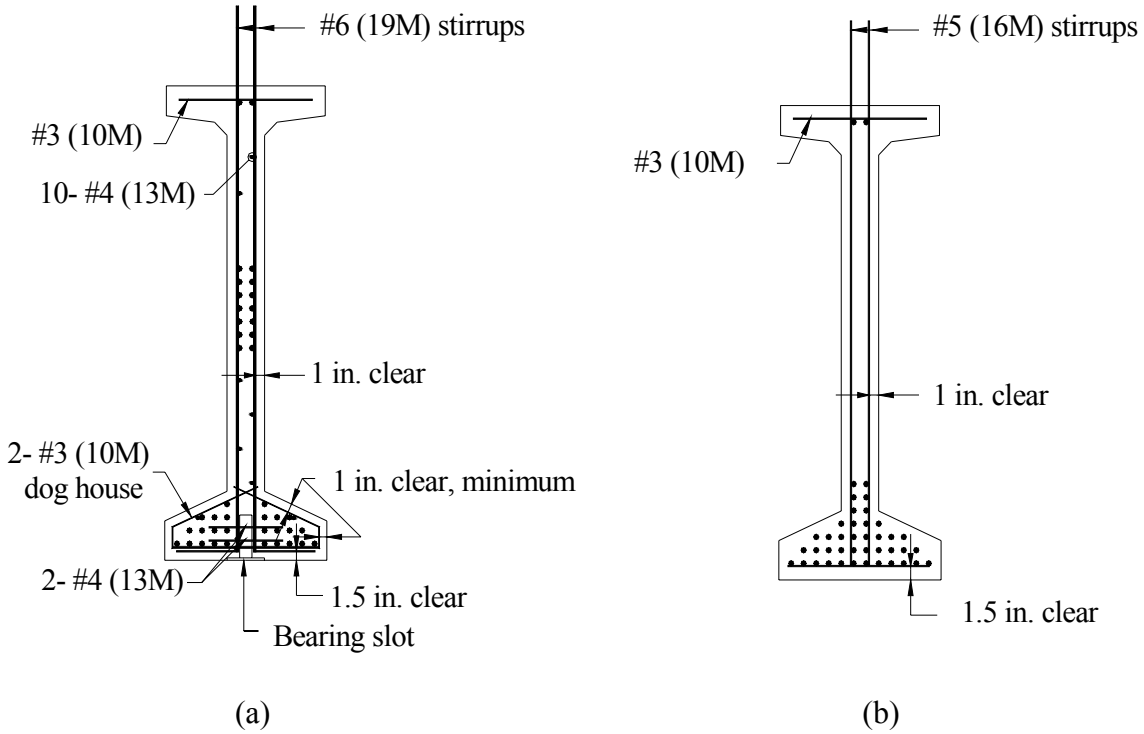

Figure 4-23. Reinforcement detail of SCC girders (a) at ends, and (b) at center

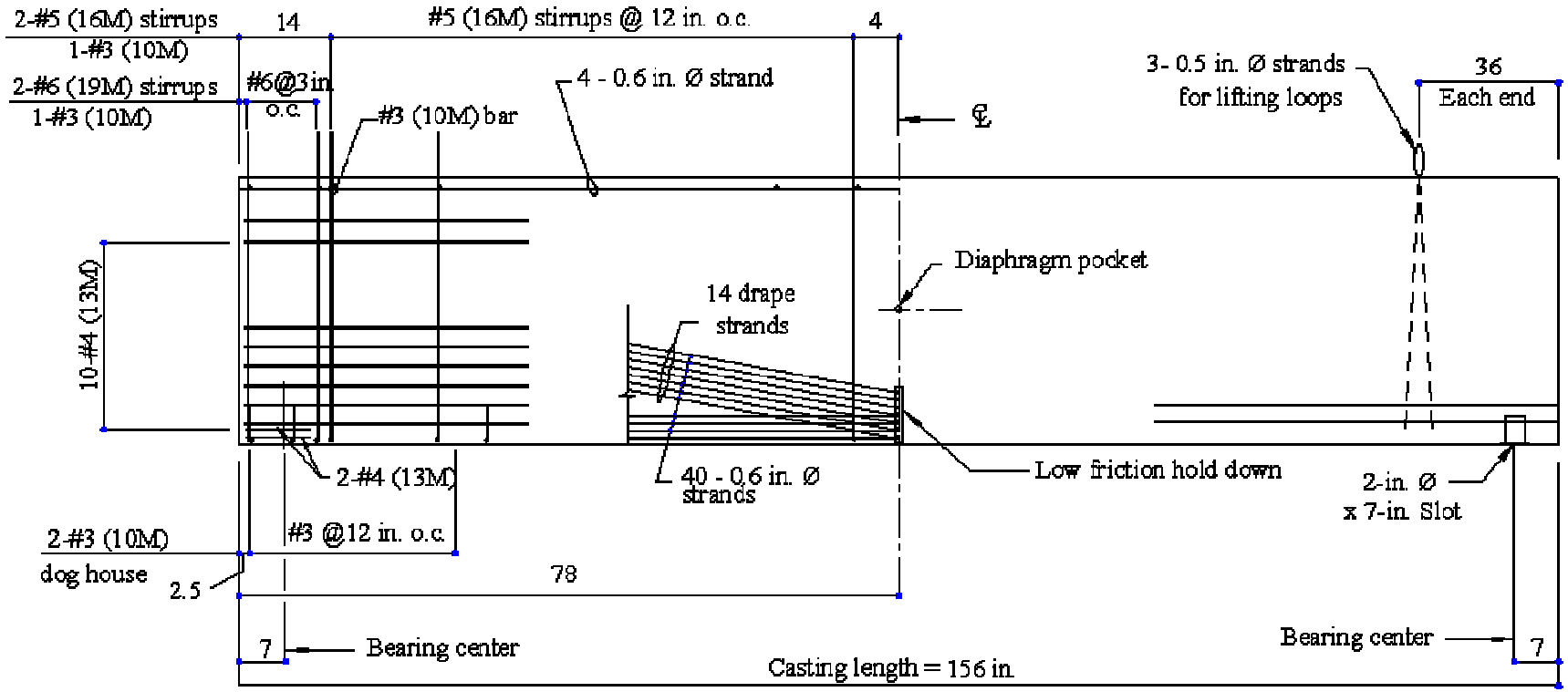

Figure 4-24. Elevation of SCC BT-72 girders

A diaphragm pocket at the center of the section, and slot devices at both bottom ends were also included in the SCC girders (Figure 4-25). The diaphragm pocket is typically used in actual bridge girders for passing of reinforcement through the girders in order to connect them to concrete diaphragms. The slot devices serve as connectors for pins which restrain lateral displacements.

Three areas in the reinforcement were apparent points of congestion: the shear reinforcement at the end of the sections, the area around the lifting loops and, the hold down location for the draped strands. The combination of tight vertical reinforcement towards the end of the girders and the seven layers of draped strands created a narrow area for passing of the concrete (Figure 4-26(a)). Lifting loops made of six ½-in. strands were located 36 inches away from each end of the sections to mimic such loops in actual girders (Figure 4-25). The clearance between the #5 (16 M) stirrups and the pick-ups was only 0.5 inches (13 mm). A low friction hold down device was placed at the bottom center of the girders to lock the draped strands in place. Adding the layers of draped strands to the four layers already placed at the bottom flange created a densely reinforced area prone to block the concrete flow (Figure 4-26(b)).

Figure 4-25. Reinforcement layout of a SCC girder section

(a) (b)

Figure 4-26. Reinforcement details of SCC girder, (a) at ends and, (b) at bottom center

All eight girders were aligned over a single prestressing bed. For ease of construction, these short sections were built at the same bed where other BT-72 concrete girders were being cast. The SCC girders utilized the same prestressed strands at the top and bottom flanges as those other sections using conventional concrete. Figure 4-27 illustrates the layout of the SCC girders on the prestressing bed; on the left a blue tarp is covering the conventional concrete sections.

The conventional formwork for BT-72 sections has a wider top flange than the one proposed. A Styrofoam piece was placed at each side of the top flange of the sections to avoid the complete filling of these areas. Figure 4-28 shows the top flange of the formwork with the Styrofoam pieces at each side.

Figure 4-27. Layout of SCC girder sections over the prestressing bed

Figure 4-28. Top flanges of formwork in SCC girders

4.5 – Casting of SCC girders

All concrete mixes were prepared at the SCP batching plant at Atlanta, Georgia. The batching sequence consisted of introducing the fine and coarse aggregates and allowing them to mix. The cementitious materials and mix water were then added and mixed until a 2-in. slump were apparent in the concrete. At this point the HRWR agent was added and the concrete was agitated for another minute. Finally, the LRWR agent and air-entraining agent were added separately and were mixed for an additional minute. The fresh concrete was tested for self-consolidating properties and air content prior to casting of the girders.

4.5.1 –Testing of Fresh SCC

Two batches were produced for every mix design, and each batch was tested for self-flowing abilities. Although the two batches were based on the same mix, they were not consistent in that their water and air content varied. Variations of the moisture content of the aggregates inside the bins produced changes in the total water added to the mixes. As a consequence, the w/cm of the mixes changed from one batch to another. Those mixes with a noticeable difference in w/cm displayed different results on the fresh state tests, as shown is Table 4-11.

In general, all batches produced self-consolidating concrete mixes of acceptable quality, but not of optimum quality. Excessive bleeding was observed in almost every mix, except mixes 7N (Mix 1) and 67N (Mix 2) which resulted in rather dry mixes. The slump flow of all mixes fell within an acceptable range varying from 22 to 29 inches (556 to 737 mm). All mixes tended to display a slump diameter closer to either the lower or upper values, resulting in a dry or watery mix, accordingly. The fresh VSI number of the mixes varied from 0 to 1.5. Only mix 67Nv (Mix 2) had an optimum stability appearance with a VSI of 0 and a middle range spread diameter of 25 in. (635 mm). Mixes with excessive bleeding got a VSI number of 1.5. The U-flow test ran with a 100% passing for all mixes, except mix 67N (Mix 2) that only achieved 86% of passing, but it was considered acceptable as it fell above the 85% passing acceptance criteria (Ramage et al., 2004). The L-box test showed similar results as those from the U-box test, although no measurements were taken of the last four batches as the apparatus was damaged during the test process. The batches tested with the L-box apparatus showed a level surface with a 3% slope, except mix 7BLv (Mix 4) that achieved a total leveled surface.

Table 4-11. Fresh state testing results for SCC girders

Mix	Batch	w/cm	Slump Flow		VSI					U-Flow	L-Flow				Air
					Index		Notes				H_d	H_{S1}	H_{S2}	H_f	
			T_{20}	D	F	H	B	A	P	% Max	(in)	(in)	(in)	(in)	(%)
Mix 1	7N	0.31	4	23	1	1				100	20	4	3	3	2.8
	7Nv	0.32	3	27	1.5	1	x	x		100	20	4	3	3	2.0
Mix 2	67N	0.30	5	22	1.5	2				86					3.5
	67Nv	0.33	4	25	0	1				100					6.0
Mix 4	7BL	0.32	2	29	1.5	1	x			100	20	4	3	3	0.5
	7BLv	0.34	3	28	1	1	x			100	21	3	3	3	5.5
Mix 5	67M	0.32	4	27	1	1	x			100					1.8
	67Mv	0.33	4	27	1	1	x			100					4.8

*Notes:

T_{20}: Time (seconds)
F: Fresh state
H: Hardened state
B: Bleed on slump flow
A: excessive air in the mix
P: Aggregate pile-up (inches)
D: mean diameter (inches)
%Max: Height percent of maximum
H_d: filling head drop
H_{S1}: depth at 6 inches away from gate
H_{S2}:depth at 13 inches away from gate
H_f: final depth

Measurement of air content of the mixes showed a lack of consistency between batches of the same mix. The air content of the mixes varied between 0.5% and 6.0%, which placed some mixes outside the specified range of 4 ± 2 %. The wide range of air content was attributed to the large amount of HRWR used in the mixes in combination with the air-entraining agent. The combination of an air-entraining agent with large amounts of HRWR can induce excessive paste fluidity and segregation resulting in loss of air. This negative aspect could have been controlled by the use of viscosity modifier agents (VMA) (Ozyildirim and Lane, 2003).

4.5.2 – Placement of SCC Mixes

A 3.0 cy (2.3 m^3) batch was needed to fully fill the section of a single bulb-tee girder. As to compare the effect of vibration on the girders, two batches were produced for every mix, one for a section that was vibrated and the other one for a section that was left without vibration. A Tucker-built truck delivered the concrete from the batching plant to the prestressing bed, less than 100 yards away. The concrete was placed from a single point located 20 in. (510 mm) away from one end of the sections, in between the pick-ups and the closed spaced stirrups. The concrete was then allowed to flow to the opposite end of the girder section, as shown in Figure 4-29.

Figure 4-29. Placement of SCC mixes in BT-72 sections

In general, all mixes flowed well through the reinforcement and reached the opposite end of the girders' section without signs of segregation. However, the pick-up areas were extremely challenging for all mixes to overcome, especially the pick-up hook at the opposite side of the casting point. The clearance between stirrups and the strand bundle of the lifting loops was less than 1 in., which produced blockage of the concrete flow in all girders, especially in mixes 7N and 67N (Figure 4-30). Eventually, the concrete flowed around the loops through the top flange area, and filled the rest of the section.

Figure 4-30. Blockage of the concrete flow at the pick-up strands bundle

After the sections were completely filled, the top surface slope was around 4% for all mixes. The top surface of the concrete was then leveled out with shovels and screeded to finish the top flange of the girders (Figure 4-31).

Figure 4-31. Leveling of top surface of bulb-tee sections

Vibration of the girders was supplied by an external vibrator connected to one side of the forms. The side vibrator was located halfway along the length of the vibrated girders, and was mounted on a rail that ran approximately 4 ft up from the bottom of the sections (Figure 4-32). The vibration was given at a single point of the sections, and was limited to 5 seconds, and was only provided after all concrete was in place. No internal vibration whatsoever was provided to any of the sections.

Figure 4-32. External vibrator on side of the forms

Finally, the girders were cover with a tarp to limit moisture and temperature loss, and steam cured at 150°F (66°C) for 18 hours. The tarp was kept in place until removal of the forms, around 20 hours after placement.

4.5.3 –Forms Removal

Before removal of the forms it was necessary to verify if the concrete had achieved the specified compressive strength at release of 6,000 psi (41 MPa). Six 4x8 in. (100 x 200 mm) control cylinders per mix, except for mix 7N, were placed under the tarp to match curing conditions of the girders. The mean compressive strength of three of the control cylinders was determined for every mix and compared with the specified release strength.

As shown in Table 4-12, all mixes tested were over the specified 6,000 psi 18 hours after placement. Although no data were available for mix 7N, the w/cm ratio of this mix was similar to that of mixes 7BL and 67M, and therefore it was considered safe to remove the forms from all sections.

Table 4-12. Mean compressive strength of steam cured control cylinders 18 hours after casting

Mix	w/cm	Compressive strength, psi [MPa]
7N	0.31	-
7BL	0.32	6,500 [45]
67N	0.30	8,400 [58]
67M	0.32	6,950 [48]

All girder sections were demolded and the continuous strands at the top and bottom flanges were cut with a torch. The sections were lifted out of the prestressing bed and stacked at the SCP plant for two more weeks to allow the concrete to gain strength. After that period they were trucked to the Georgia Tech Structures Laboratory (Figure 4-33).

Figure 4-33. Delivery of SCC girder sections to Georgia Tech Laboratory

4.6 –Testing for Homogeneity of SCC Girders

The concrete girders were tested for uniformity of the mixes considering the three testing methods used for the end-wall panels: surface finish evaluation, compressive strength analysis of core samples, and aggregate distribution estimation of different cross sections. A comparison of the qualitative and quantitative values of these methods was also performed.

4.6.1 – Surface Finish Evaluation

A visual inspection of the surface finish of the girders found that different mixes produced different results. In general, the surface of the girders was not air-void free and bleeding marks traced the position of the interior reinforcement. The top surface of the bottom flange area was not as smooth as the web surface in the majority of the sections (Figure 4-34).

Figure 4-34. Surface finish of the bottom flange area of SCC girdes

In all girders, except mix 7BL (Mix 4), air bubbles as well as bleeding marks were clustered around the areas of heavier reinforcement, particularly the lifting loops and the draped strands. The bleeding marks were thicker and more common at the end of the girders where the SCC was placed (termed near end) (Figure 4-35).

Vibrated and non-vibrated girders presented similar surface finish quality, except mixes 67N and 67Nv (Mix 1 non-vibrated and vibrated, respectively). The surface of girder 67N showed multiple voids which varied in size from 1/8-in. to 1-in. diameter. The bottom flange was particularly affected by these bug holes as seen in Figure 4-36 (a). On the other hand, Mix 67Nv showed a smoother surface, with bleeding lines along the pick-up area (Figure 4-36(b)). In all photos, the spray painted and stenciled specimen designators were placed on the side to which the vibrator was attached and the end where the Tucker-built truck poured the SCC.

(b)

Figure 4-35. Surface finish comparison of SCC girders (a) mix 7N, and (b) mix 7Nv (Mix 1)

(a)

(b)

Figure 4-36. Surface finish comparison of SCC girders (a) mix 67N, and (b) mix 67Nv (Mix 2)

Mixes 67M and 67Mv (Mix 5) showed a particularly poor surface finish. Large voids (honeycombing) and bleeding lines around the area of the draped strands were observed for both girders. These voids were signs of poor consolidation. However, the central area of the web of these girders displayed a smooth, good quality surface finish, as shown for mix 67Mv in Figure 4-37. This difference in the quality of the surface finish within the girders showed that mixes 67M and 67Mv were in essence self-flowing, but with limited ability to flow in the highly congested reinforcement of the BT-72 sections. The quality of the surface finish of the bottom flanges was not as good as in the center of the web, but not as poor as around the draped strands. The appearance of the bottom flanges was no better than that achieved in girders with conventional concrete.

(a) (b)

Figure 4-37. Surface finish comparison of SCC girders (a) mix 67M, and (b) mix 67Mv (Mix 5)

Mixes 7BL and 7BLv (Mix 4) presented similar surface finishes (Figures 4-38 and 4-39). Both girders showed smooth and clean surfaces with minimal presence of air bubbles, especially mix 7BLv. The bottom flanges of these girders looked the best when compared with the rest of the mixes. Although the finish of the bottom flanges was not optimum and completely air-void free, the sizes of the bubbles were small and reduced in number. The quality of the surface finish of the girder using mixes 7BL and 7BLv was superior to that obtained in vibrated girders using conventional concrete.

Figure 4-38. Surface finish of girder using mix 7BL (Mix 4 non-vibrated)

Figure 4-39. Surface finish of girder using mix 7BLv (Mix 4 vibrated)

In a quantitative analysis of the surface finish, 1-ft by 1-ft areas were drawn on the surface of the girders at three locations of the web: top, center and bottom, and a fourth area at the top surface of the bottom flange (Figure 4-40). The top web position was located at the near end of the girders, where the concrete was placed, and over the layers of draped strands. The center area was over the diaphragm pocket and at the mid-length of the girders. The bottom web position was located at the far end, the opposite end to the casting point, and underneath the layers of draped strands. The location at the bottom flange was placed at mid-length and coincided with the strand hold-down position. The location of these points in the web followed the critical path of the concrete. The hold-down position was identified as a potential source of blockage and segregation of the mixes; therefore, the fourth area was located at this point.

The number of air bubbles inside the designated areas was registered and organized by diameter sizes in four groups. The groups were divided in bubbles 1/8-in. ± 1/16, 1/4-in. ± 1/16, 3/8-in. ± 1/16, and larger than 7/16-in. diameter. The smallest size diameter recorded was 1/16 in. and the largest was 1 in.

The results of this analysis were graphed in Figures 4-41 to 4-44. For these charts the y-axis represented the number of bubbles found for a given diameter of the bubbles, represented in the x-axis. Vibrated and non-vibrated girders using the same mix were represented in a single chart. In general, the observed trend for all girders was that the larger the size of the bubbles the fewer the number of occurrences. The higher number of bubbles was found to be 1/8-in. in diameter. The region with the greatest number of air bubbles was the bottom flange location for all girders.

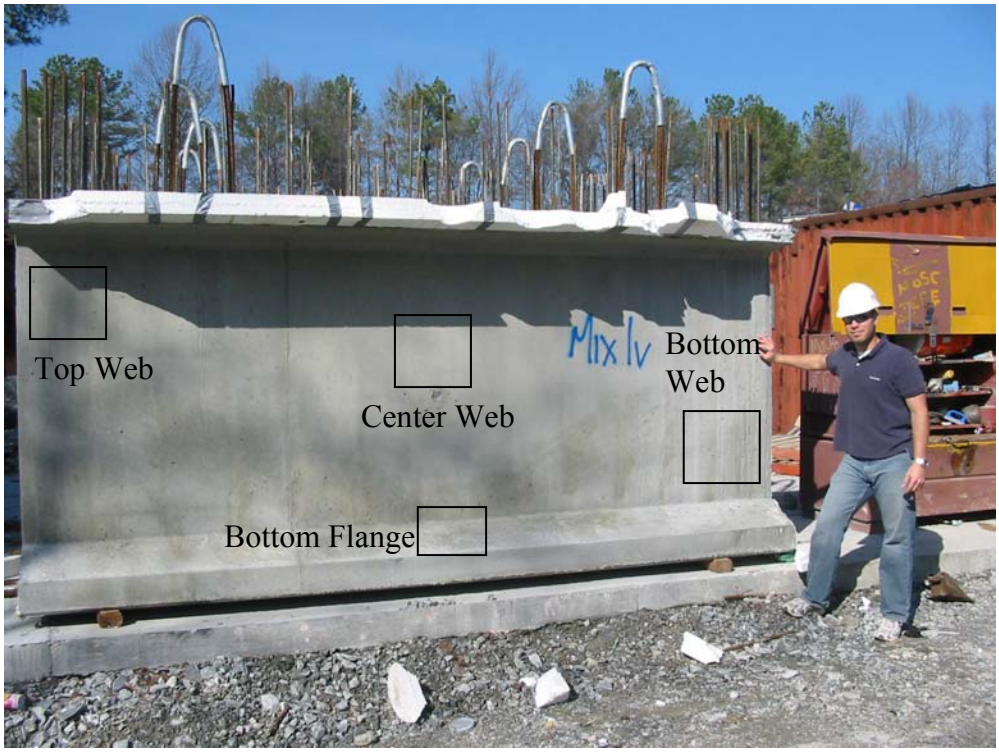

Figure 4-40. Areas for surface-finish study

The center web location was the area with the fewest number of air bubbles for all girders, if compared with end locations. As shown in Figure 4-24, the reinforcement at both ends of the girders was more congested than that at the center of the sections. The tight spacing of the reinforcement along with the boundary effect created by the edges of the girders were the causes for the greater number of air bubbles in these areas.

Although bigger size bubbles had lower occurrences than the small size bubbles, not all mixes displayed this the same way. Mixes 7N and 7BL showed a bigger difference between the number of 1/8-in. and 3/8-in. diameter bubbles (Figure 4-41 and 4-42) than mixes 67N and 67M did (Figure 4-43 and 4-44). The greater presence of large bubbles in mixes 67N and 67M, including 3/8-in. and >7/16-in. diameter, were an indication of poor consolidation of these mixes. The maximum area fraction of air bubbles to surface of the girders for mixes 67N and 67M were 2.11% and 3.41%, respectively, both greater than the 2% maximum of entrapped air required for properly consolidated concrete (Walker, 1992). For mixes 7N and 7BL the maximum air-bubbles to surface ratio were only 0.90% and 0.45%.

The non-vibrated girders displayed a higher number of air-bubble occurrences than the vibrated ones. However, this difference was only significant for mix 67N. Mix 67N performed poorly at the fresh state testing compared with mix 67Nv (Table 4-11); therefore, the difference in surface finish of these two girders could not be attributed solely to the vibration process. For the rest of the mixes the difference between vibrated and non-vibrated girders was minimal and only observed in the 1/8 in. diameter bubbles.

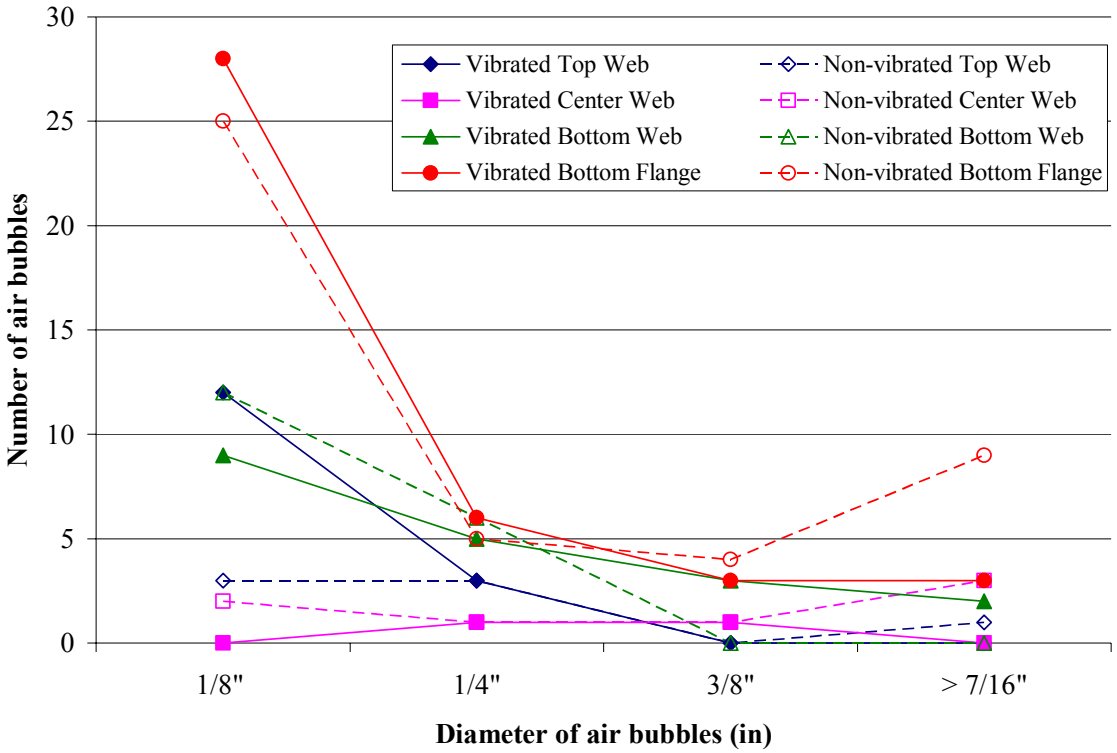

Figure 4-41. Air bubbles in SCC girders. Mixes 7N and 7Nv (Mix 1)

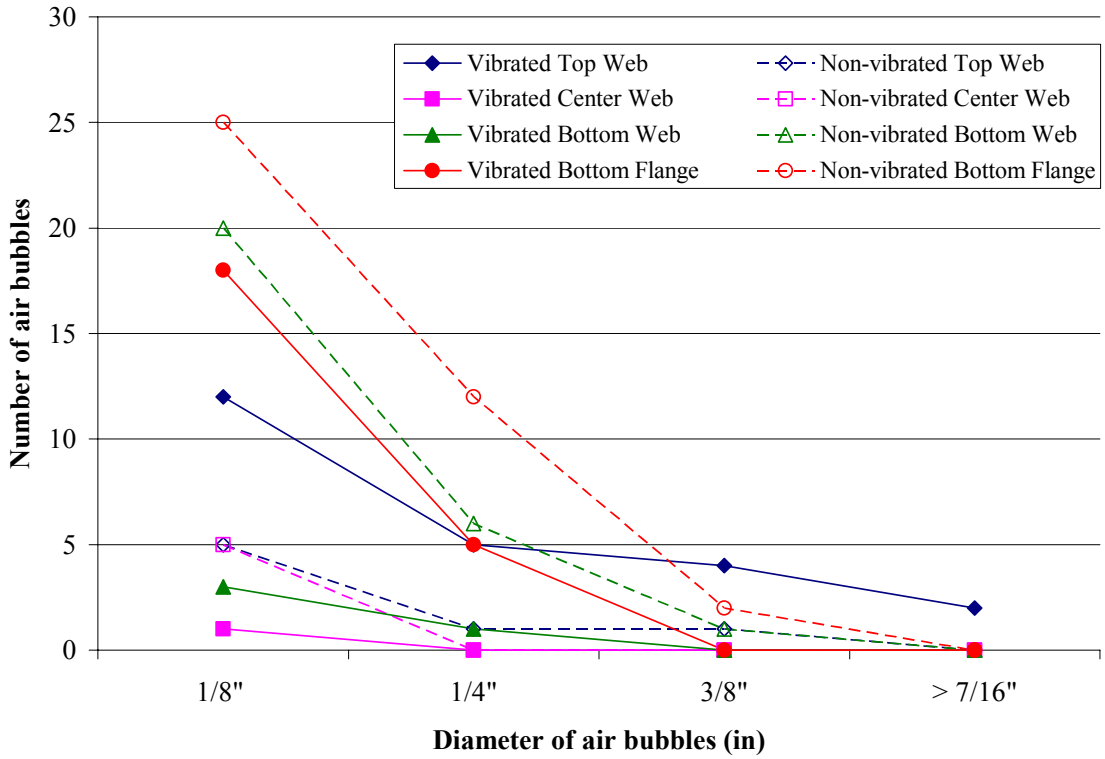

Figure 4-42. Air bubbles in SCC girders. Mixes 7BL and 7BLv (Mix 4)

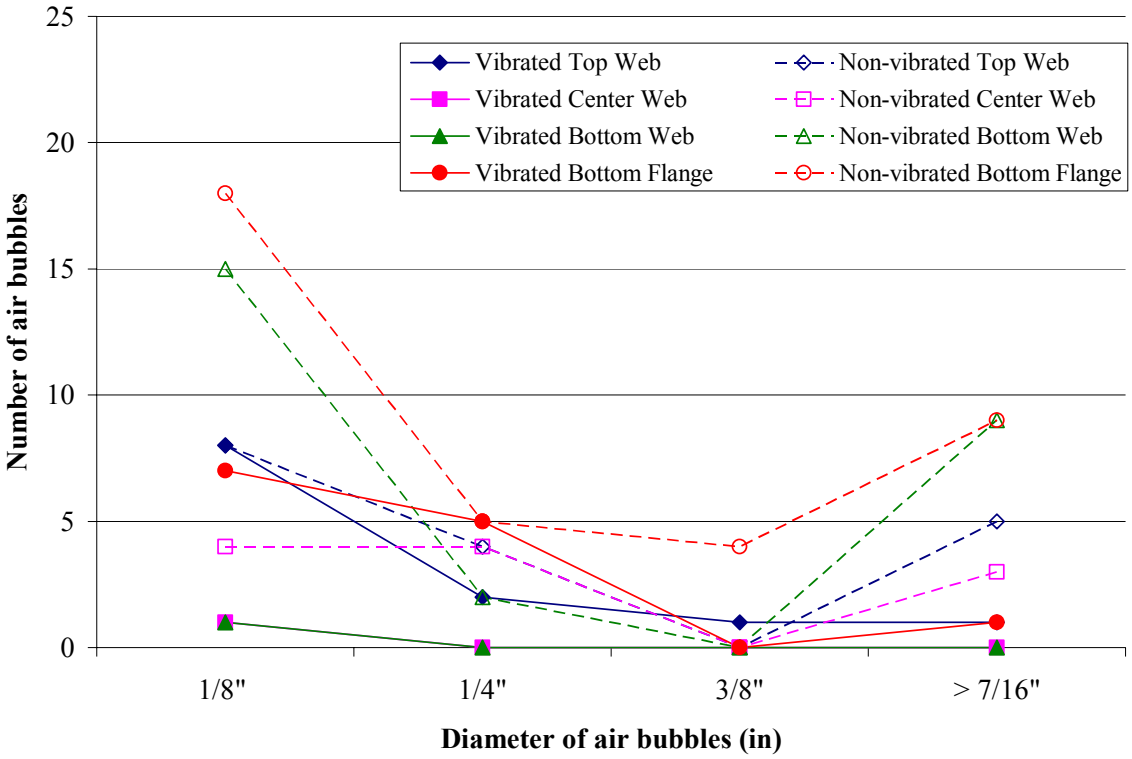

Figure 4-43. Air bubbles in SCC girders. Mixes 67N and 67Nv (Mix 2)

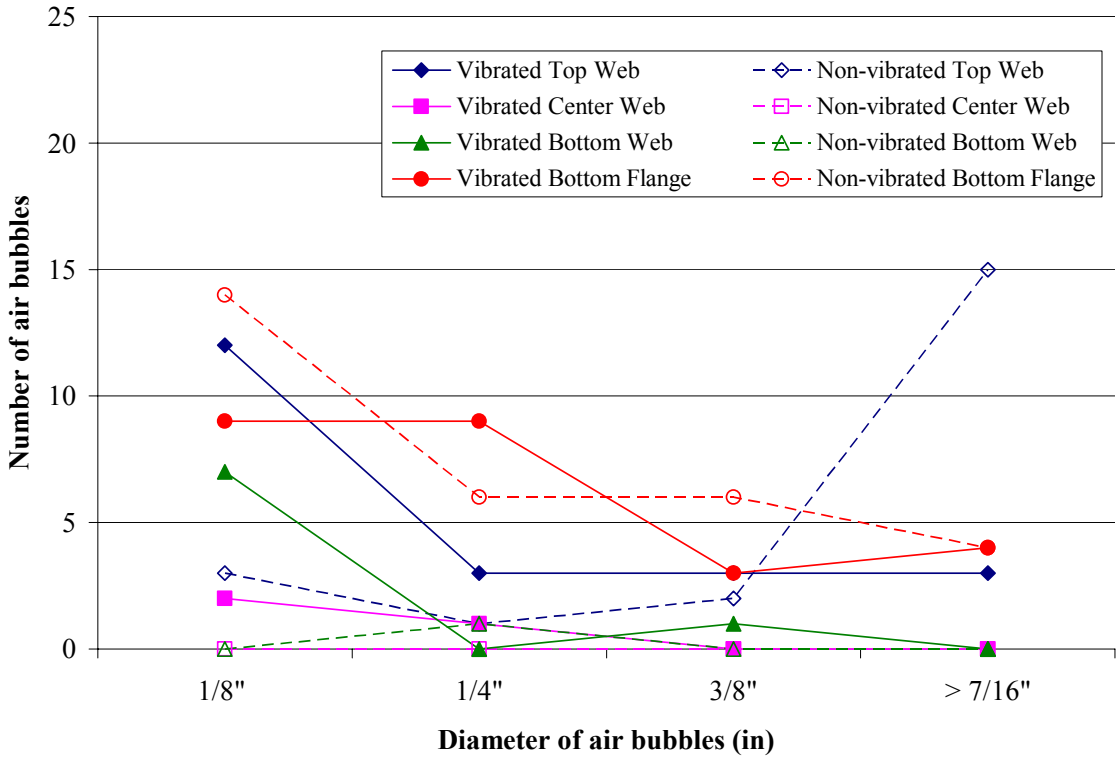

Figure 4-44. Air bubbles in SCC girders. Mixes 67M and 67Mv (Mix 5)

The top surface of the bottom flange area was the location with the largest number of bubble occurrences. Also, this area was particularly prone to create a large number of the bigger size bubbles, including 3/8-in. and >7/16-in. diameter. This was particularly true for mixes 7N and 67N (Figure 4-41 and 4-43). The maximum area fraction of air bubbles to bottom flange surface for mixes 7N and 67N was 2.61% and 2.55%, respectively, both over the required 2% for proper consolidation. The mixes with the lowest area fraction of air bubbles to surface were 7BL and 7BLv with 0.78% and 0.32%, respectively.

In general, the surface finish of the girders was acceptable but not optimum. There was excessive bleeding present in the majority of the mixes, and there were a large number of air bubbles across the surface of the girders, especially on the top surface of the bottom flange. Only in the case of mixes 7BL and 7BLv were the surface finishes superior to those in girders using conventional concrete. The quantitative analysis corroborated the visual inspection conclusion about the quality of the surface finish of the girders, identifying mixes 67N and 67M as the ones with the poorest surface finish quality and 7BL and 7BLv as the ones with the best quality.

4.6.2 – Compressive Strength of Core Samples

Nine 3-in. diameter cores were taken from each girder in order to evaluate the in-place properties of the SCC mixes (Figure 4-45). The cores were taken only from the web; each position characterized the compressive strength of that given area. The number and distribution of the cores were limited by the dimensions of the web, the size of the coring machine, and the distribution of reinforcement in the girders (Figure 4-46). At the near and far ends of the girders, the layout for the draped strands only allowed for cores to be taken closer to the upper region of the web. Therefore, two cores were taken at the top position at both ends of the girders.

Figure 4-45. Coring of SCC girders

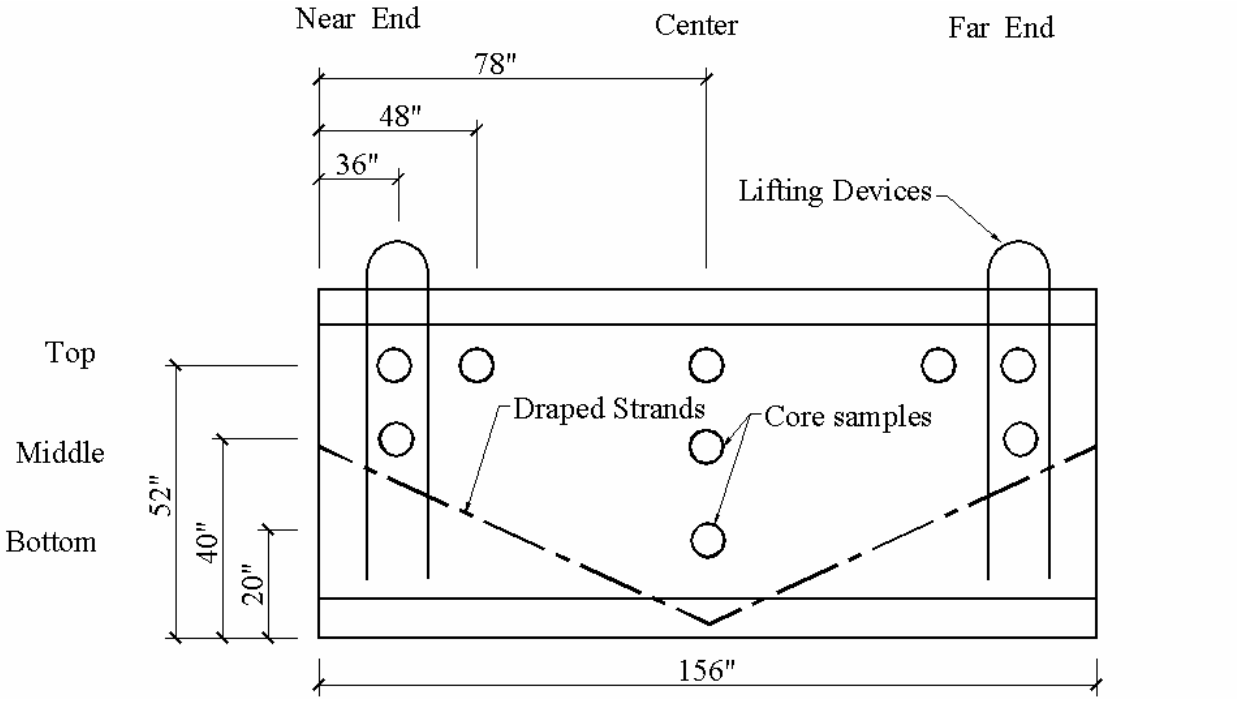

Figure 4-46. Distribution of cores along SCC girders

The surface of the cores mirrored the surface finish of the girders, except for Mix 5 (67M and 67Mv). The large honeycombs found on the surface of girders 67M and 67Mv were not present in the core samples taken from these sections. An examination of the cores' surface revealed multiple air bubbles, particularly for mix 67M, but no honeycombs (Figure 4-47). The lack of large bubbles confirmed the self-consolidating abilities of mixes 67M and 67Mv in areas with lower congestion of the reinforcement.

(a)

(b)

Figure 4-47. Comparison of surface in cores samples (a) mix 67M, and (b) mix 67Mv (Mix 5)

The differences in surface quality previously observed in mixes 67N and 67Nv (Mix 2) were also exposed in the surface of the core samples (Figure 4-48). Cores taken from mix 67N presented a large number of air bubbles well distributed in the core's body, while cores from mix 67Nv showed a smooth bubble-free surface. Mix 67Nv had a w/cm of 0.33 and air content of 3.5% while mix 67N had a w/cm of 0.30 and air content of 6.0%.

(a) (b)

Figure 4-48. Comparison of surface in core samples (a) mix 67N, and (b) mix 67Nv (Mix 2)

The cores were drilled and tested 56 days after casting of the girders. As the web of the girders had a thickness of 6 in., it was not necessary to trim the length of the cores to achieve an L/D of 2. In order to compare the core results with the compressive strength of the control cylinders, the compressive strength values obtained from the cores where reduced by 2% to adjust them for equivalent 4x8 in. cylinder strength (Mehta and Monteiro, 1996). Figure 4-49 shows the core location with the non-adjusted strength of each core sample.

The core samples taken from vibrated girders showed a lower compressive strength than that for cores taken from non-vibrated girders of a given mix. These values corresponded with the w/cm of the mixes, which was in general lower for vibrated girders than for non-vibrated ones.

The coefficient of variation (COV) of the compressive strength of the cores within a given girder varied among the mixes, but all remained below 9.5% indicating a good reproducibility of the test results. The majority of the mixes displayed a COV that range in between 4.6% and 6.4% which was an indicative of uniform distribution of the concrete. Table 4-13 summarizes the mean values and COV obtained for the adjusted compressive strength of all mixes.

Both mixes 67M and 67Mv (Mix 5) showed a low COV of 4.6% and 2.0%, respectively, which contrasted with the results of the surface finish analysis of section 4.6.1. No significant variation in the compressive strength of the cores was observed for mixes 67M and 67Mv due to the fact that the core samples were taken on areas above the draped strands, where no air voids or segregation were observed in the girders.

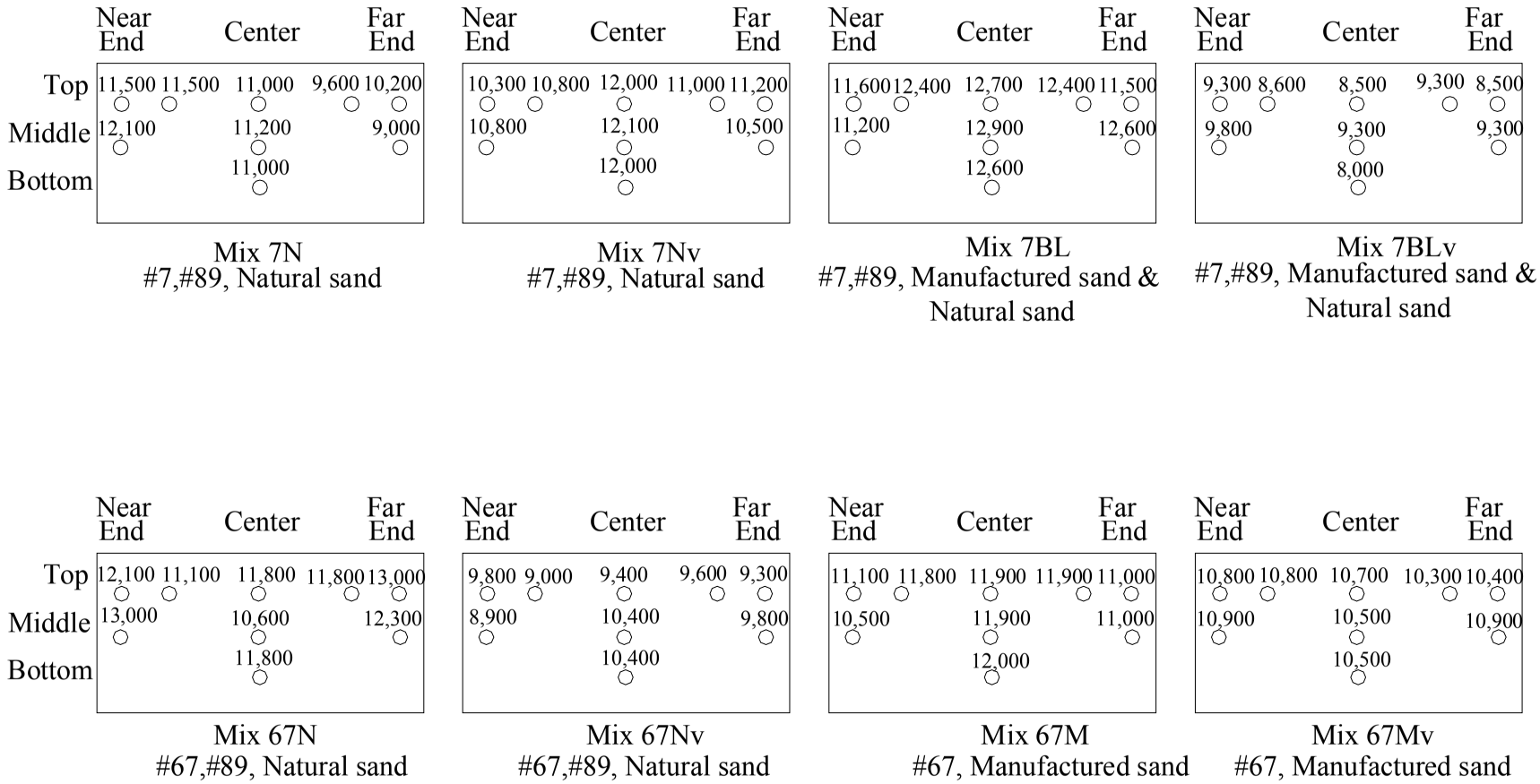

Figure 4-49. Distribution of core compressive strength at 56 days (psi) for SCC BT-72 girders

Table 4-13. Adjusted mean compressive strength of 3 x 6 in. cores at 56 days of SCC girders

Mix	Mean (psi)	COV
7N	10,600	9.4%
7Nv	11,000	6.4%
7BL	12,000	5.2%
7BLv	8,800	6.8%
67N	11,800	6.7%
67Nv	9,500	5.6%
67M	11,200	4.6%
67Mv	10,500	2.0%

No analysis of variance (ANOVA) of the compressive strength of the cores was performed as the number of core samples was too small to achieved statistically significant results. The fact that the w/cm differed for vibrated and non-vibrated girders from a single mix made the comparison of compressive strength between girders inconsequential. Nevertheless, the homogeneity of the mixes was corroborated by the low values of the COV obtained for all mixes.

4.6.3 – Aggregate Distribution throughout Cross Sections

The girders were sawn vertically in order to analyze the distribution of aggregate throughout their cross sections. This study looked for significant differences in the aggregate-to-concrete ratio produced by blockage of the concrete when flowing from the point of casting to the opposite end. Three cuts were made to the girders, two at 24 in. away from each end of the girder, and a third cut at mid-length. The cut closer to the casting point was defined as the “near end” surface; the cut at the opposite end was labeled “far end” surface. The center cut defined the “middle” surface.

After cutting, all sections were labeled and laid out so the surfaces of the cross sections were exposed, facilitating the visual evaluation of the aggregate distribution. For easiness of comparison, all surfaces were grouped by mixes and aligned side by side as shown in Figure 4-50.

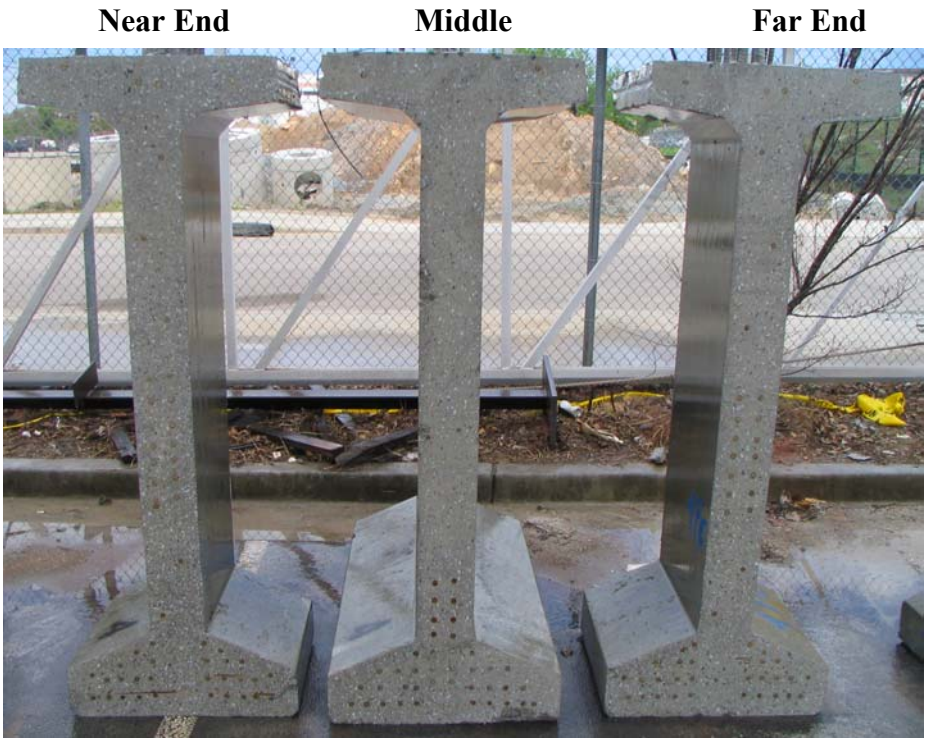

Figure 4-50. Cross sections for aggregate distribution analysis (Mix 7BL)

A visual inspection of the sawn surfaces revealed no significant differences in the aggregate distribution for any of the girders, except mix 67M (Mix 5). No major variations were observed between top and bottom areas of a given cross section (Figure 4-51), nor between near and far end surfaces, as shown in Figure 4-52. Also, no voids were observed around the reinforcement in any of the girders, except mix 67N and 67M, indicating good consolidation of the concrete and that no bleeding occurred.

(a)

(b)

Figure 4-51. Comparison of aggregate distribution within a single surface, far end mix 7N (a) Top flange, and (b) Bottom flange

Figure 4-52. Comparison of aggregate distribution in bottom flange for mix 7BLv. From top to bottom: near end, middle, and far end surfaces

Cross sections of mixes 67N and 67M exhibited a large amount of entrapped air bubbles and water pockets underneath the reinforcement, as shown in Figure 4-53. This confirmed previous observations of core samples and surface finish of these girders. The voids detected around the draped strands indicated bleeding and poor consolidation of concrete around this area.

Mix 67 presented noticeable differences in aggregate distribution throughout the girder. Although no perceptible differences were observed within a given sawn surface, considerable change in the aggregate to concrete ratio was detected when comparing the near end surface with the far end surface. As shown in Figure 4-54, coarse aggregate at the near end surface occupied a large percentage of the area of the bottom flange of the girder, and a similar amount was present at the middle surface of the girders. However, the bottom flange at the far end surface showed a considerable reduction of the area occupied by the aggregate.

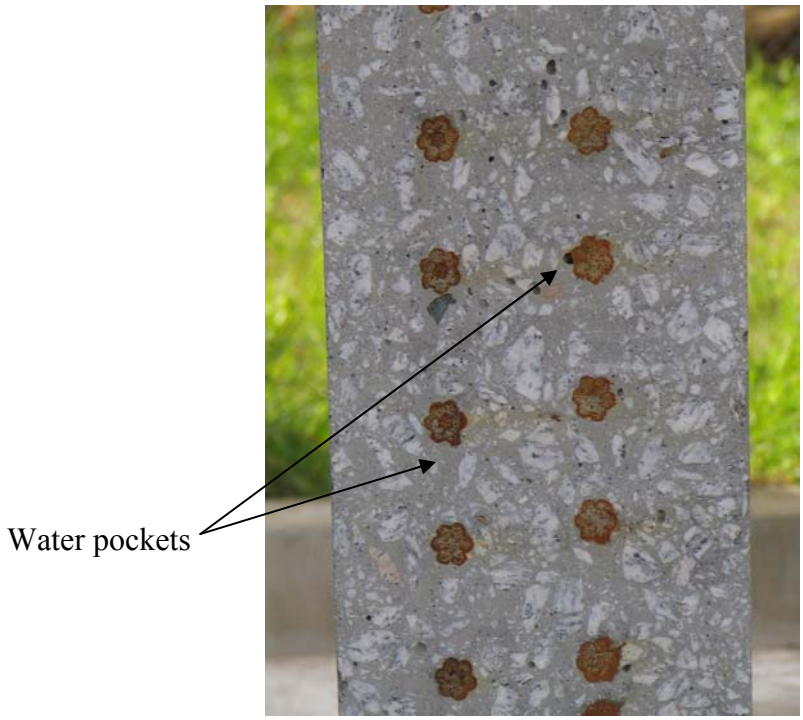

Figure 4-53. Bleeding in near end cross section of girder 67M

Figure 4-54. Comparison of presence of aggregate in bottom flange, mix 67M. From top to bottom: near end, middle, and far end surfaces

Every girder cross-section was divided in five regions, top and bottom flanges, and three 18-in. long regions at the depth of the web. The regions were labeled and studied using the Digital Image Analysis (DIA) method. Figure 4-55 illustrates the results obtained for aggregate distribution from the DIA for every girder. The values found were different for every girder. The mean aggregate percentage of each mix is given in Table 4-14. The theoretical value for the coarse aggregate-to-concrete ratio of the mixes by volume was 32.7%, except for mixes 67N and 67Nv (Mix 2) which was 31.5%. The general trend found with the DIA method was that the greatest differences in percentage of aggregate were between the bottom flange at the near end and the top flange at the far end.

The maximum COV within a girder was 9.4% for mix 67M (Mix 5 not vibrated), which was greater than the required 6% specified in ASTM C94 for uniformity of the concrete. For the rest of the girders, the COV remained around 3.5%, except for mix 7N that showed a COV equal to 6%, yet complying with the ASTM specifications.

Table 4-14. Percentage of coarse aggregate-to-concrete ratios by volume for SCC girders

Mix	Mean	COV	Theoretical
7N	28.3%	6.0%	32.7%
7Nv	30.2%	3.8%	
7BL	31.1%	3.2%	32.7%
7BLv	31.9%	2.2%	
67N	29.2%	3.7%	31.5%
67Nv	29.7%	3.5%	
67M	30.1%	9.4%	32.7%
67Mv	30.6%	3.5%	

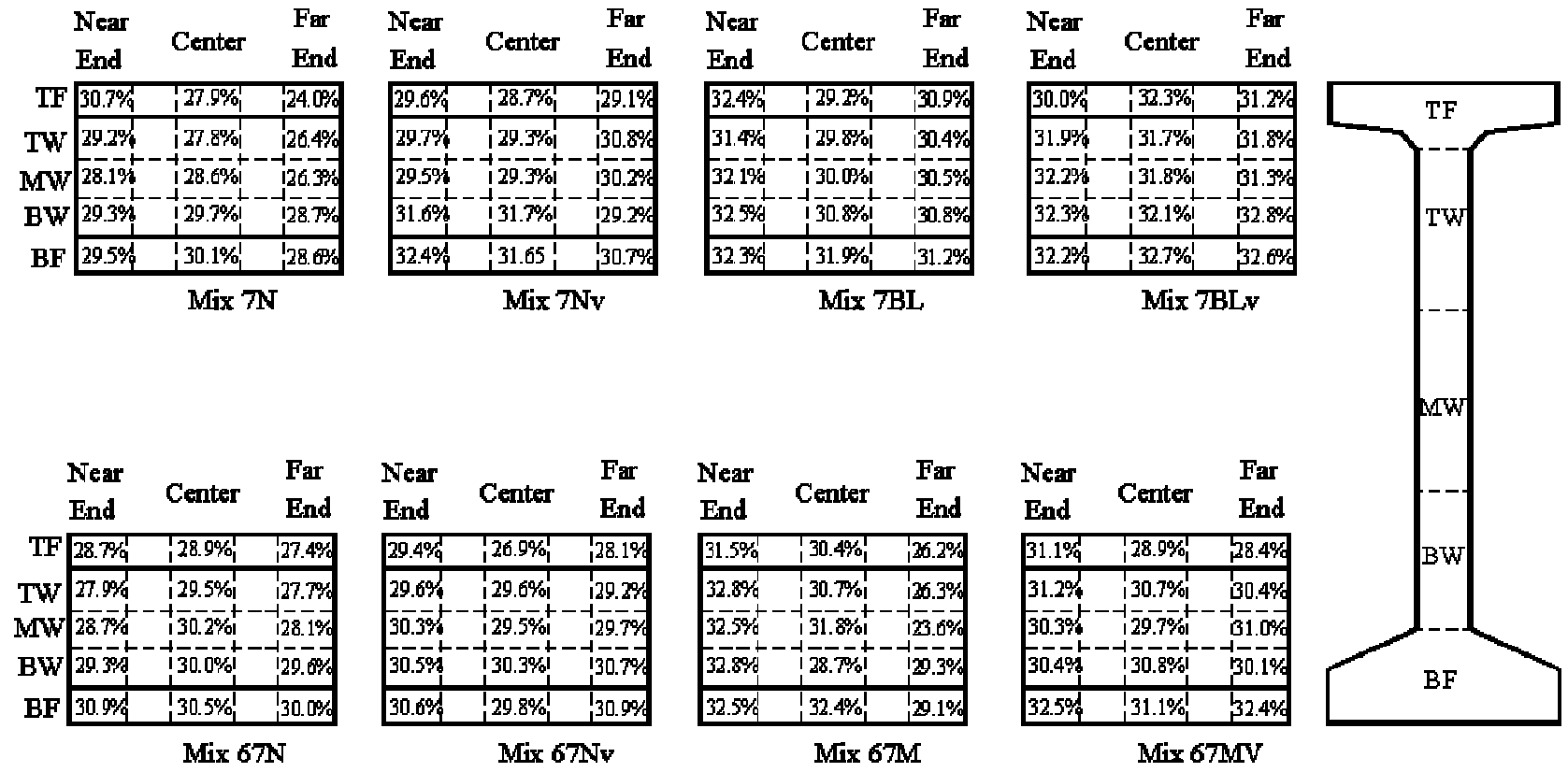

Figure 4-55. Aggregate distribution for SCC girders. Values are aggregate-to-concrete area ratios

Only mixes 7N and 67M had COV values significantly different from those of the vibrated mixes 7Nv and 67Mv, respectively. This difference could not be attributed solely to the vibration process; it was also due to the difference in w/cm between the vibrated and non-vibrated mixes, which varied their respective self-flowing and consolidation abilities.

The results obtained in the DIA corresponded with the visual inspection of the sawn surfaces. No significant aggregate segregation was found in the studied cross-sections, except for those of mixes 67M and 67Mv (Mix 5). For the girders were no segregation was observed, the maximum difference obtained between the theoretical and in-place aggregate percentage was 4.6%, which is about equal to the COV obtained for these girders.

In general, the aggregate-to-concrete ratio was lower at the far end than at the near end. Also, the ratio was lower at the top than at the bottom. These two trends showed that there was some, though slight, aggregate separation as the SCC flowed from near end to far end and as it filled the girder from bottom to top. The difference within a column or level was less than the COV.

4.7 –Mechanical and Material Properties of SCC used in BT-72 Girders

A number of control cylinders were cast during placement of the girder sections (Figure 4-56). The filling of all cylinders was accomplished in two lifts, each of them rodded five times with a standard steel rod, following the same technique as explained in section 3.7. Six control cylinders per mix were kept at the prestressing bed along with the girders and steam cured for 18 hours. The rest of the cylinders were kept under wet

burlap for 24 hours, after which they were transported to the Georgia Tech Structures Laboratory. After stripping the molds, the cylinders were stored in a fog room with constant temperature of 73°F (23°C) and 100% humidity until testing.

Figure 4-56. Preparation of control cylinders at SCP plant

4.7.1 – Compressive Strength of Control Cylinders

Of the batch of steam-cured cylinders, three cylinders per mix were tested for compressive strength after 18 hours to determine if the mixes had achieved their release strength. The rest of the steam-cured cylinders were taken along with the ASTM moist-cured cylinders to the Georgia Tech Laboratory, stored in the fog room, and tested at 28 days.

The compressive strength of the mixes was tested using 4 by 8 in. (100 by 200 mm) cylinders at 1, 3, 7, 28 and 56 days according to ASTM C39 specifications. The average of four cylinders was reported at each time period for every mix. Figure 4-57 shows the mean compressive strength achieved by all mixes used in casting of the girders at different ages.

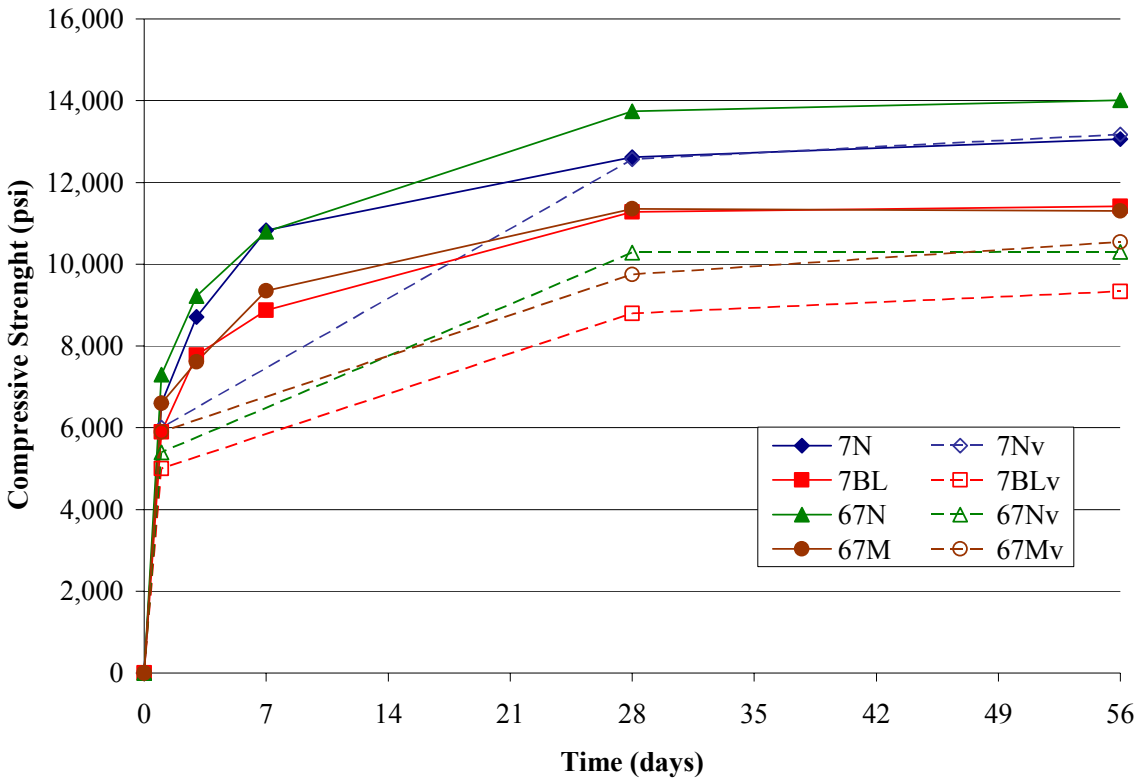

Figure 4-57. Compressive strength of control cylinders for SCC mixes (ASTM cured)

The target compressive strength at 28 days for all SCC mixes was 8,000 psi (55 MPa). All moist-cured SCC mixes developed high strength at early ages; mix 7BLv with the lowest value of compressive strength developed 63% of the target strength after 24 hours. Although some mixes had w/cm over the specified 0.32, like mix 7BLv with a w/cm of 0.34, all mixes surpassed the target strength at 28 days.

Inconsistencies in the moisture content of the aggregates and the air introduced in the mixes produced large variations in the compressive strength of vibrated and non-vibrated mixes. Table 4-15 compares the w/cm and percentage of air of the SCC mixes with their compressive strength at 28 days.

Table 4-15. Influence of the w/cm and air percentage on 28-day compressive strength of SCC mixes

Mix	w/cm	Air (%)	Control cylinders, psi [MPa]
7N	0.31	2.8	12,600 [87]
7Nv	0.32	2.0	12,500 [86]
7BL	0.32	0.5	11,000 [76]
7BLv	0.34	5.5	8,800 [61]
67N	0.30	3.5	13,750 [95]
67Nv	0.33	6.0	10,300 [71]
67M	0.32	1.8	11,350 [78]
67Mv	0.33	4.8	9,700 [67]

Non-vibrated girders had lower w/cm than vibrated girders; and, as a consequence, non-vibrated mixes were in general stronger than the vibrated ones. The greatest difference in compressive strength was observed between mix 67N with a w/cm of 0.30 and mix 67Nv with a w/cm of 0.33, with a 25% decrease in strength. Mixes 7N and 7Nv showed more consistency in their proportions and therefore more uniformity in their strength results, with a variation of only 0.8% of their compressive strength.

The compressive strength at different ages of the steam-cured cylinders was compared with that of the moist-cured cylinders. All steam-cured cylinders exceeded the required compressive strength of 6,000 psi (41 MPa) for release of the prestressed strands

18 hours after placement of the girders, as presented in section 4.5.3. Moist-cured cylinders of the same mix showed a strength between 87% and 95% of the strength achieved by the steam-cured cylinder after 1 day. Testing of moist-cured cylinders 28 days after placement of the girders revealed a similar strength to that of the steam-cured cylinders, as shown in Figure 4-58. Only non-vibrated mixes were included in this study.

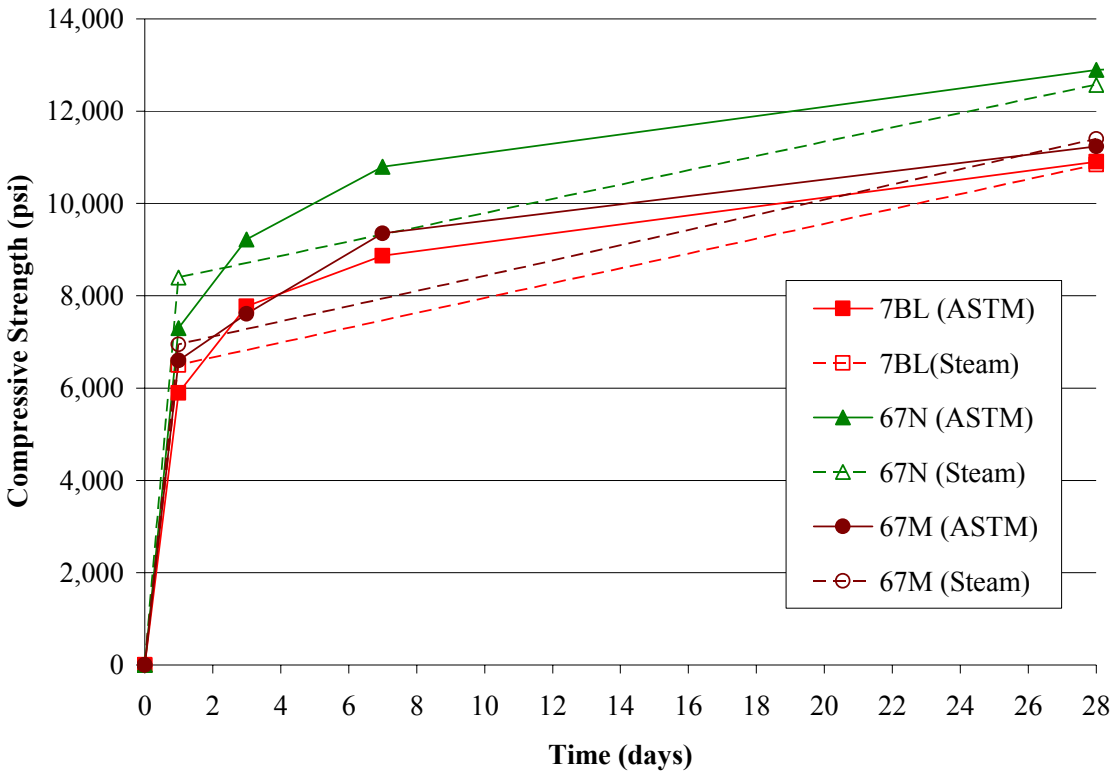

Figure 4-58. Compressive strength comparison between steam-cured and moist-cured control cylinders

The compressive strength of control cylinders was also compared with that obtained from the core samples. No significant differences were observed between the strength of cores and control cylinder, except for mixes 7N, 7Nv and 67N (Table 4-16). For these last three mixes, the cores' adjusted compressive strength were 15% weaker than the control cylinder strengths, indicating a poorer consolidation and curing of the

concrete in the girders than the one achieved by the control cylinders which were cured in the fog room. The compressive strength of core sample from mixes 67M and 67Mv (Mix 5) was very similar to that of their control cylinders. This confirmed that proper consolidation was achieved by this mixes in the upper areas of the girders, where less congested reinforcement was present.

Table 4-16. Comparison of compressive strength at 56 days of control cylinders versus core samples* of SCC girders

Mix	Control cylinders (psi)	3x6 in. cores (psi)	Cores/Control
7N	13,000	10,600	81.5%
7Nv	13,200	11,000	83.3%
7BL	11,400	12,000	105.3%
7BLv	9,300	8,800	94.6%
67N	14,000	11,800	84.3%
67Nv	10,300	9,500	92.2%
67M	11,300	11,200	99.1%
67Mv	10,600	10,500	99.1%

*3x6 in. core strength were adjusted to equivalent 4x8 in. cylinder strength by multiplying the strength by a factor of 0.98

A set of 30 4x8 in. cylinders were tested to determine the required average compressive strength (f_{cr}') for mix 7BL (Mix 4). This mix was selected due to its high stability and excellent self-consolidating abilities. The specified compressive strength for this mix was 8,000 psi (55 MPa) at 28 days, and the required mean strength according to ACI 318 specifications was 8,740 psi (60 MPa). At 28 days the mean compressive strength for mix 7BL was 10,900 psi (75 MPa), with a standard deviation of 554 psi (3.8 MPa) and a COV of 5.0%. Based on this result, mix 7BL satisfied the criteria for a design strength f_c' of 10,180 psi (70 MPa).

4.7.2 –Modulus of Elasticity

The static modulus of elasticity test was performed using three 6 x 12 in. (150 x 300 mm) cylinders at 3 and 28 days, according to ASTM C469 specifications (Figure 4-59). Only non-vibrated mixes were tested. The average value of modulus of elasticity and Poisson ratio found for each SCC mix at each time period is presented in Tables 4-17 and 4-18. Equation 4-1 is given by ACI 318 for the modulus of elasticity for normal weight concrete. Concrete mixes with compressive strength that exceeds 6,000 psi (41 MPa) are considered high-strength concrete. Equation 4-2 is given by ACI Committee 363 as the modulus for high strength concrete.

$$E = 33 * w_c^{1.5} \sqrt{f_c'} \qquad \text{Equation 4-1}$$

$$E = \left(\frac{w_c}{145}\right)^{1.5} * (40{,}000\sqrt{f_c'} + 1 * 10^6) \qquad \text{Equation 4-2}$$

Where

E: Modulus of elasticity (psi);

w_c: unit weight of concrete (lb/ft^3);

f_c': compressive strength of concrete (psi)

Table 4-17. Comparison of modulus of elasticity at 3 days for SCC versus conventional concrete and high strength concrete

Mix	f_c' (psi)	E_{SCC} (ksi)	$E_{ACI\ 318}$ (ksi)	$E_{ACI\ 363}$ (ksi)	$E_{SCC}/E_{ACI\ 318}$	$E_{SCC}/E_{ACI\ 363}$	Poisson (ν)
7N	8,951	4,686	5,393	4,934	86.9%	95.0%	0.26
7BL	7,582	3,581	4,963	4,623	72.2%	77.5%	0.25
67N	9,524	4,293	5,563	5,057	77.2%	84.9%	0.23
67M	7,703	4,242	5,003	4,651	84.8%	91.2%	0.23

Figure 4-59. Modulus of elasticity test set up

At 3 days all mixes displayed similar mean values of modulus of elasticity, independently of their compressive strength. The average value for modulus of elasticity at 3 days for all mixes ranged between 72% and 87% of the value defined by Equation 4-1, and between 77% and 95% of those defined by Equation 4-2. The values predicted by Equation 4-2 were closer to the experimental results; however, considering the few number of tests done, there was a wide scattering of the experimental data. Figure 4-60 illustrates the dispersion of the values of modulus of elasticity for the SCC mixes at 3 days.

The Poisson ratio was also similar for all the SCC mixes, varying from 0.23 to 0.26 at 3 days and from 0.26 to 0.28 at 28 days. These values were higher than those reported for conventional concrete, which range between 0.15 and 0.20.

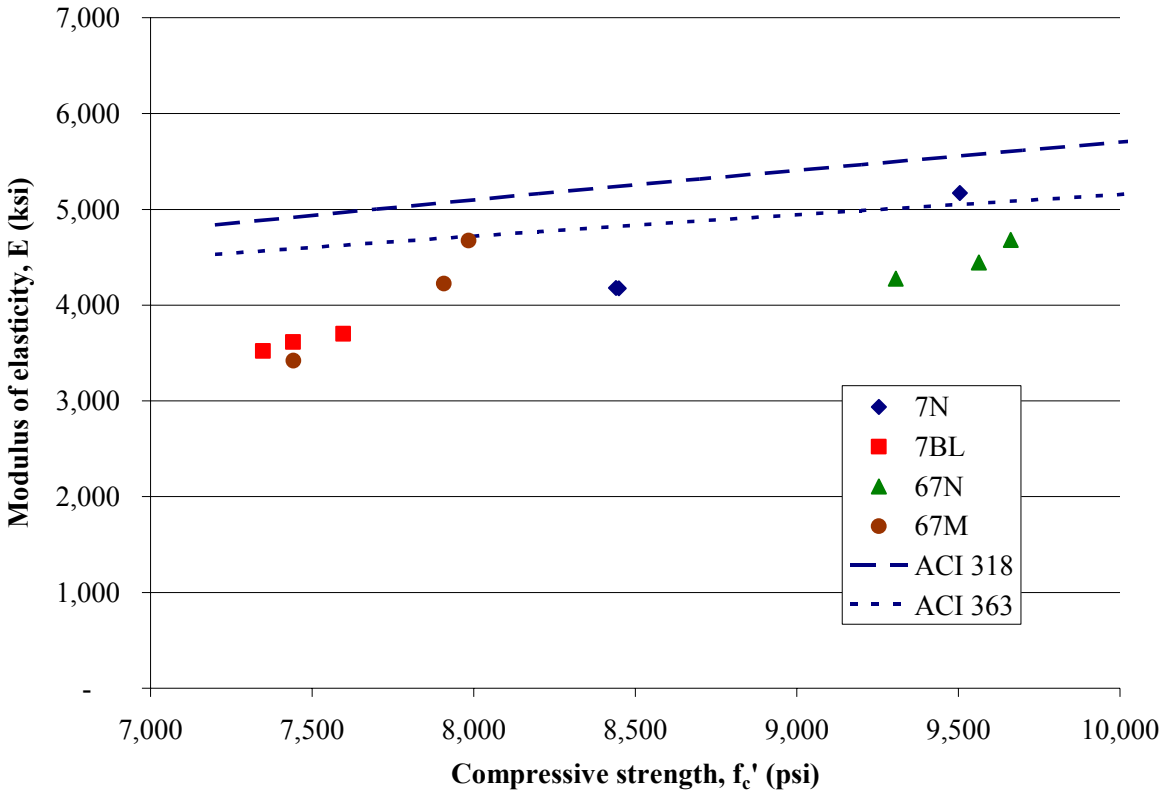

Figure 4-60. Experimental and predicted SCC modulus of elasticity versus 3-day compressive strength

Table 4-18. Comparison of modulus of elasticity at 28 days for SCC versus conventional concrete and high strength concrete

Mix	f_c' (psi)	E_{SCC} (ksi)	$E_{ACI\ 318}$ (ksi)	$E_{ACI\ 363}$ (ksi)	$E_{SCC}/E_{ACI\ 318}$	$E_{SCC}/E_{ACI\ 363}$	Poisson (ν)
7N	12,623	4,901	6,404	5,665	76.5%	86.5%	0.28
7BL	11,280	4,333	6,054	5,412	71.6%	80.1%	0.28
67N	13,742	4,968	6,682	5,867	74.3%	84.7%	0.28
67M	11,352	4,445	6,073	5,426	73.2%	81.9%	0.26

After 28 days all mixes showed an increase in their modulus of elasticity values. For mix 7BL an increase of 21% in modulus of elasticity was registered, yet other mixes like 7N only registered an increase of 4.6%. A direct relationship between the mixes compressive strength and their respective modulus of elasticity was observed at 28 days. Mix 67N with the highest compressive strength displayed the highest modulus of elasticity with 4,968 ksi (34.2 GPa). Mixes with similar w/cm presented similar values of modulus of elasticity. All SCC mixes showed a modulus of elasticity of around 73% of what Equation 4-1 predicted for conventional concrete and 83% of the values given by Equation 4-2 for high strength concrete. Figure 4-61 illustrates a comparison between modulus of elasticity of the experimental data and what is predicted for conventional concrete and high strength concrete.

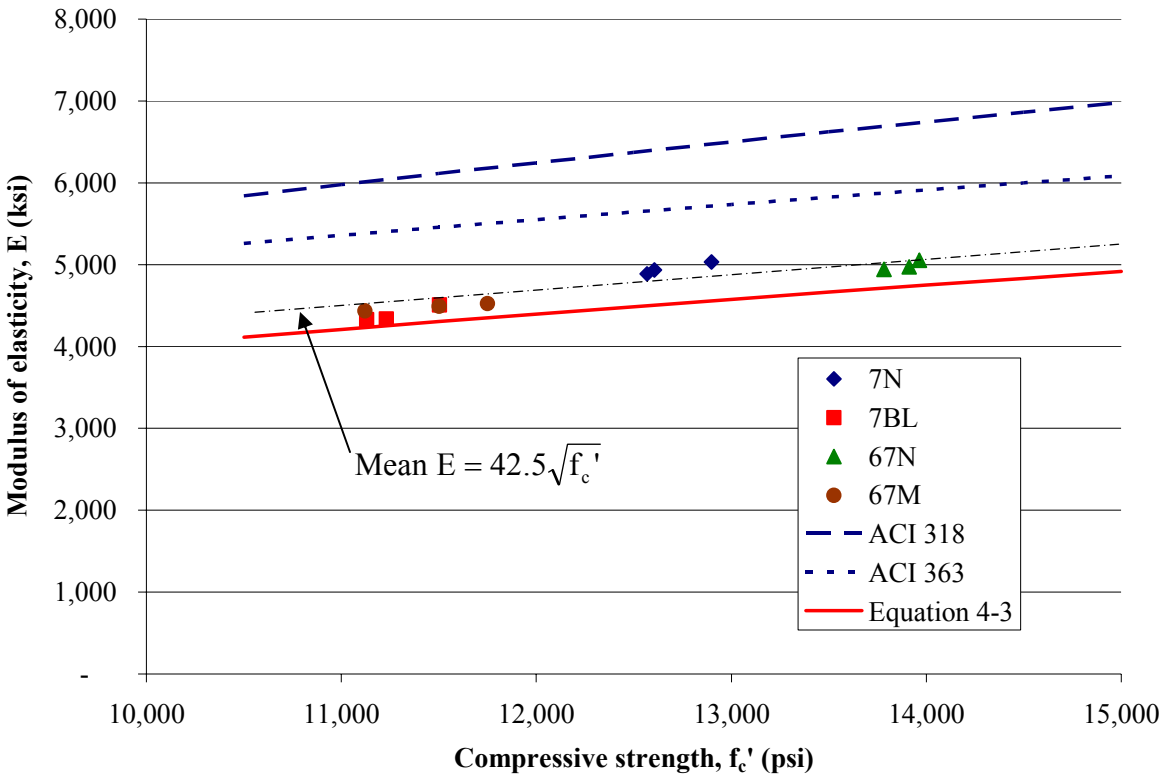

Figure 4-61. Experimental and predicted SCC modulus of elasticity versus 28-day compressive strength

A new expression for modulus of elasticity that better accommodated to the results obtained for the SCC mixes is presented below (Equation 4-3). This expression represented the mean value for modulus of elasticity of the SCC mixes with a 95% confidence limit (p=0.05). The experimental data for this experiment was reduced, and although equation 4-3 was conservative with respect to the values obtained, further investigation is necessary to properly asses the accuracy of these results.

$$E = 40{,}135\sqrt{f_c'} \qquad \text{Equation 4-3}$$

Where

E: Modulus of elasticity for self-consolidating concrete (psi);

f_c': compressive strength of concrete (psi)

4.7.3 – Modulus of Rupture

The standard test for modulus of rupture, ASTM C78; was conducted using 4 x 4 x 16 in. (100 x 100 x 400 mm) model beams. The beams were cured the same way as the control cylinders, covered the first 24 hours in wet burlap and stored afterwards in a fog room under constant temperature and relative humidity until testing. Three specimens per mix were tested at 28 days and the average modulus of rupture was reported. Figure 4-62 shows the typical failure mode for the beams and the test set up used for the SCC specimens.

Figure 4-62. Modulus of rupture test at Georgia Tech laboratory

Table 4-19 summarizes the results obtained for every SCC mix. Only non-vibrated mixes were used in this study. The modulus of rupture found for the SCC mixes were compared with those predicted by the ACI 318 equation for conventional concrete (Equation 4-3). As shown in Table 4-19 all SCC mixes displayed a modulus of rupture around 60% higher than those given by Equation 4-4.

$$f_r = 7.5\sqrt{f_c'} \qquad \text{Equation 4-4}$$

Where

f_r: Modulus of rupture (psi);

f_c': compressive strength of concrete (psi)

Table 4-19. Comparison of Modulus or Rupture of SCC versus conventional concrete

Mix	f_c', psi [Mpa]	$f_{r\ SCC}$, psi [Mpa]	$f_{r\ ACI\ 318}$, psi [Mpa]	$f_{r\ SCC}/f_{r\ ACI\ 318}$
7N	12,623 [87]	1,472 [10.1]	843 [5.8]	175%
7BL	11,028 [76]	1,303 [9.0]	788 [5.4]	165%
67N	13,742 [95]	1,492 [10.3]	879 [6.1]	170%
67M	11,352 [78]	1,286 [8.7]	799 [5.5]	161%

An analysis of the relationship between modulus of rupture and compressive strength of the mixes was performed. Figure 4-63 presents the variation of the modulus of rupture to the square root of compressive strength ratio as a function of the modulus of rupture. A comparison between the experimental data and the expression for conventional concrete was also included.

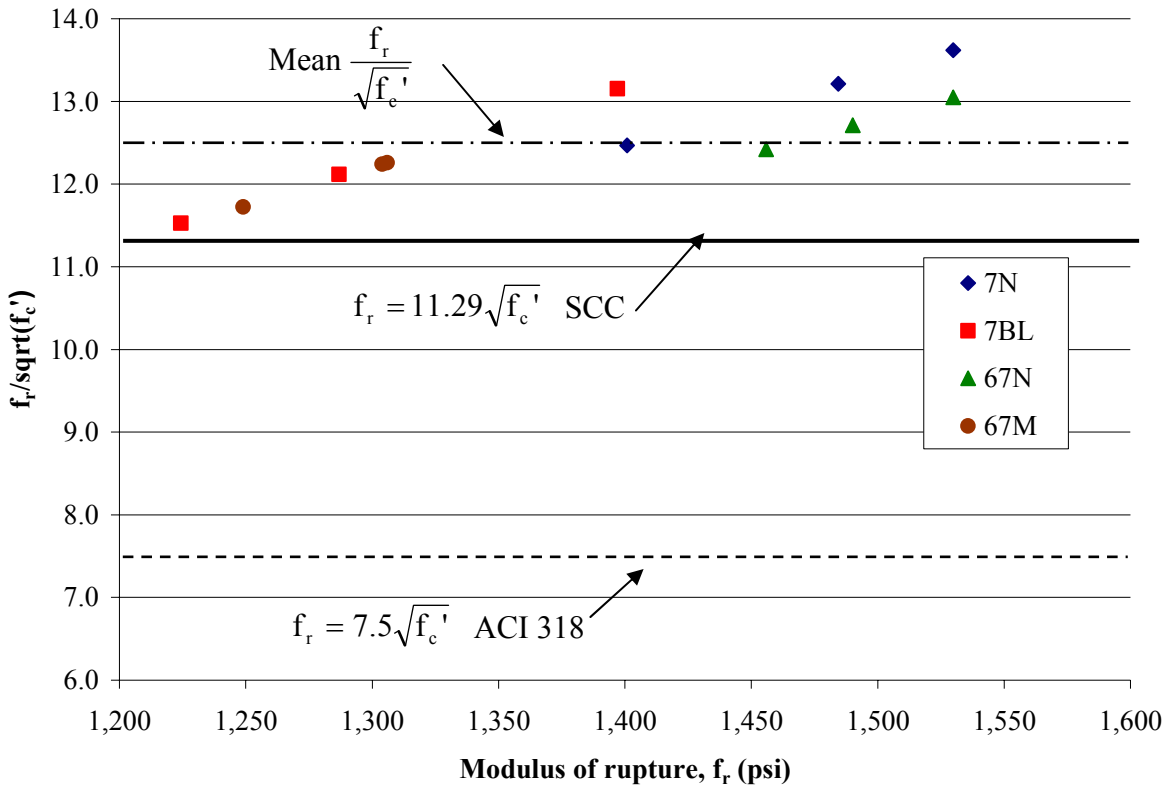

Figure 4-63. Comparison of modulus of rupture to the square root of compressive strength ratio for SCC and conventional concrete

Equation 4-4 underestimated the actual flexural capacity of the concrete for the SCC mixes. A new expression that better accommodates the experimental data is presented in Equation 4-5. This equation was found by calculation of the mean and standard deviation of the experimental modulus of rupture to the square root of compressive strength ratio ($f_r / \sqrt{f_c'}$), and establishing the mean value for the mixes' values with a 95% confidence (p=0.05). The mean value for the $f_r / \sqrt{f_c'}$ ratio was 12.54 psi/psi, with a standard deviation of 0.63 psi/psi and COV of 5%. Given the scattering of the experimental data and the few number of samples used, further research is needed to properly asses the validity of the proposed expression.

$$f_r = 11.29\sqrt{f_c'} \qquad \text{Equation 4-5}$$

Where

f_r: Modulus of rupture for self-consolidating concrete (psi);

f_c': compressive strength of concrete (psi)

CHAPTER 5

LONG-TERM AND DURABILITY PROPERTIES OF SCC MIXTURES

5.1 – Introduction

Long-term properties of self-consolidating concrete are an important concern. The higher paste content of SCC mixtures can potentially increase the concrete's shrinkage and creep compared to normal mixes of the same strength, because it is the paste fraction which is believed to experience the greatest strain, while the aggregate fractions acts to restrain shrinkage and creep (Mehta and Monteiro, 1996). This is particularly important for precast prestressed girders, because excessive deformation by shrinkage and creep contributes to long-term prestress losses. Also, the long-term durability of self-compacting concrete should be considered. Concrete permeability can be used as one measure of potential durability.

This research studied long-term shrinkage and creep of the SCC mixtures used in casting of the wall panels and girder sections discussed in Chapters 3 and 4, respectively. Also, chloride permeability was investigated as an indicator of the SCC's durability.

5.2 – Specimen Preparation

Five 6 x 12 in. (150 x 300 mm) cylinders were cast for every SCC mixture. Three cylinders per mix were tested for creep and the other two were tested for shrinkage of the concrete. Demountable mechanical gage (DEMEC) points were embedded in the specimens at a spacing of 10 in. (254 mm) on opposite side of the cylinders to measure

the long-term deformations. A total of eight DEMEC points were inserted, which allowed for four distinct readings on opposite sides of each cylinder (Figure 5-1).

(a) (b)

Figure 5-1. DEMEC inserts (a) interior of cylinder molds, and (b) DEMEC reader

The cylinders were filled in two lifts, each rodded five times with a standard 3/8-in. diameter steel rod, as described before for casting of the control cylinders. The cylinders were kept under wet burlap at the job site the first 24 hours, after which the molds were stripped and the cylinders were transported to the Georgia Tech Structures Laboratory. All cylinders we,re stored at a fog room with a constant temperature of 73°F (23°C) and 100% relative humidity for 28 days. After this period the cylinders were removed from the fog room, and those selected for creep test were capped to assure a perfect flat surface at both ends of the specimens. All cylinders were then moved to the testing room where they were kept at 50% relative humidity and 73°F (23°C).

Three cylinders of every mixture were mounted in a loading frame to measure creep according to ASTM 512 specifications (Figure 5-2). Two companion cylinders were left besides the loading frames to measure shrinkage of the mixture. The applied stress to the creep specimens was 40% of the compressive strength at 28 days.

Figure 5-2. Cylinders in loading frame for creep test; companion cylinders for shrinkage measurements are on the floor

5.3 –Shrinkage results

The average readings of two 6 x 12 in. cylinders per mixtures were used for measuring shrinkage of the mixtures. Each shrinkage test started 28 days after placement of the concrete and immediately after the cylinders were removed from the fog room. It was assumed that all autogenous shrinkage had already occurred; therefore, drying shrinkage was the only deformation to be measured. Readings for drying shrinkage were

continued for 200 days for the mixtures used in the wall panels. The shrinkage readings reported for the mixes used in the girders account for the first 70 days of testing.

The ACI 209 (1997) committee and AASHTO-LRFD (2004) specifications describe models for drying shrinkage of conventional concrete that define hyperbolic curves that tend to an asymptotic value, which is identified as ultimate shrinkage. The models for drying shrinkage of conventional concrete for both ACI 209 and AASHTO-LRFD follow Equations 5-1.

$$(\varepsilon_{sh})_t = \frac{(t-t_0)^{\alpha}}{f+(t-t_0)^{\alpha}}(\varepsilon_{sh})_u \qquad \text{Equation 5-1}$$

where

t: age of concrete (days)

t_0: age at the beginning of drying (days)

$(\varepsilon_{sh})_t$: shrinkage strain after "t-t_0" days under drying ($\mu\varepsilon$)

α: constant depending on member shape and size

f: constant depending on member shape and size

$(\varepsilon_{sh})_u$: ultimate shrinkage strain ($\mu\varepsilon$)

ACI 209 recommends a value for f of 35 and 55, for 7 days moist curing and 1 to 3 days steam curing, respectively. The typical value recommended for α is 1.0. The value recommended by ACI 209 for average ultimate shrinkage is 780 $\mu\varepsilon$, which is then adjusted depending on the particular conditions of the test by a series of factors (Equation 5-2).

$$(\varepsilon_{sh})_u = 780 \cdot \gamma_\lambda \cdot \gamma_{vs} \cdot \gamma_s \cdot \gamma_\psi \cdot \gamma_c \cdot \gamma_\alpha \qquad \text{Equation 5-2}$$

where

$(\varepsilon_{sh})_u$: ultimate shrinkage strain ($\mu\varepsilon$)

γ_λ: ambient relative humidity factor; $\gamma_\lambda = \begin{cases} 1.40 - 1.0*h \text{ for } 0.40 \le h \le 0.80 \\ 3.00 - 3.0*h \text{ for } h > 0.80 \end{cases}$

h: relative humidity in decimals

γ_{vs}: volume-to-surface factor; $\gamma_{vs} = 1.2 \cdot e^{(-0.12\frac{V}{S})}$

V: specimen volume (in^3)

S: specimen surface area (in^2)

γ_s: slump factor; $\gamma_s = 0.89 + 0.041*s$

s: slump (in.)

γ_ψ: fine aggregate content factor; $\gamma_\psi = \begin{cases} 0.30 + 1.4*\psi \text{ for } \psi \le 0.50 \\ 0.90 + 0.2*\psi \text{ for } \psi > 0.50 \end{cases}$

ψ: fine aggregate-to-total aggregate ratio in decimals

γ_c: cement content factor; $\gamma_c = 0.75 + 0.00036*c$

c: cement content (lb/yd^3)

γ_α: air content factor; $\gamma_\alpha = 0.95 + 0.08*\alpha$

α: air content (%)

The AASHTO-LRFD model uses a different expression for calculating the ultimate drying shrinkage value (Equation 5-3). This is a more general model that only considers the test conditions and does not take into account the specific mix design of a given concrete specimen.

$$(\varepsilon_{sh})_u = K \cdot k_s \cdot k_\lambda \qquad \text{Equation 5-3}$$

where

$(\varepsilon_{sh})_u$: ultimate shrinkage strain (με)

K: ultimate shrinkage base value; $K = \begin{cases} 510\ \mu\varepsilon \text{ for moist curing} \\ 560\ \mu\varepsilon \text{ for steam curing} \end{cases}$

k_s: size factor; $k_s = \left[\frac{(t - t_0)}{\frac{26 \cdot e^{0.36\frac{V}{S}} + (t - t_0)}{(t - t_0)}} \right] \cdot \left[\frac{1064 - 0.94\frac{V}{S}}{923} \right]$

$45 + (t - t_0)$

t: age of concrete (days)

t_0: age at the beginning of drying (days)

V: specimen volume (in^3)

S: specimen surface area (in^2)

k_λ: ambient relative humidity factor; $k_\lambda = \begin{cases} 2.00 - 1.43 * h \text{ for } h < 0.80 \\ 4.29 - 4.29 * h \text{ for } h \geq 0.80 \end{cases}$

h: relative humidity in decimals

Table 5-1 summarizes the predicted values for ultimate drying shrinkage using both ACI and ASSHTO models for the SCC mixes tested. Mix design parameters used in calculation of the ultimate drying shrinkage, including cementitious content, air content, and fine aggregate-to-total aggregate (FA/TA) ratio are also included. Equation 5-2 gave more conservative values for ultimate drying shrinkage than those predicted by Equation 5-3, as seen in Table 5-1.

Table 5-1. Ultimate drying shrinkage for SCC mixes predicted by ACI 209 (1997) and AASHTO-LRFD (2004) models

Structure	Mix	w/cm	CM (lb/yd^3)	Air Content (%)	FA/TA	$(\varepsilon_{sh})_u$ (με)	
						ACI 209	AASHTO-LRFD
Wall panels	S-Slag/Ash	0.30	1010	1.5	0.389	975	659
	G-Slag	0.37	955	0.5	0.458	959	
	Tindall	0.38	750	1.0	0.477	926	
Girders	7N	0.31	946	2.8	0.455	1,162	659
	7BL	0.32	939	0.5	0.478	1,011	
	67M	0.32	923	1.8	0.485	1,123	

The values obtained for drying shrinkage for both the SCC mixes used in the wall panels and girder sections are presented in Figures 5-3 and 5-4, respectively. The G-Slag mix showed the highest drying shrinkage value with 495 με after 200 days. Both S-Slag/Ash mix and the Tindall mix reported 30% less drying shrinkage than the G-Slag mix, with a final value of about 350 με, as seen in Figure 5-3. Both mixes 67M and 7BL showed similar drying shrinkage values at 70 days of 245 με. Mix 7N displayed a lower value than those of mixes 67M and 7BL, achieving 157 με (Figure 5-4). In all cases, the reported drying shrinkage was directly related to the percentage of water and paste content of the mixes (Table 5-2). Those mixes with similar water content displayed similar shrinkage strain independent of their w/cm, as in the case of S-Slag/Ash mix and the Tindall mix, both with about 18% water content. Mix G-Slag with 20% water content, the largest water content, and also displayed the largest shrinkage strains. As for the mixes used in the girder section, they all had similar water and paste contents, and all showed similar values for drying shrinkage considering the early stage of the test at which these values were reported.

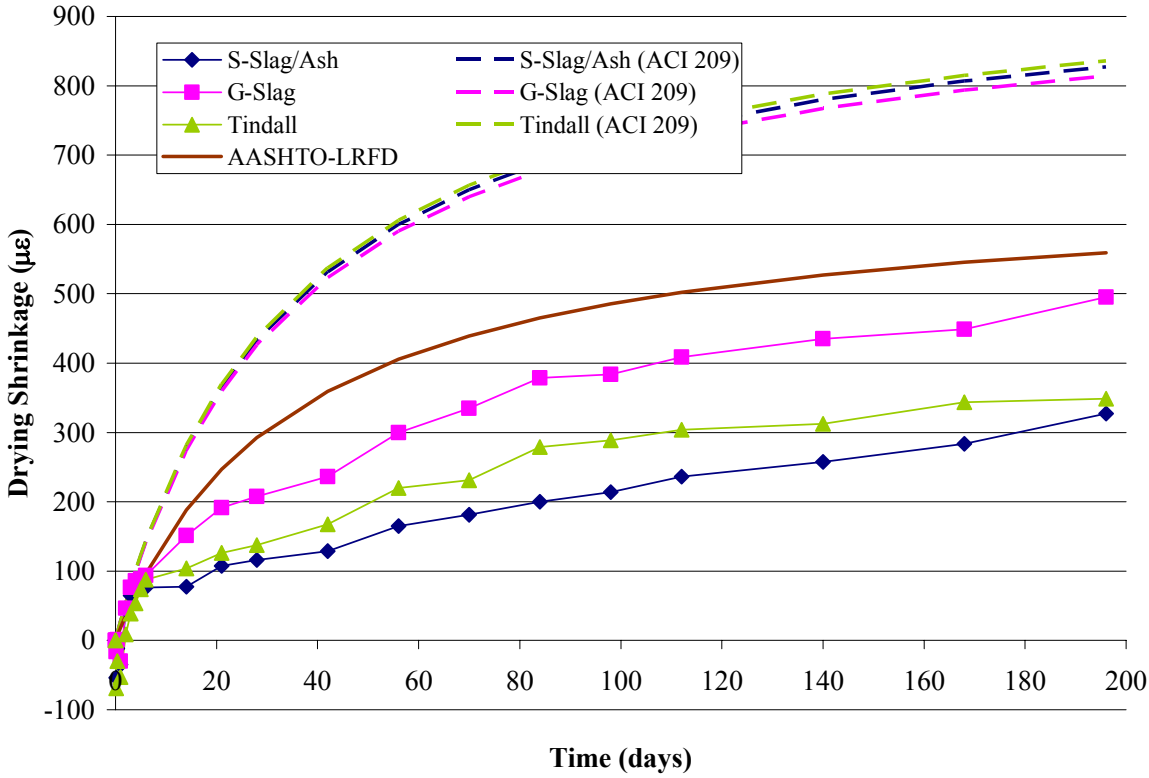

Figure 5-3. Predicted and measured drying shrinkage of SCC mixes used in wall panels

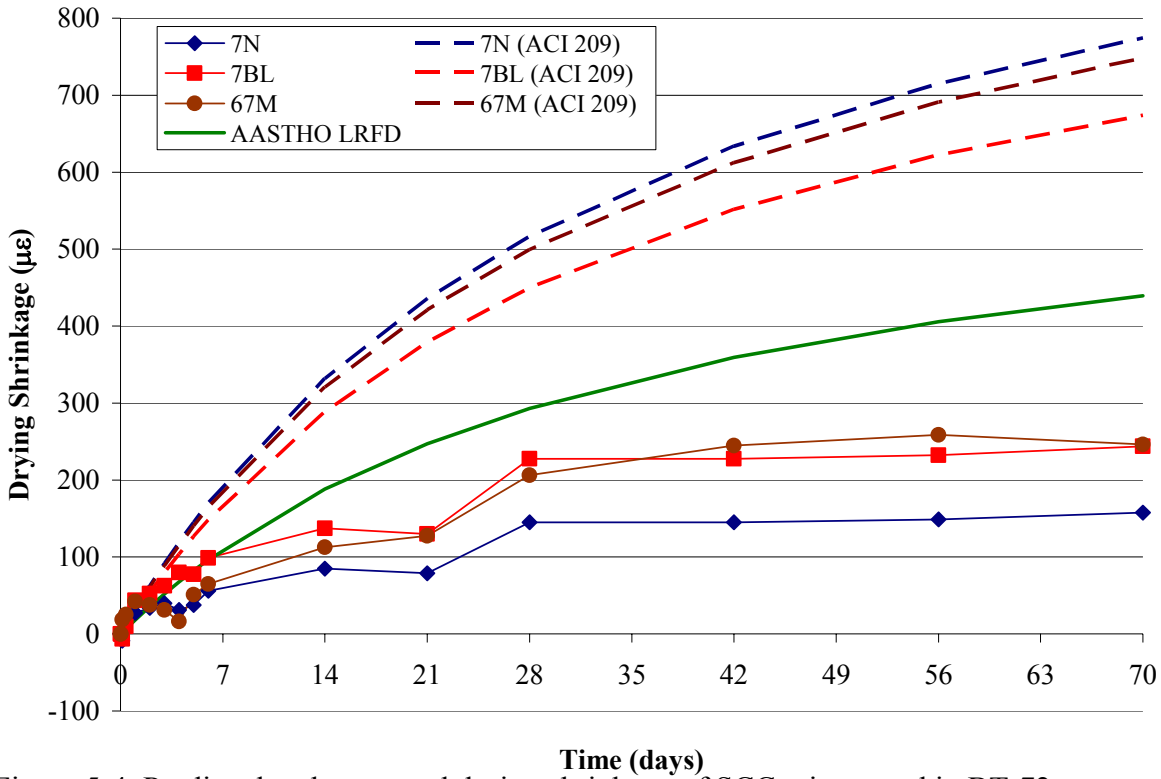

Figure 5-4. Predicted and measured drying shrinkage of SCC mixes used in BT-72 girders

Table 5-2. Paste and water content by volume in mix design of SCC mixes tested for drying shrinkage

Structure	Mix	w/cm	Paste Content (%)	Water Content (%)
Wall panels	S-Slag/Ash	0.30	38.3	18.2
	G-Slag	0.37	39.2	20.8
	Tindall	0.38	32.1	17.6
Girders	7N	0.31	36.0	17.6
	7BL	0.32	36.3	18.1
	67M	0.32	35.3	17.5

The drying shrinkage strains of the mixes used in the walls in general were greater than the shrinkage in the girder sections at 70 days of testing. The SCC mixes used in the walls had strains between 190 με and 330 με, while the mixes used in the girders showed values between 160 με and 250 με. This difference in shrinkage strain seemed to be related to the paste content of the SCC mixes. The walls averaged about 38% paste content compared with the 36% paste content for the girders mixes.

After 28 days of testing the mixtures used in the girder sections showed a plateau in their respective deformations, which inferred no significant difference between the shrinkage at 70 days and ultimate shrinkage of the mixes. The same plateau was observed in the mixes used in the wall panels after 80 days of testing. Turcry et al., (2002) reported similar plateaus for SCC mixes with a decrease in the drying rate after 20 days and almost constant shrinkage after 60 days of testing.

The long-term drying shrinkage curves predicted by ACI 209 and AASHTO-LRFD for conventional concrete were also included in the charts. All SCC mixes showed drying shrinkage deformations lower than those predicted by models for conventional concrete. The ACI model differed with the actual measurements of drying shrinkage in

SCC mixes, giving values up to 2 times greater than those observed in the SCC mixes used in the walls after 200 days, and 3 times greater than the drying shrinkage values measured in the mixes used in the girder sections after 70 days of testing. The ASSHTO-LRFD model predicted values about 50% greater than those measured after 200 days in the SCC mixes of the wall panel. In the case of the SCC mixes used in the girder sections, the AASHTO-LRFD model predicted values of drying shrinkage 75% greater than those measured after 70 days in the SCC specimens.

5.4 – Creep results

Creep was measured for all three mixes used for casting of the wall panels (Chapter 3), and three selected mixes from those used in the girder sections (Chapter 4). Mixture S-Slag/Ash with a w/cm of 0.30 had a compressive strength of 10,641 psi (73 MPa) at 28 days; G-Slag mix with a w/cm of 0.37 had a compressive strength of 8,294 psi (57 MPa); and the Tindall mix with a w/cm of 0.38 had compressive strength of 8,313 psi (57 MPa). The mixes selected from the girder sections had w/cm ranging from o.31 to 0.32. Mix 7N had a higher compressive strength at 28 days of 12,620 psi (87 MPa) compared with mix 7BL with 11,280 psi (78 MPa) and 67M with 11,350 psi (78 MPa). All specimens were loaded at 40% of the compressive strength at 28 days of each mix. Table 5-3 summarizes the compressive strength at 28 days and loading stresses applied to the mixtures in the creep test.

Table 5-3. Stresses applied in creep test for SCC mixes

Structure	Mix	w/cm	Compressive Strength at 28 days, psi [MPa]	Stress applied in Creep test, psi [MPa]
Wall panels	S-Slag/Fly	0.30	10,641 [73]	4,256 [29]
	G-Slag	0.37	8,294 [57]	3,318 [23]
	Tindall	0.38	8,313 [57]	3,325 [23]
Girders	7N	0.31	12,620 [87]	5,048 [35]
	7BL	0.32	11,280 [78]	4,512 [31]
	67M	0.32	11,350 [78]	4,540 [31]

Four DEMEC readings were performed for each cylinder, and the average creep deformation obtained from three cylinders per mixture was reported. The direct reading taken from the cylinders were reported as total creep. Creep of the SCC mixes was determined by subtracting drying shrinkage strain from the total strain measured. The creep coefficient, which is the creep strain divided by initial elastic strain, and specific creep, which is the creep strain divided by the applied stress, were also reported. All creep readings for the mixes used in the walls were continued for 200 days. The creep readings reported for the mixes used in the girder sections account for the first 70 days of testing.

Figures 5-5 and 5-6 illustrates the total creep measured for the wall mixes and the BT-72 girder section mixes, respectively. In general, the total creep strains developed by the wall mixes was lower than those of the girder mixes at 70 days of testing. The SCC mixes used in the walls showed a total creep of about 1,300 με after 70 days, while the mixes used in the girders had creep in range of about 1,400 με and 1,650 με. After 200 days all the mixes used in the walls showed similar creep strains around 1,600 με.

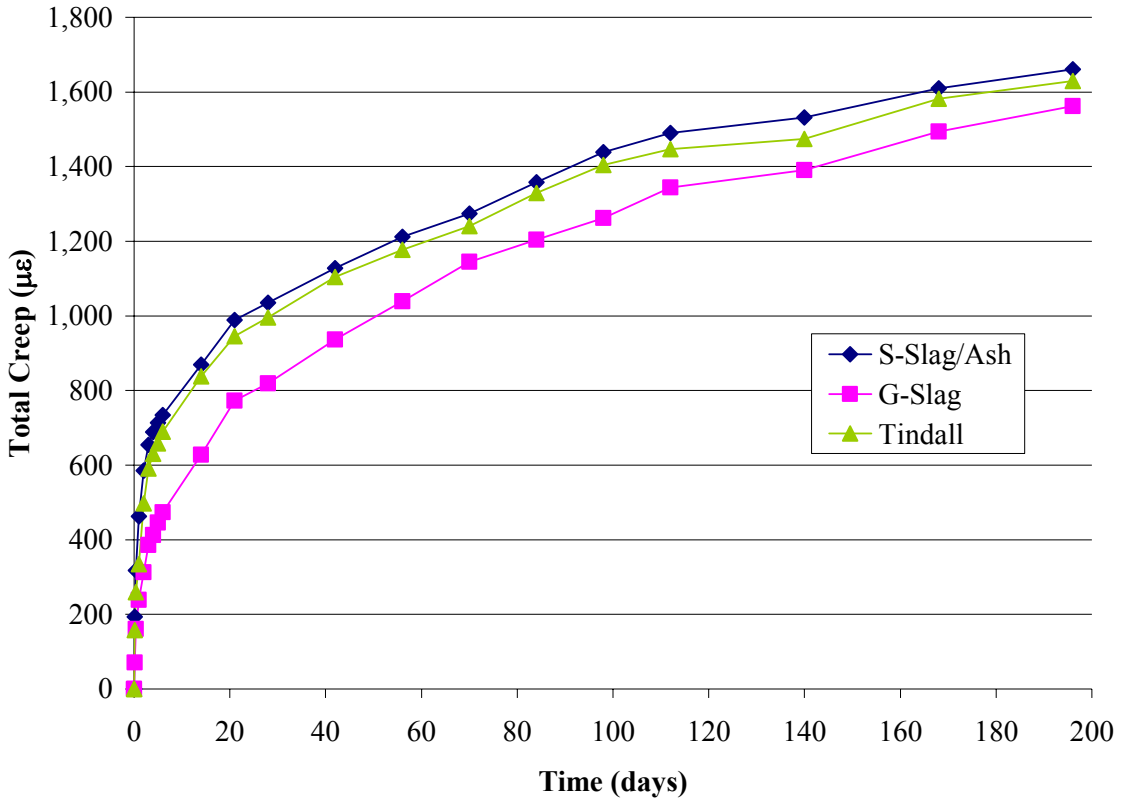

Figure 5-5. Total creep of SCC mixes used in the wall panels

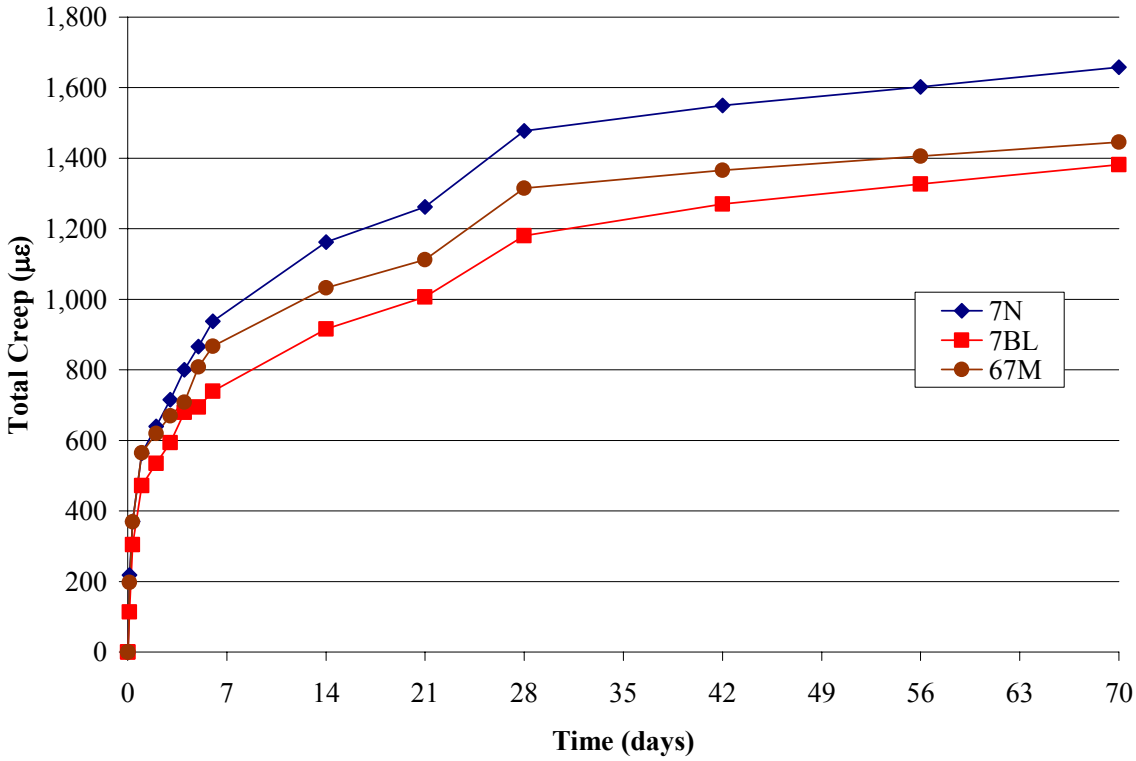

Figure 5-6. Total creep of SCC mixes used in the BT-72 girder sections

The creep strain of the mixes is shown in Figures 5-7 and 5-8. The values presented here were calculated based on the total creep minus the drying shrinkage of the mixes. In general, the creep observed in each of the SCC mixes was proportional to the corresponding applied stress. The mixes with a higher compressive strength at 28 days displayed larger creep values (Table 5-3). Mix S-Slag/Ash showed the largest creep at 200 days of the mixes used in the walls with 1,333 με, while mix G-Slag showed the lowest value with 1,068 με. For the mixes used in the girder sections, mix 7N showed the greatest creep at 70 days with 1,500 με, while mix 7BL displayed the lowest value with 1,138 με. The creep values found in the mixes used in the BT-72 girder sections were higher after 70 days than those reported by the wall mixes, due to the higher stresses applied to the girder mixes.

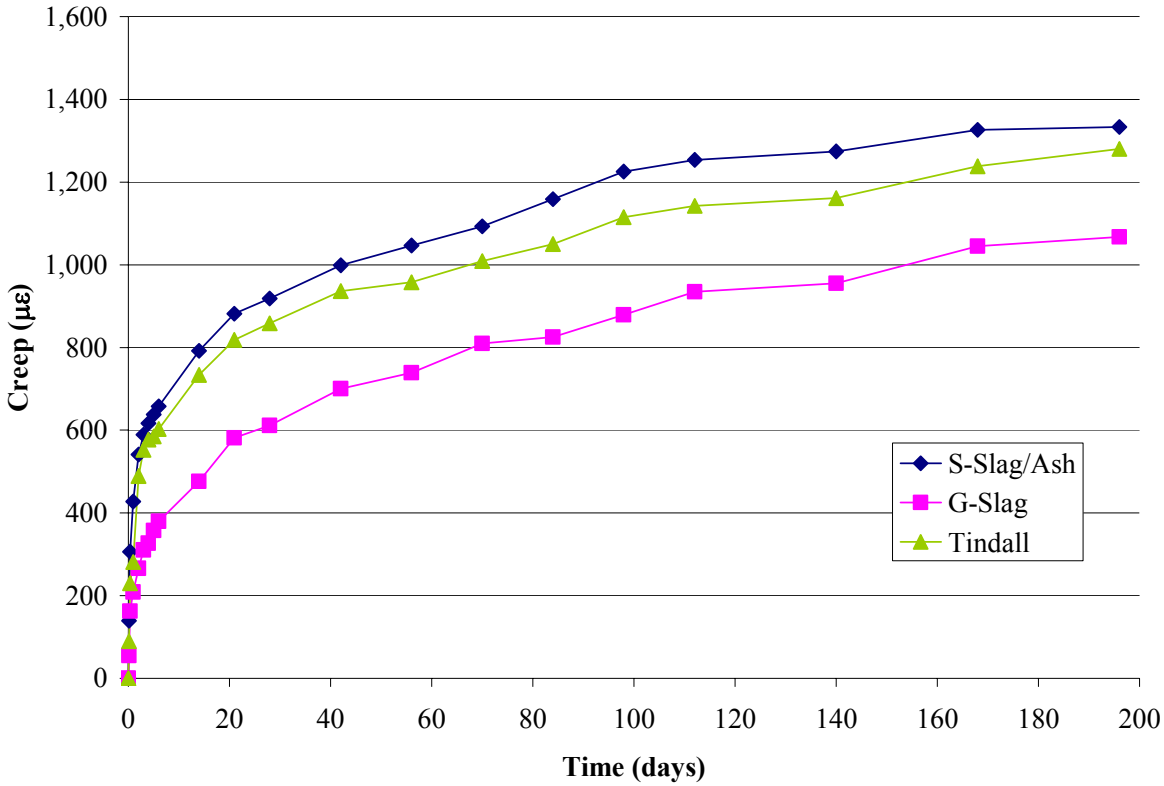

Figure 5-7. Creep strain of SCC mixes used in the wall panels

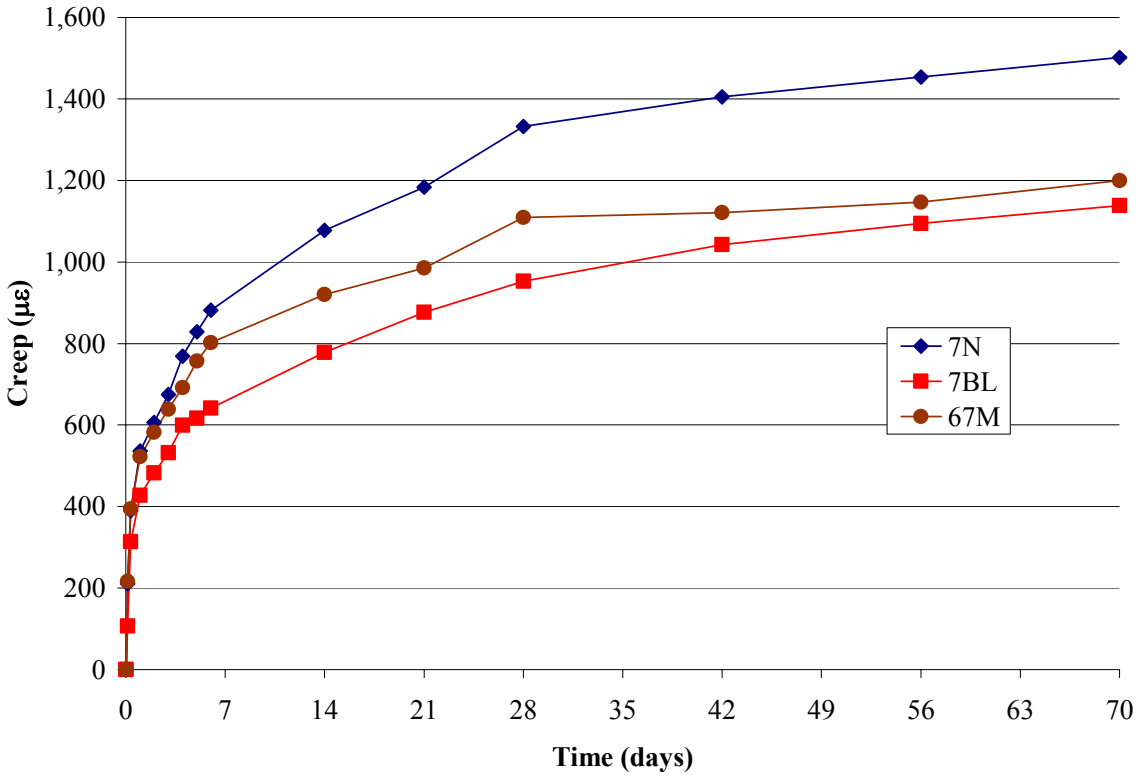

Figure 5-8. Creep strain of SCC mixes used in the BT-72 girder sections

The creep coefficient and specific creep of the SCC mixes of both the walls and girder sections were compared with the respective models given by ACI 209 and AASHTO-LRFD for conventional concrete mixes. These models were based on curing conditions, age at application of load, mix design, ambient temperature, and humidity of the samples. The predicted parameter of these models is not creep strain but creep coefficient, so that the value is not dependant on the applied stress. Equation 5-4 presents the general expression used by both ACI 209 and AASHTO-LRFD models for creep coefficient.

$$\phi_t = \frac{(t-t')^{\psi}}{d+(t-t')^{\psi}} \cdot \phi_u \qquad \text{Equation 5-4}$$

where

t: age of concrete (days)

t': age of concrete at loading (days)

ϕ_t: creep coefficient at age "t" loaded at t'

ψ: constant depending on member shape and size

d: constant depending on member shape and size

ϕ_u: ultimate creep coefficient

ACI 209 recommends values of 0.6 and 10 for ψ and d, respectively. The value recommended by ACI 209 for average ultimate creep coefficient is 2.35, which is then adjusted depending on the particular conditions of the test by a series of factors (Equation 5-5).

$$\phi_u = 2.35 \cdot \gamma_{la} \cdot \gamma_{\lambda} \cdot \gamma_{vs} \cdot \gamma_s \cdot \gamma_{\psi} \cdot \gamma_{\alpha} \qquad \text{Equation 5-5}$$

where

ϕ_u: ultimate creep coefficient

γ_{la}: age at loading factor; $\gamma_{\lambda} = \begin{cases} 1.25*t'^{-0.118} & \text{for moist curing} \\ 113*t'^{-0.094} & \text{for steam curing} \end{cases}$

t': age of concrete at loading (days)

γ_{λ}: ambient relative humidity factor; $\gamma_{\lambda} = \begin{cases} 1.27 - 0.67*h & \text{for } h \geq 0.40 \\ 1.00 & \text{otherwise} \end{cases}$

h: relative humidity in decimals

γ_{vs}: volume-to-surface factor; $\gamma_{vs} = \frac{2}{3}\left[1 + 1.13 \cdot e^{(-0.54\frac{V}{S})}\right]$

V: specimen volume (in^3)

S: specimen surface area (in^2)

γ_s: slump factor; $\gamma_s = 0.88 + 0.067 * s$

s: slump (in.)

γ_ψ: fine aggregate content factor; $\gamma_\psi = 0.88 + 0.24 * \psi$

ψ: fine aggregate-to-total aggregate ratio in decimals

γ_α: air content factor; $\gamma_\alpha = 0.46 + 0.09 * \alpha$

α: air content (%)

The AASHTO-LRFD model uses a different expression for calculating the ultimate creep coefficient value (Equation 5-6). The main difference in the models is that Equation 5-6 uses a compressive strength factor, instead of mix design factors like fine aggregate content and air content, in order to adjust the ultimate creep coefficient to the specific sample.

$$\phi_u = 3.50 \cdot k_{la} \cdot k_\lambda \cdot k_s \cdot k_f \qquad \text{Equation 5-6}$$

where

ϕ_u: ultimate creep coefficient

k_{la}: age of loading factor; $k_{la} = 1.00 * t'^{-0.118}$ for moist curing

t': maturity of concrete at loading (days)

k_λ: ambient relative humidity factor; $k_\lambda = 1.58 - 0.838 * h$

h: relative humidity in decimals

k_s: size factor; $k_s = \left[\frac{t}{\frac{26 \cdot e^{0.36\frac{V}{S}} + t}{\frac{t}{45+t}}} \right] \cdot \left[\frac{1.80 + 1.77 \cdot e^{-0.54\frac{V}{S}}}{2.587} \right]$

t: maturity of concrete (days)

V: specimen volume (in^3)

S: specimen surface area (in^2)

k_f: concrete strength factor; $k_f = \frac{1}{0.67 + \frac{f_c'}{9}}$

f_c': compressive strength if concrete cylinders at 28 days (ksi)

Table 5-4 summarizes the ultimate creep coefficients calculated for the SCC mixes using both ACI 209 and ASSHTO-LRFD models. The parameters used for calculation of the ultimate creep coefficient, including compressive strength, air content and fine aggregate-to-total aggregate ratio for every given mix are also shown. The ultimate creep coefficient values varied in every mix depending on the model used.

Table 5-4. Ultimate creep coefficient for SCC mixes predicted by ACI 209 (1997) and AASHTO-LRFD (2004) models

Structure	Mix	w/cm	f_c' (psi)	Air Content (%)	FA/TA	Ultimate Creep Coefficient, ϕ_u	
						ACI 209	AASHTO-LRFD
Wall panels	S-Slag/Ash	0.31	10,641	1.5	0.389	1.71	1.49
	G-Slag	0.37	8,294	0.5	0.458	1.38	1.74
	Tindall	0.38	8,313	1.0	0.436	1.62	1.74
Girders	7N	0.31	12,620	2.8	0.455	2.08	1.42
	7BL	0.32	11,280	0.5	0.478	1.48	1.51
	67M	0.32	11,350	1.8	0.485	1.83	1.45

The creep coefficient values for the mixes used in the walls and girder sections are presented in Figures 5-10 and 5-12, respectively. Table 5-5 shows the applied stresses and the correspondent initial elastic strain of every mix used to calculate the creep coefficient. As shown in Figure 5-10, G-Slag mix had the lowest creep coefficient of 1.02, the S-Slag/Ash mix and Tindall mix showed a creep coefficient equal to 1.28. The mixes used in the girder sections showed a creep coefficient after 70 days, ranging from 1.10 to 1.21 (Figure 5-12). Mix 7BL had the lowest creep coefficient, while mix 7N displayed the highest value. The creep coefficient of the mixes used in the girders was in general greater than those from the walls at 70 days. This result was not expected as the paste content of the girder mixes were lower than that of the wall mixes. At 70 days, mix S-Slag/Ash had the highest creep coefficient value of the walls mixes, and it was equal to 1.05.

Table 5-5. Applied stress and initial elastic strain of the SCC mixes for the creep test

Structure	Mix	w/cm	Applied Stress (psi)	Initial elastic strain (με)
Wall panels	S-Slag/Ash	0.31	4,256	1,044
	G-Slag	0.37	3,318	1,049
	Tindall	0.38	3,325	1,004
Girders	7N	0.31	4,615	1,236
	7BL	0.32	4,163	1,038
	67M	0.32	4,434	1,022

The ACI 209 model for creep coefficient was compared with the measured values of the SCC mixes used in the walls and the girder sections in Figures 5-10 and 5-12, respectively. The AASHTO-LRFD model was also presented for comparison in Figures 5-11 and 5-13. In all cases the ACI 209 curves were closer to the measured creep curves of the SCC mixtures than the curves predicted by the AASHTO-LRFD model. However, the values given by ACI 209 model for conventional concrete were lower than those observed in the SCC mixes. The measured creep coefficients of the SCC mixes ranged from 5% to 32% higher than those expected by ACI 209. In general, the AASHTO model for conventional concrete also underestimated the creep coefficient of the SCC mixes, except in G-Slag mix for which the predicted value is higher than the measured one. The measured creep coefficients of the SCC mixes ranged between 4% and 53% higher than those given by the AASHTO model. The AASHTO model underestimation of creep coefficient of the SCC mixes was greater for the mixes used in the girder sections, but this could be related to the early stage of the test when these values were reported.

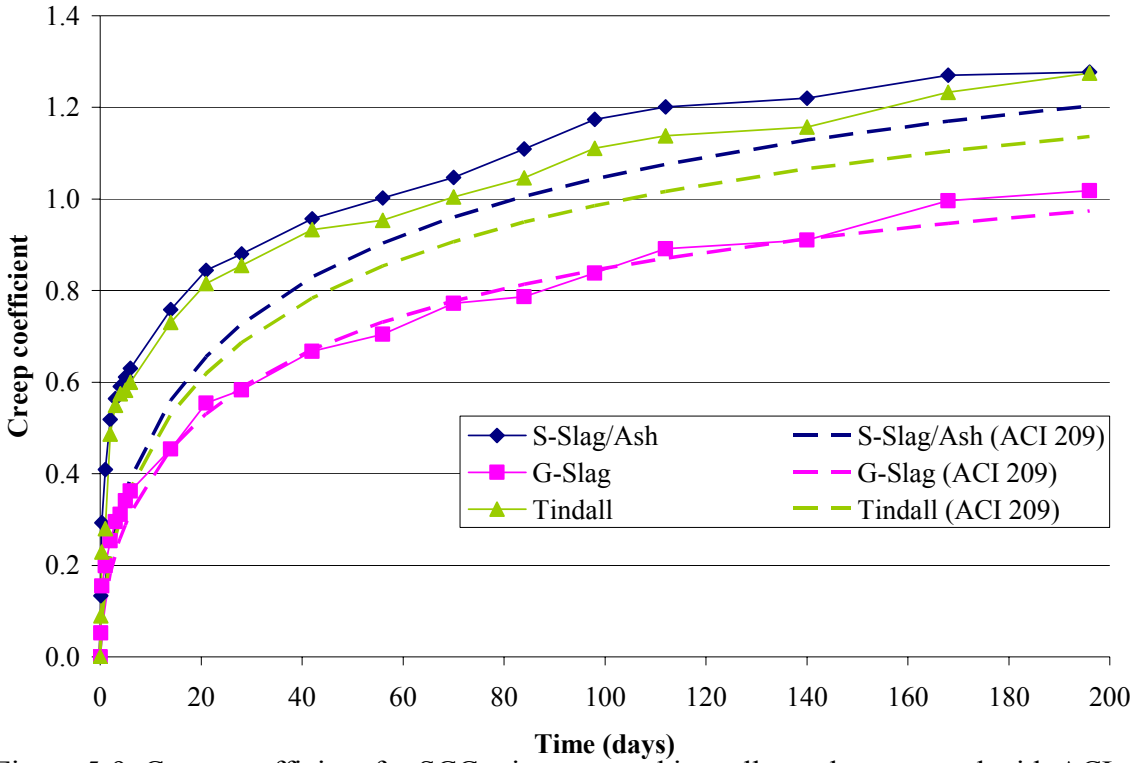

Figure 5-9. Creep coefficient for SCC mixtures used in wall panels compared with ACI 209 model for conventional concrete

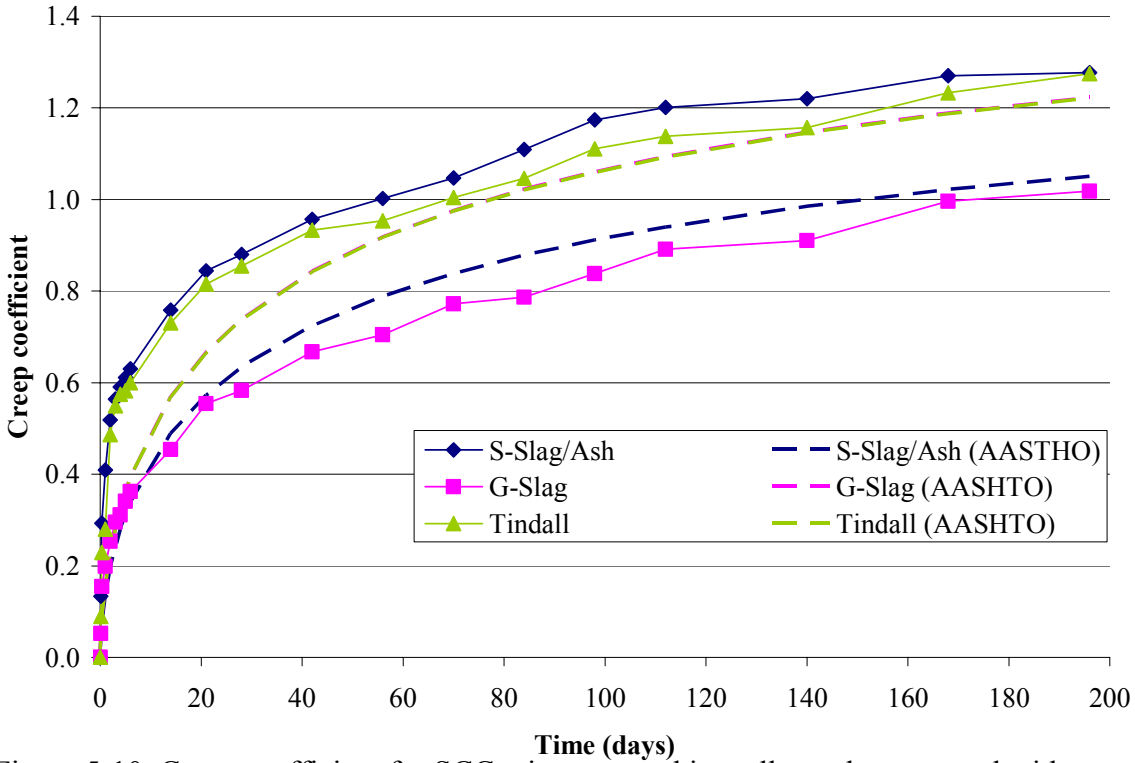

Figure 5-10. Creep coefficient for SCC mixtures used in wall panels compared with AASHTO-LRFD model for conventional concrete

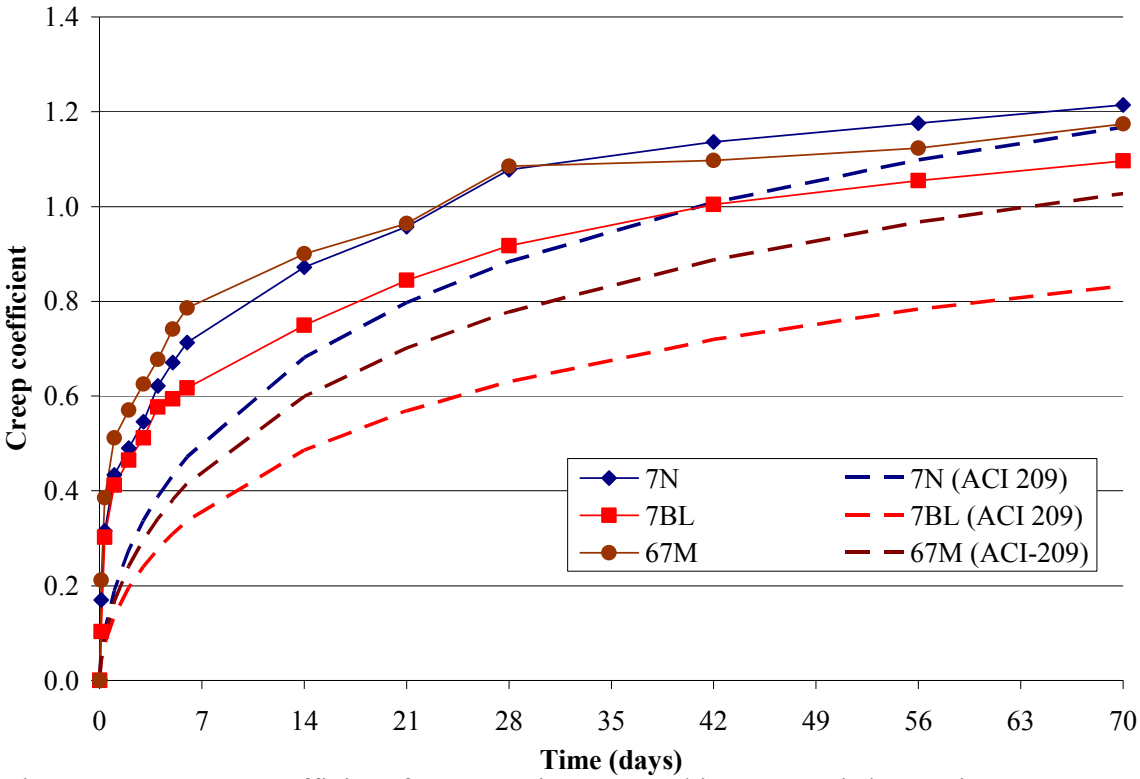

Figure 5-11. Creep coefficient for SCC mixtures used in BT-72 girder sections compared with ACI 209 model for conventional concrete

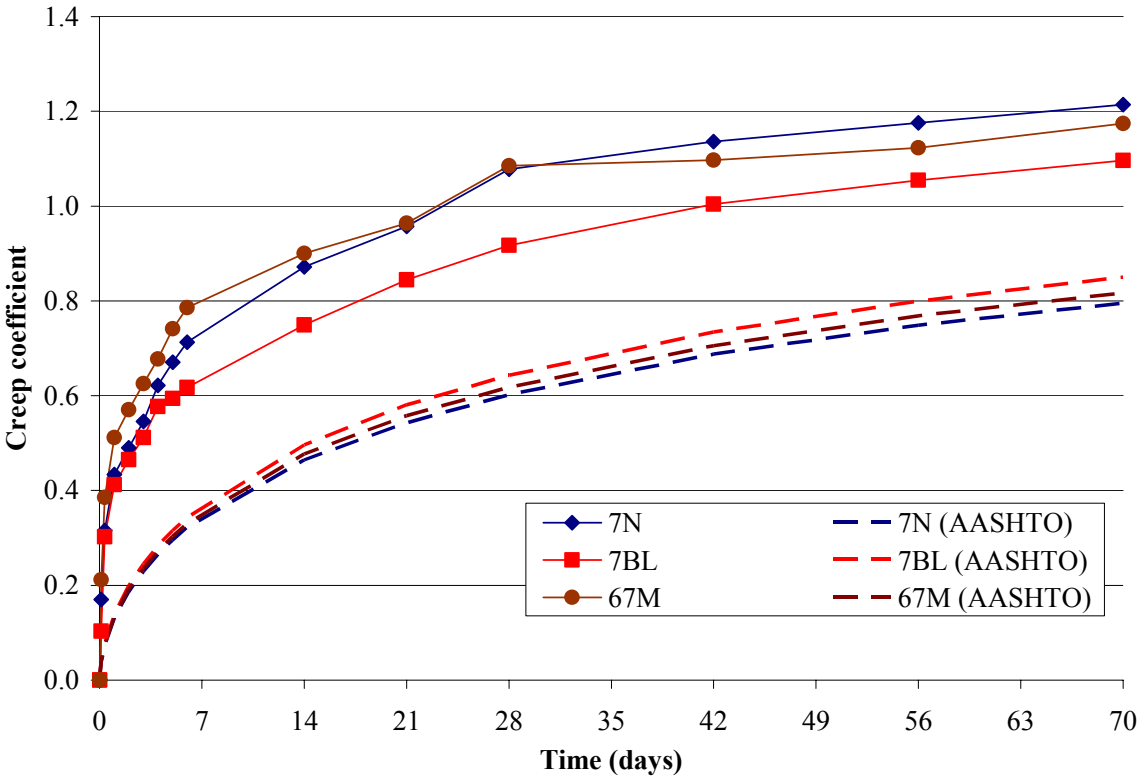

Figure 5-12. Creep coefficient for SCC mixtures used in BT-72 girder sections compared with AASHTO-LRFD model for conventional concrete

The specific creep of the SCC mixes is presented in Figures 5-14 to 5-17. Mixes S-Slag/Ash and G-Slag had similar results after 200 days, with a specific creep of 0.32 με/psi (46 με/MPa). Tindall mix presented a slight higher value of specific creep with 0.38 με/psi (55 με/MPa). After 70 days, all SCC mixes used in the girder sections achieved similar specific creep values. Mix 7N reported the largest value with 0.32 με/psi (46 με/MPa), which was 14% higher than those achieved by mixes 7BL and 67M, with 0.28 με/psi (40 με/MPa). The values of specific creep reported for the mixes used in the girders were similar to those achieved by the mixes used in the walls after 70 days. This seemed to be related to the fact that all SCC mixes presented a similar water-to-paste (w/p) ratio of about 0.50, independently of their respective w/cm as seen in Table 5-6.

A comparison of the ACI 209 and AASHTO-LRFD models of specific creep for conventional concrete showed similar results as found in creep coefficient. The SCC mixes displayed higher values of specific creep than those expected for conventional concrete. The ACI 209 model showed values closer to those measured in the SCC mixes, than the values given by AASHTO model. Yet, ACI 209 reported specific creep values about 5% to 32% lower than those of the SCC mixes.

Table 5-6. Water-to-paste ratio and paste content by volume of the SCC mixes

Structure	Mix	w/cm (by mass)	Water/Paste (w/p)	Paste content (%)
Wall panels	S-Slag/Ash	0.31	0.47	38.3
	G-Slag	0.37	0.53	39.2
	Tindall	0.38	0.55	32.1
Girders	7N	0.31	0.49	36.0
	7BL	0.32	0.50	36.3
	67M	0.32	0.49	35.3

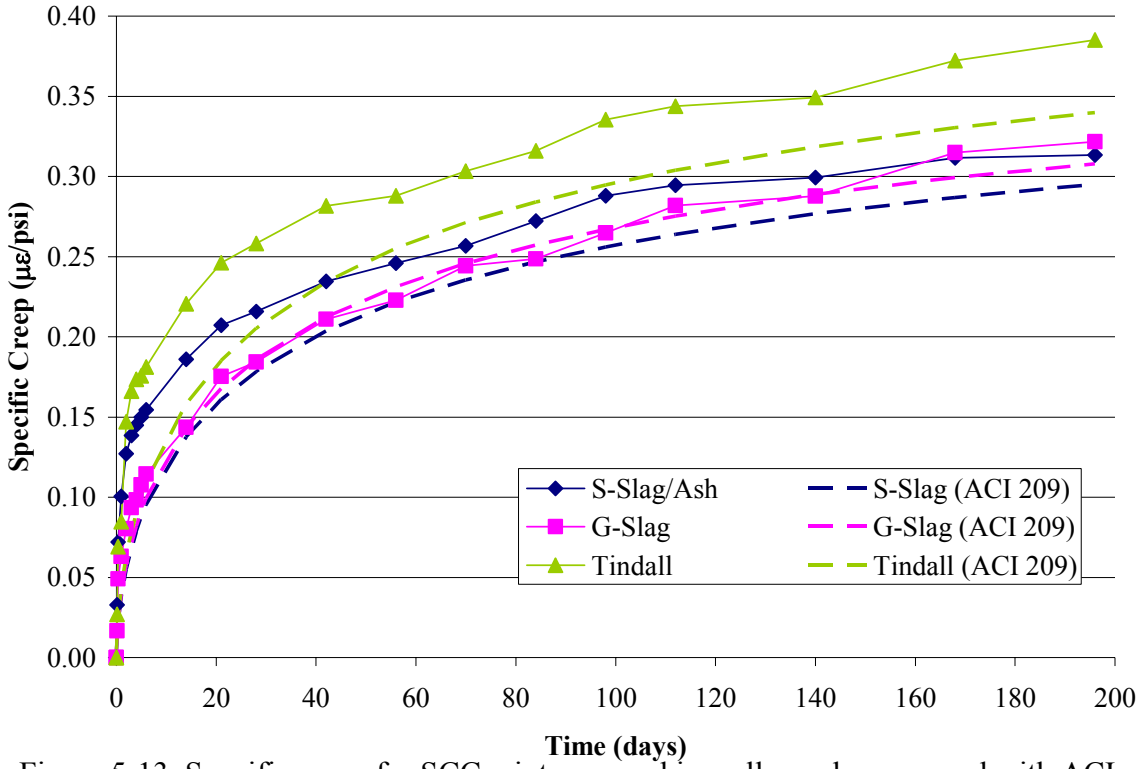

Figure 5-13. Specific creep for SCC mixtures used in wall panels compared with ACI 209 model for conventional concrete

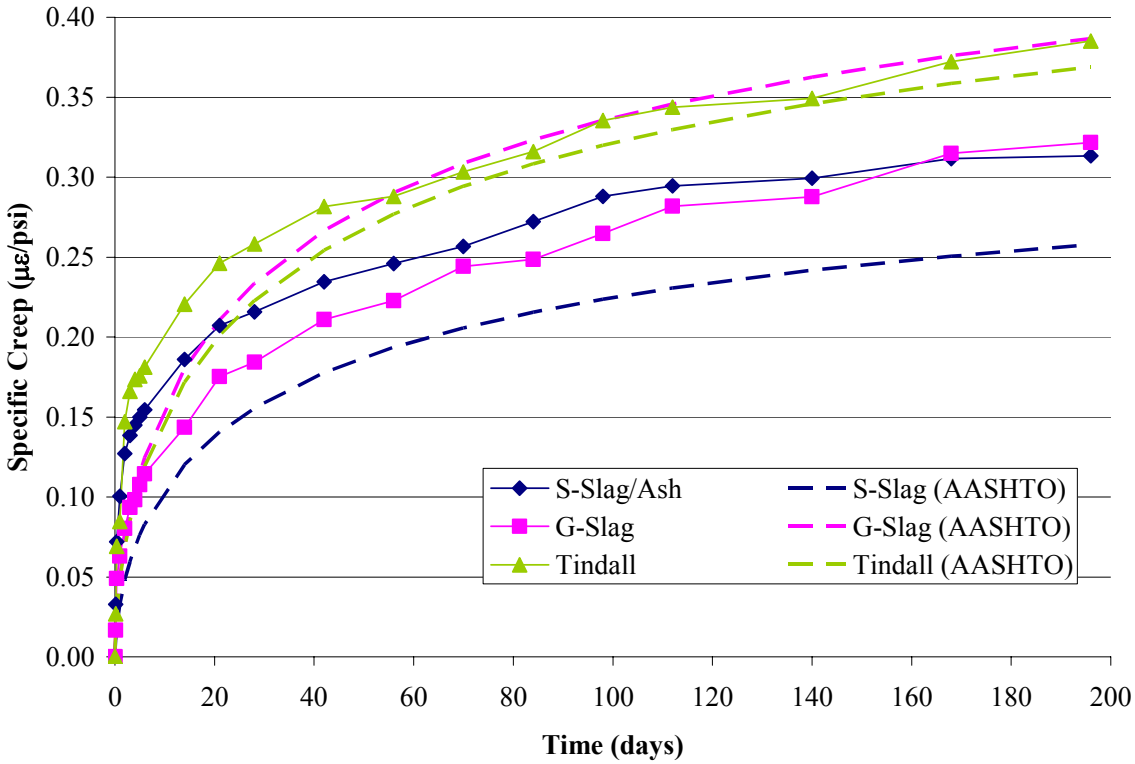

Figure 5-14. Specific creep for SCC mixtures used in wall panels compared with AASHTO-LRFD model for conventional concrete

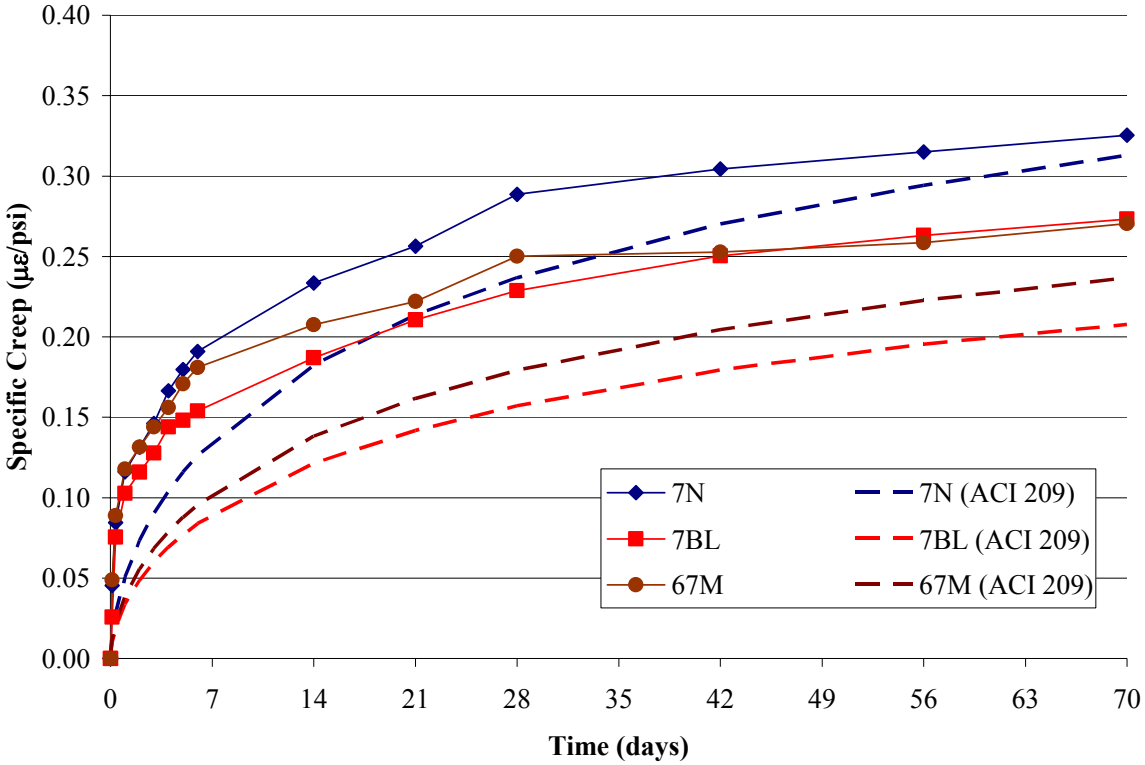

Figure 5-15. Specific creep for SCC mixtures used in BT-72 girder sections compared with ACI 209 model for conventional concrete

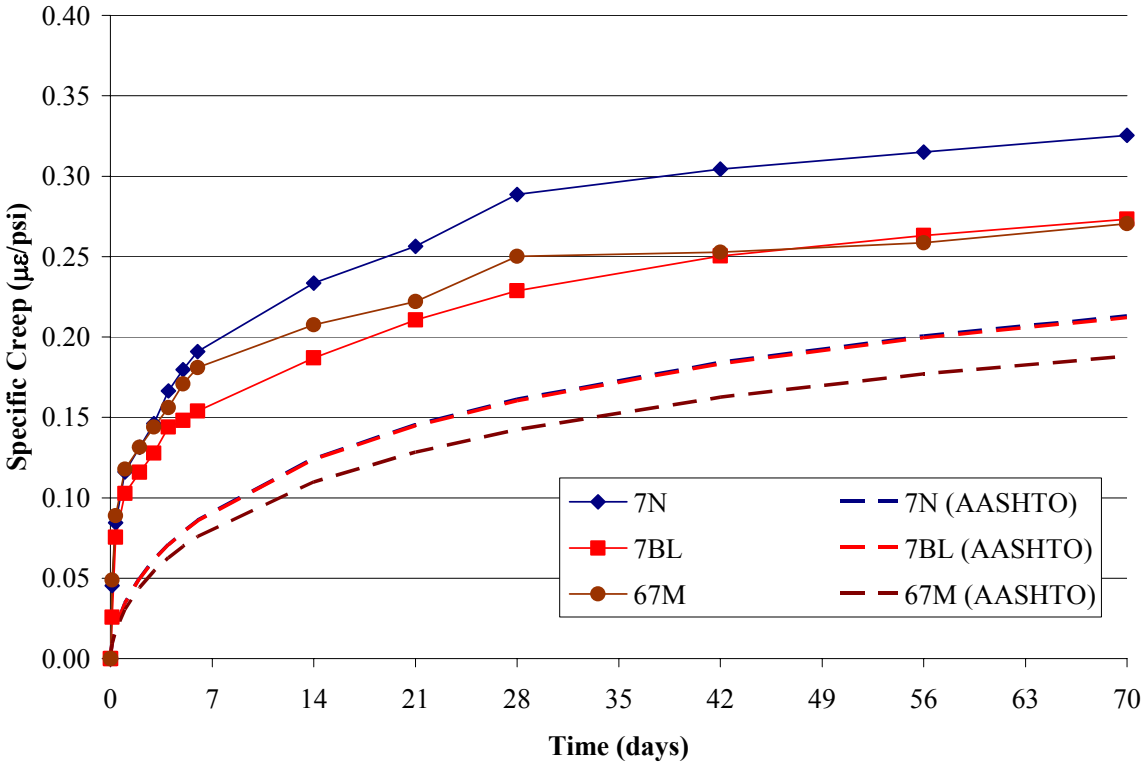

Figure 5-16. Specific creep for SCC mixtures used in BT-72 girder sections compared with AASHTO-LRFD model for conventional concrete

Drying shrinkage and creep strain of the SCC mixes used in the wall panels and the BT-72 girder sections were compared in Figures 5-17 and 5-18, respectively. In order to compared values of creep strain that were not dependant on the level of stress applied, the creep strains presented in these charts were not the measured creep, but the potential creep strains produced by a fixed value of stress applied to all mixes. Thus, these values of creep were calculated based on the specific creep of each mix multiply by this assumed fixed stress. The assumed value of stress was the average value of the applied stresses for each group of mixes. For the mixes used in the wall panels the assumed stress was 3,600 psi (25 MPa); while for the girder mixes the assumed stress was 4,400 psi (30 MPa). Creep curves are shown in solid lines, while drying shrinkage curves are represented in dashed lines.

In general, the trend found for drying shrinkage of the SCC mixes was not the same than that of creep, as seen in Figures 5-17 and 5-18. The mixes with the lowest creep strain showed the highest value of drying shrinkage, as in the case of mix G-Slag for the wall panels and the mix 7BL for the girders. Also, mixes with high values of creep showed low values of shrinkage, as in the case of the Tindall mix and mix S-Slag/Ash. These results were unexpected, as is commonly stated that creep and drying shrinkage are interrelated phenomena and both are affected by the same experimental parameters (Midness et al., 2002). No explanation could be found to account for the observed discrepancy between the tendencies of creep and drying shrinkage of the mixes.

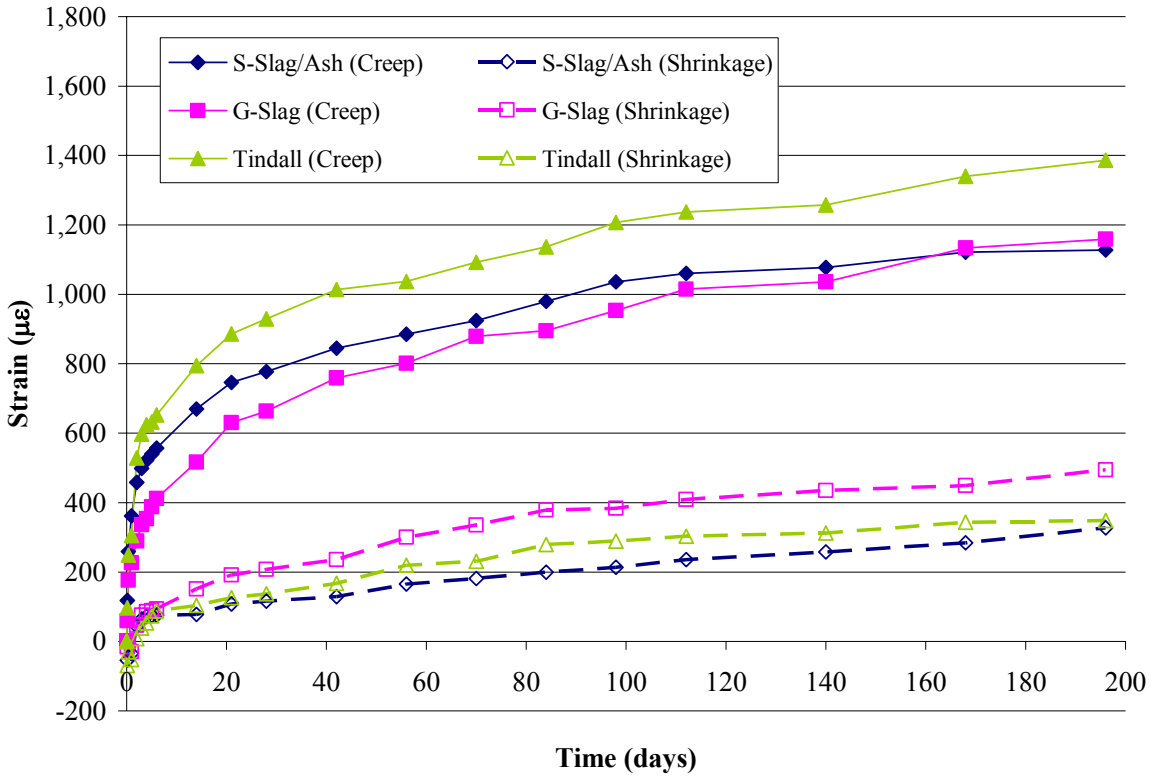

Figure 5-17. Drying shrinkage and creep strain for SCC mixes used in the wall panels

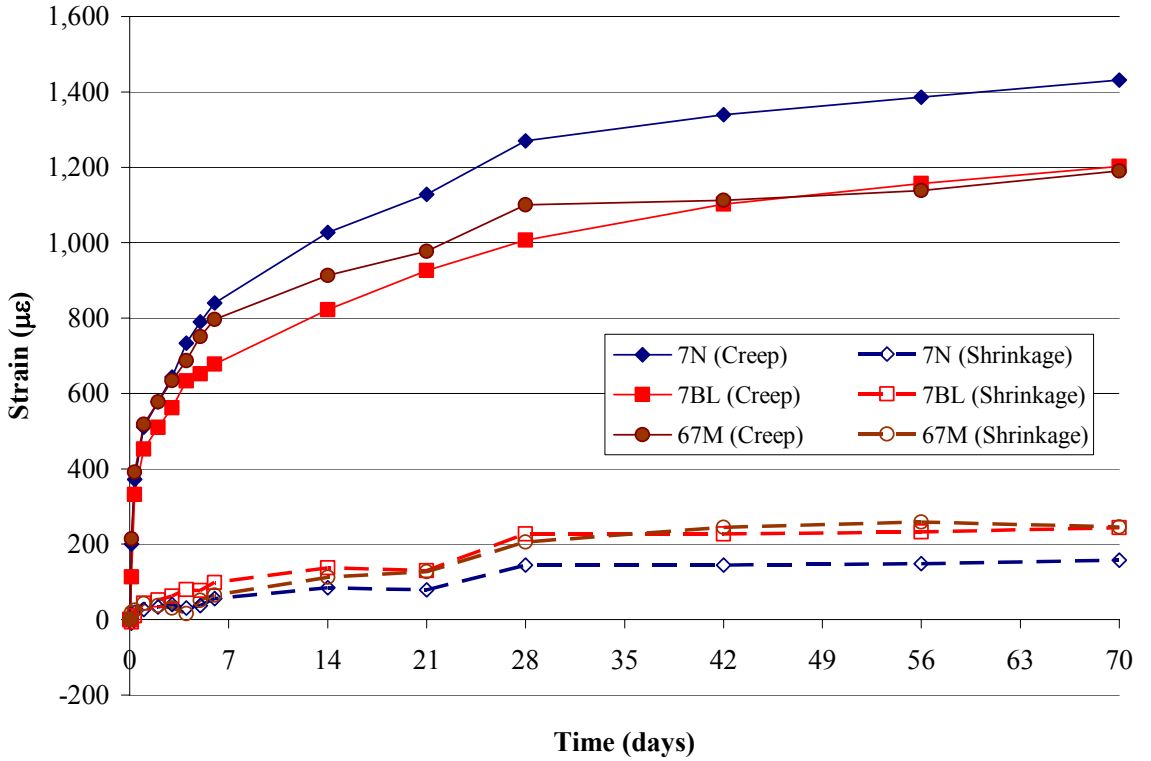

Figure 5-18. Drying shrinkage and creep strain for SCC mixes used in the BT-72 girders

5.5 – Rapid Chloride Permeability Test

The rapid chloride permeability test (RCPT, ASTM C 1202) was measured for all SCC mixtures used for casting of the BT-72 girders. Three 4 x 8 in. moist cured cylinders were tested for every mixture. The cylinders were kept in the fog room for 56 days and then were sawed into 2-in. thick disks (Figure 5-19). The central section of each cylinder was used for the RCPT test according to ASTM C1202 specifications. The concrete sections were tested using special electric cells as shown in Figure 5-20. Samples were monitored by a computer that allowed testing of four specimens simultaneously, as illustrated in Figure 5-21.

Figure 5-19. Sawing of control cylinders for chloride permeability test

Figure 5-20. Samples preparation for chloride permeability test

Figure 5-21. Chloride permeability test set up. Four concrete samples were tested simultaneously monitored by a computer

The average charge passed during RCPT for each mix is presented in Figures 5-22 and 5-23. Both vibrated and non-vibrated mixes were included in this study in order to assess the influence of w/cm on the permeability of the mixtures. In general, mixes with higher w/cm gave larger RCPT values than those for mixtures with lower w/cm, as shown in Figure 5-22.

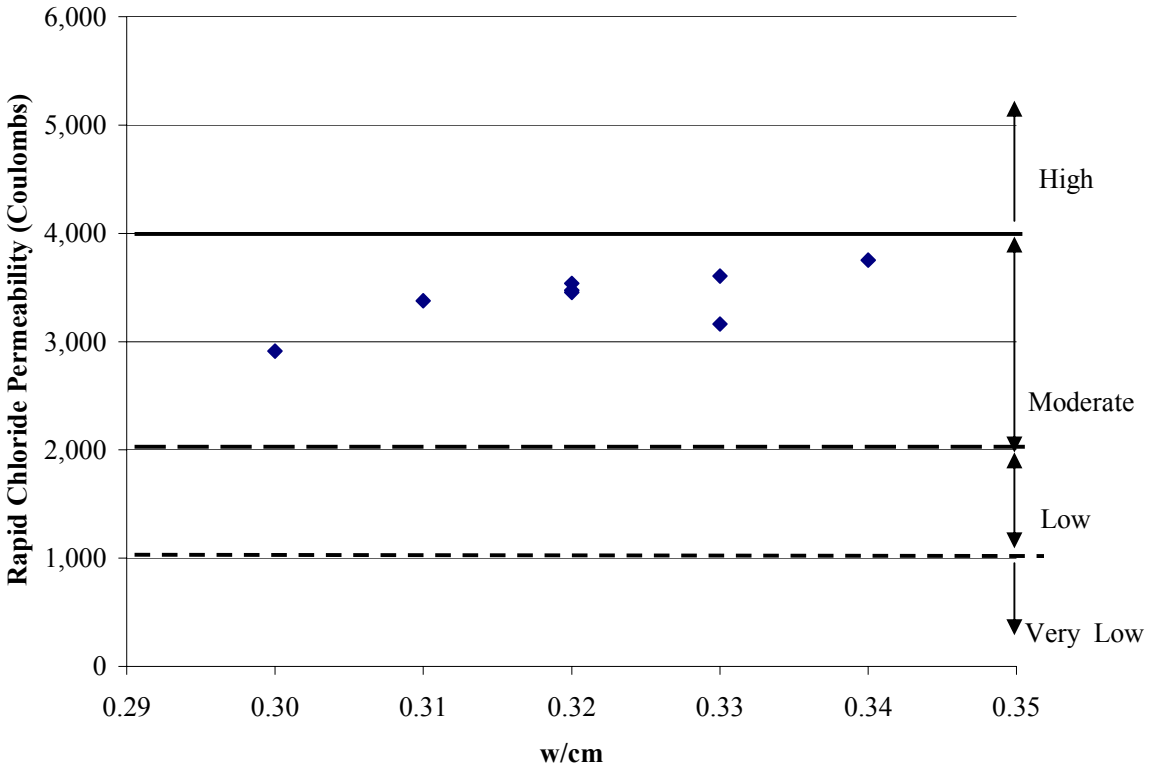

Figure 5-22. Rapid chloride permeability versus w/cm for SCC mixtures

The reported chloride permeability of all SCC mixtures was in the Moderate range, between 2,000 and 4,000 Coulombs (Figure 5-22). Mix 67N showed the lowest permeability value with 2,911 Coulombs, while mix 7BLv showed the highest value with 3,752 Coulombs. These values were higher than those reported in the literature for SCC mixtures of similar w/cm (Ozyildirim and Lane, 2003). However, the SCC mixes in Ozyildirim and Lane (2003) incorporated about 20% to 25% of Class F fly ash as supplementary cementitious material , while the SCC mixes used for casting of the girders used about 17% of Class C fly ash.

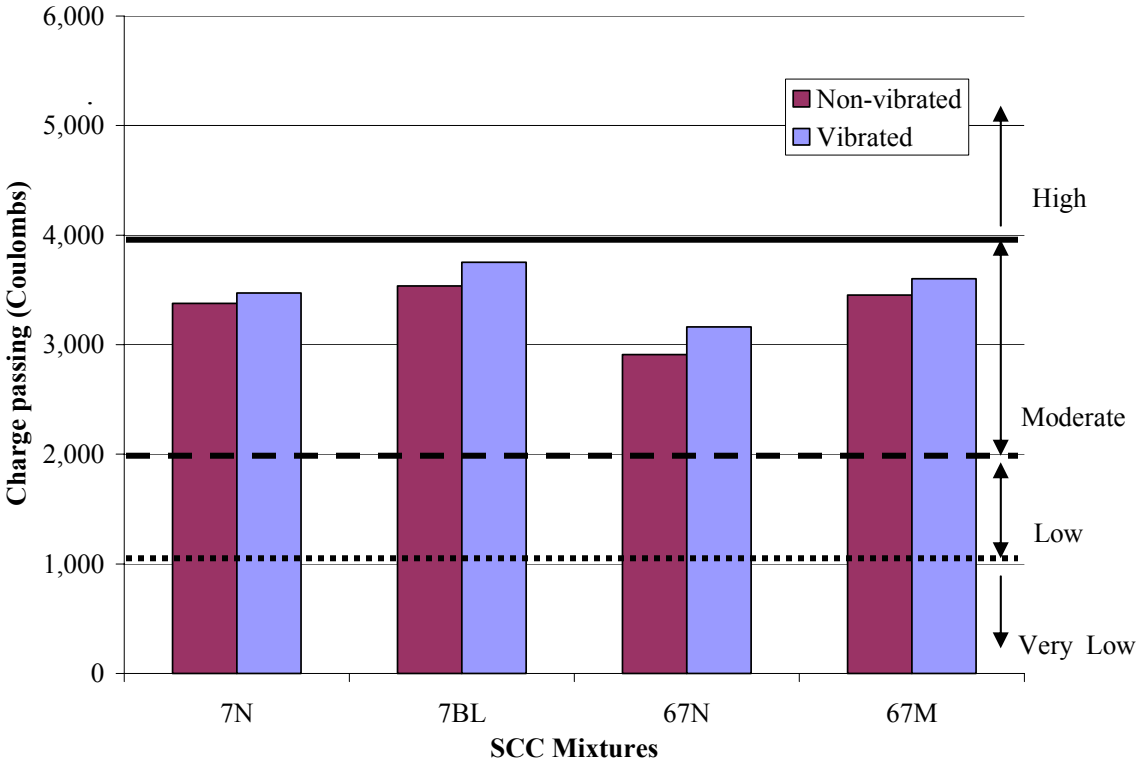

Figure 5-23. Rapid chloride permeability test results at 56 days for SCC mixtures used in BT-72 girders

Also, the excessive bleeding observed in the SCC mixes used in the BT-72 girder sections may have produced more trapped bleed water around the aggregate, which created a more porous and permeable transition zone, thus producing higher RCPT values. Inclusion of finer cementitious materials including silica fume or metacaolin is recommended in the design of SCC mixes, as they produce a denser transition zone which increases the water retaining capability of the paste slurry, thus reducing the chloride permeability of the concrete (Westerholm et al., 2002).

CHAPTER 6

DISCUSSION OF RESULTS

6.1 – Introduction

In this chapter, mixes from both the wall panels and the girders with the best and worst results are compared. The intent of this chapter is to identify which properties of the SCC mixes in the sections cast were responsible for the variations in SCC performance. Also, the results obtained in this study are compared with previous research findings.

6.2 –Effect of Mix Proportioning on Workabilty

Table 6-1 summarizes the mix proportioning for those mixes selected for comparison of excellent and poor self-consolidating performance. These mixes were selected based on the results of both visual inspection and quantitative analysis of the properties of the concrete sections. The walls and girders with the least percentage of air bubbles present on their surfaces, both on the web and bottom flanges in the case of the girders, and lowest COV values for compressive strength and percentage of aggregates throughout the sections were chosen as those mixes with the best performance. On the other hand, the poor performance mixes displayed significant segregation of the concrete, including multiple voids and honeycombing and also an uneven distribution of the aggregate throughout the concrete sections. Two mixes recommended by Ramage et al. (2004) in Task 1 report of this research are also included. Ramage mixes produced

satisfactory results in all fresh state and hardened state testing, including VSI numbers, slump flow, U-box test and L-box test.

Table 6-1. Mix proportioning of SCC with good and poor performances

	Recommended		**Good Performance**		**Poor Performance**	
	G-TA-1	**S-TA-1**	**G-Slag**	**7BLv**	**67M**	**Tindall**
Mix Components	**Ramage et al. (2004)**		**Mix 2 (Tindall)**	**Mix 4v (SCP)**	**Mix 5 (SCP)**	**Mix 3 (Tindall)**
Cementitious (lb/yd^3)						
Cement Type I	524	640	730	-	-	750
Cement Type III	-	-	-	754	770	-
Slag	401	180	225	-	-	-
Silica Fume	31	-	-	-	-	-
Fly Ash, Class F	-	80	-	-	-	-
Fly Ash, Class C	-	-	-	147	153	-
Total Powder	*956*	*900*	*955*	*901*	*923*	*750*
Water (lb/yd^3)	366	282	350	308	294	288
w/cm	*0.38*	*0.31*	*0.37*	*0.34*	*0.32*	*0.38*
Coarse Aggregates (lb/yd^3)						
# 67 stone	-	-	-	-	1439	1465
# 7 stone	917	928	910	1223	-	-
# 89 stone	494	500	485	182	-	-
Total Coarse	*1411*	*1428*	*1395*	*1405*	*1439*	*1465*
Fine Aggregates (lb/yd^3)						
Natural sand	589	538	600	211	-	1331
Manufactured sand	589	360	580	1155	1357	-
Total Fine	*1178*	*898*	*1180*	*1366*	*1357*	*1331*
Total Aggregates	*2589*	*2326*	*2575*	*2771*	*2796*	*2796*
Admixtures (fl oz./cwt)						
HRWR	8.4	7.1	6.9	6.0	6.0	5.5
LRWR	-	-	-	1.9	2.0	-
AEA	-	-	-	0.18	0.18	0.4

6.2.1 – Cementitious Materials

The use of either Type I or Type III cement did not influence the performance of the mixes. For the two types of cement, mixes with both excellent and poor self-consolidating abilities were found. The increase in fineness of Type III cement did not affect the general workability of the mixes where it was used.

Different supplementary cementitious materials (SCMs) were used with no significant differences in performance of the SCC mixes depending on the type or percentage of SCM employed. The SCM replacement percentage recommended by Ramage et al. was 45% by weight of cement, suggesting the use of slag in greater percentage. A lower percentage of SCM replacement ranging from 16% to 24% by weight produced mixes with equally good and poor performances. In general, mixes using slag showed a more uniform pattern of air-bubble sizes and distribution when compared with mixes using Class C fly ash. However, this can not be attributed to the type of SCM used, as the area fraction of air bubbles to surface of the section was about 0.35% for both mix G-Slag and mix 7BLv, even when one used slag and the other used Class C fly ash, respectively.

Inclusion of SCMs in proportioning of SCC mixes is recommended not only to reduce the greater heat of hydration produced by the large amount of cementitious material incorporated in this type of concrete (Tang et al., 2001), but also to increase the workability of fresh concrete (Sonebi, 2001). The Tindall mix, which did not incorporate any SCM, showed a poor workability and an overall inferior performance. Futhermore, inclusion of SCMs in the mix desing of SCC improves the durability properties of the concrete, including the resistance to chloride permeability (Westerholm et al., 2002).

6.2.2 – Aggregates

The size and gradation of the aggregates were considered the most important factors affecting the performance of SCC mixes. Not only the individual gradation of each aggregate, but the combine gradation of both coarse and fine aggregates should be taken into account when designing a workable SCC mix. Figure 6-1 illustrates the gradation by weight retained of all mixes presented in Table 6-1. Mixes with a good performance were represented in solid lines, while those mixes with poor performance were represented in dashed lines. The mixes recommended by Ramage et al. were also included in the chart in solid lines.

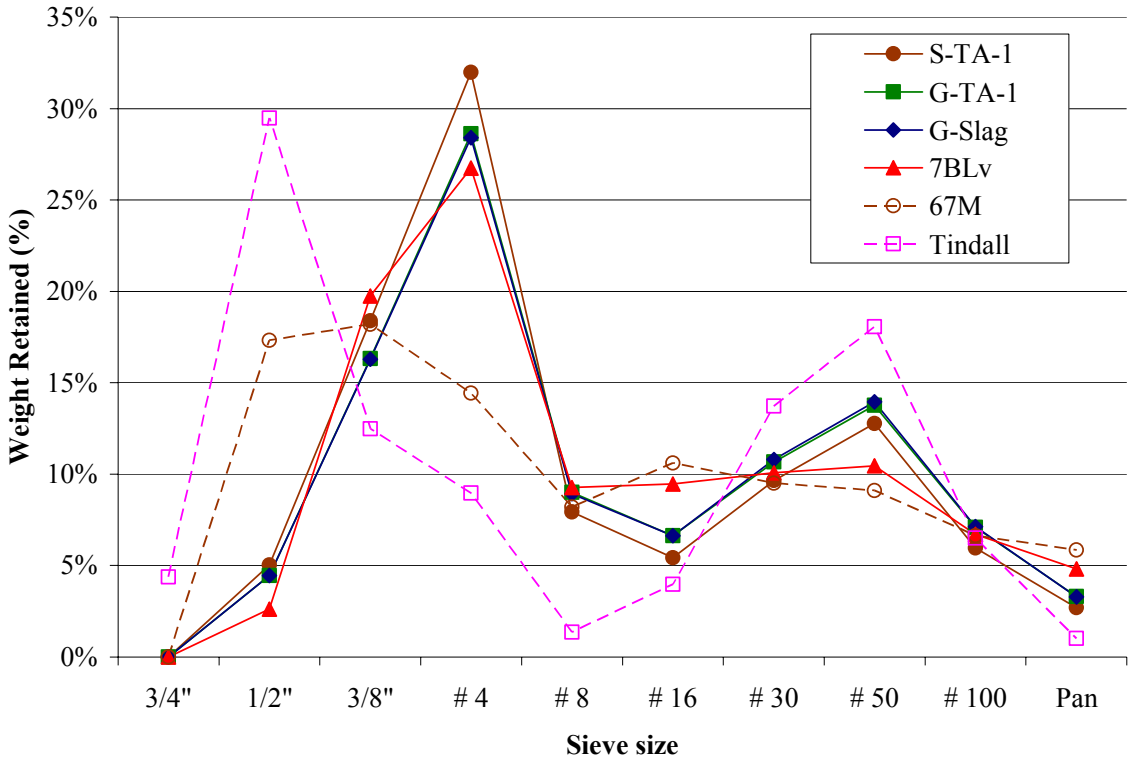

Figure 6-1. Gradation comparison of mixes with good performance (solid lines) versus mixes with poor performance (dashed lines)

The mixes with the best performance showed a lower percentage of stones retained on large size sieves, such as ¾-in. (19 mm) and ½-in. (13 mm), than those mixes with a poor performance. This was intuitive: the larger the size of the stone used, the greater the blockage potential of the mix when flowing through congested reinforcement. Also, the workable mixes displayed a more uniform gradation of the fine aggregate, with a maximum difference of 7% between the weight of aggregates retained on sieve No. 16 and that retained on sieve No. 50. This uniform gradation was not achieved by the Tindall mix, which displayed large gaps for both coarse and fine aggregates and which corresponded with its poor performance in field applications. Poor performing Mix 67M showed similar uniform fine aggregate gradation as that of good performance mixes, and it slightly differed with those in its coarse aggregate gradation. Yet, the performance of mix 67M was not as good as mixes G-Slag or 7BLv which indicated that other factor besides gradation of the aggregates must be taken into account (Section 6.5).

In order to produce a more uniform gradation is often useful to incorporate more than one coarse aggregate. Mixes G-Slag and 7BLv used a blend of #7 stone with #89 stone; the mixes showed excellent performance. The same was valid for proportioning of fine aggregates. Mixes with a good performance used a blend of natural with manufactured sands. These results confirmed Ramage et al. studies, which had proposed SCC mixes with blended aggregates because they performed the best in fresh state testing. The gradation curves of the mixes S-TA-1 and G-TA-1, proposed by Ramage et al. were close to that of mixes G-Slag and 7BLv.

Blending of different aggregates is not necessary if the gradation of a single stone provides a uniform size distribution of the aggregates. It should be noted that every quarry produces a specific gradation for a given size aggregate. For example, a significant difference was observed when comparing the gradation of the #67 stone provided by Vulcan Materials quarry and that of the #67 stone provided by Florida Rock Industries quarry (Figure 6-2). As shown in Table 6-1, mix 67M used only manufactured sand as fine aggregate while mix 7BLv used a blend of manufactured and natural sands; however, the gradation showed in Figure 6-1 for the fine aggregates of both mixes was very similar. Testing for actual gradation of the specific aggregates used in a given mix is recommended to properly assess the compliance of the aggregate with the gradation requirements presented here.

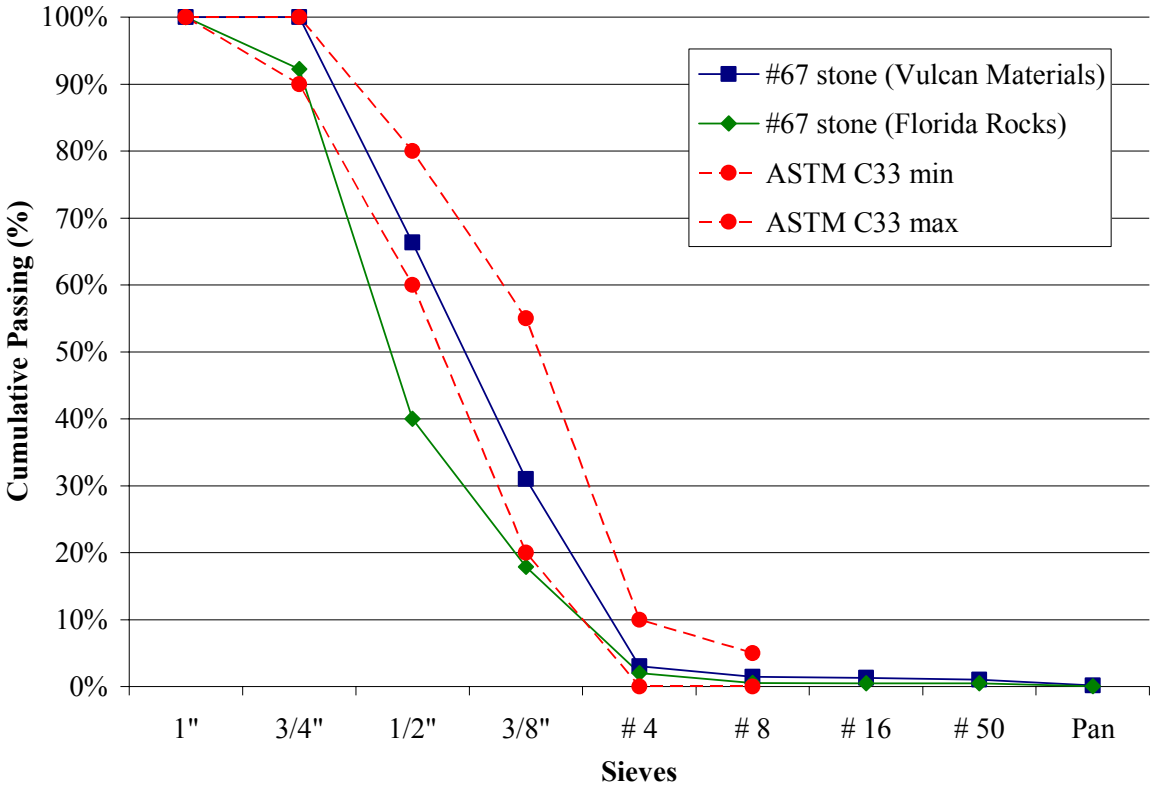

Figure 6-2. Comparison of #67 stone gradation from different quarries

Moisture content of the aggregates, especially fine aggregates, was also an important factor influencing the performance of SCC mixes. Small fluctuations in moisture content lead to segregation or affected the self-consolidating abilities of the mixes. Furthermore, these variations in moisture content from batch to batch significantly affected the consistency of the concrete. Blending of different aggregates made the mixes less sensitive to fluctuations in moisture content as demonstrated by the performances of mixes 7BL and 7BLv (Mix 4) (Section 4.6).

6.2.3 – Chemical Admixes

All HRWR agents used proved to effectively reduce the yield stress of the concrete paste. However, the effectiveness of a given dosage rate in producing self-consolidating abilities in a mix was totally dependant on the type of HRWR and the specific proportioning of the mix, including w/cm and aggregate gradation. Grace ADVACast® 540 required higher dosages than Sika Viscocrete® 6100 to produce mixes with good performances, even though both are polycarboxilate-polymer based HRWR agents. Mix G-Slag required 6.9 fl. oz/cwt (450 mL/100 kg) of ADVACast by weight of cementitious material, while mix 7BLv used 6.0 fl.oz/cwt (390 mL/100 kg) of ViscoCrete. On the other hand, the same dosage rate of a given HRWR agent did not produce the same effect in different mixes. Mix 7BLv and mix 67M used the exact same dosage rate of ViscoCrete® 6100, but the performance of mix 67M was poor compared with that in mix 7BLv when casting the BT-72 girder sections. Differences in aggregate gradation seemed to be the cause for the discrepancy in performance of the two mixes.

It should be noted that the proposed dosage rate for the HRWR agent given by Ramage et al. based on laboratory research was higher than those required in the field to achieved quality SCC. This was attributed to the reduce size of the pan mixer used in the laboratory research; the small mixer was unable to provide a uniform blending of the mix components, particularly the water-reducing agents.

Usage of LRWR agents in combination with HRWRs was not recommended by Task 1 report, suggesting that "mixes produced with only HRWR agents gave more consistent and predictable results" in their self-consolidating abilities. Mixes used for casting of the wall panels did not included any LRWR agent, and satisfactory results were obtained. In the case of the girder sections where a dosage rate of 2.0 fl.oz/cwt (130 mL/100 kg) by weight of cementitious material of Sika Plastiment® was used, the VSI number of the workable mixes was slightly higher than 0 due to observation of bleeding and small halos in the slump flow test (Table 4-11).

The effectiveness of the AEAs in producing quality SCC was also dependant on the gradation of the aggregates and the w/cm of the mixes; its effectiveness was not dependant on the dosage rate used. The same dosage rate of 0.18 fl.oz/cwt (12 mL/100kg) by weight of cementitious material was incorporated in both mixes 7BLv and 67M producing completely different results in performance. Ozyildirim and Lane (2003) reported that certain combination dosages of AEA, HRWR and w/cm induced excessive paste fluidity and segregation resulting in loss of air. The wide scattering in percentage of air obtained in the mixes used in BT-72 girder sections confirmed their finding, especially for mixes with low w/cm (Section 4.5.1). Trial batches are recommended to assess the proper dosage rate of AEA for a specific mix proportioning.

6.3 – Vibration

Vibration did not produce significant variations in the quality of the surface finish of the wall panels. Both vibrated and non-vibrated walls showed a low percentage of air bubbles, with a maximum size of air-bubble diameter of 3/8-in. For the girder sections, no significant differences were observed in surface finish between vibrated and non-vibrated beams.

6.4 – Comparison of Field Mixes with Laboratory Results

Task 1 report of this research, by Ramage et al. (2004), studied the relationship between mix proportion parameters and workability properties of SCC mixes produced in the Georgia Tech Structures Laboratory. The mix proportion parameters analyzed were: the coarse aggregate content (CA/TA), the total aggregate content (TA/Concrete) and, the percent replacement of SCMs in the mix. The workability of the mixes was dictated by their performance in the slump flow test and U-flow test. The laboratory mixes were organized according to their fresh state VSI number, which ranged from 0 to 3, with zero being highly stable working up to a value of 3, considered a highly unstable mix. Instability of the mixes produced by excess of superplasticizer agent dosage was classified as superplasticicer overdose (SP). A series of charts relating the mix proportion parameters with the respective workability performance of the mixes were presented. Each chart included a "workability box" grouping highly stable mixes with VSI of 0 and 1 (Figures 6-3 to 6-10).

The mix proportion parameters and workability results of the SCC mixes used in the walls and BT-72 girders were plotted in the laboratory mix charts to compare the accuracy of the workability boxes for field mixes (Table 6-2). The two mixes recommended by Task 1 report are identified in the charts with a VSI 0. Field mixes with a good performance were represented with dark blue squares; while poor performance mixes were represented with hallow blue squares.

Table 6-2. Field mixes comparing the coarse aggregate-to-total aggregate ratio, total aggregate-to-concrete ratio and SCM percent replacement organized by fresh VSI

Mix	VSI					Slump Flow		U-Flow	w/cm	SCM/CM	CA/TA (%)		TA/Concrete (%)	
	Index		Notes											
	F	H	B	A	P	T_{20}	D	% Max			by weight	by volume	by weight	by volume
S-TA-1	0	1				6	26	98	0.31	28.9%	61.4	61.3	66.3	59.1
G-TA-1	0	1				8	25	98	0.38	45.2%	54.5	54.5	66.2	58.0
G-Slag	0	0				2	26	100	0.37	23.6%	54.2	54.2	66.4	58.6
7BLv	1	1	x			3	28	100	0.34	16.3%	50.7	50.7	69.6	60.4
67M	1	1	x			4	27	100	0.32	16.6%	51.5	51.5	69.7	62.8
Tindall	1.5	1.5			1	-	18	50	0.38	0.0%	56.4	56.4	71.4	64.4

*Notes:

T_{20}: Time (seconds)
F: Fresh State
H: Hardened State
B: Bleed on slump flow
A: excessive air in the mix
P: Aggregate pile-up (inches)
D: mean diameter (inches)
%Max: Height percent of maximum
H_d: filling head drop
H_{S1}: depth at 6 inches away from gate
H_{S2}:depth at 13 inches away from gate
H_f: final depth

Figures 6-3 and 6-4 present the relation between the coarse aggregate-to-total aggregate ratio (CA/TA) by weight and the slump flow diameter and U-flow final height, respectively. The workability boxes defined by Ramage et al., were represented with a solid line and limited the coarse aggregate-to-total aggregate ratio of stable mixes between 50% and 62%. The slump flow diameter of stable mixes was between 22 in. and 26 in., and the lower limit of acceptance for the U-flow final height was 85%.

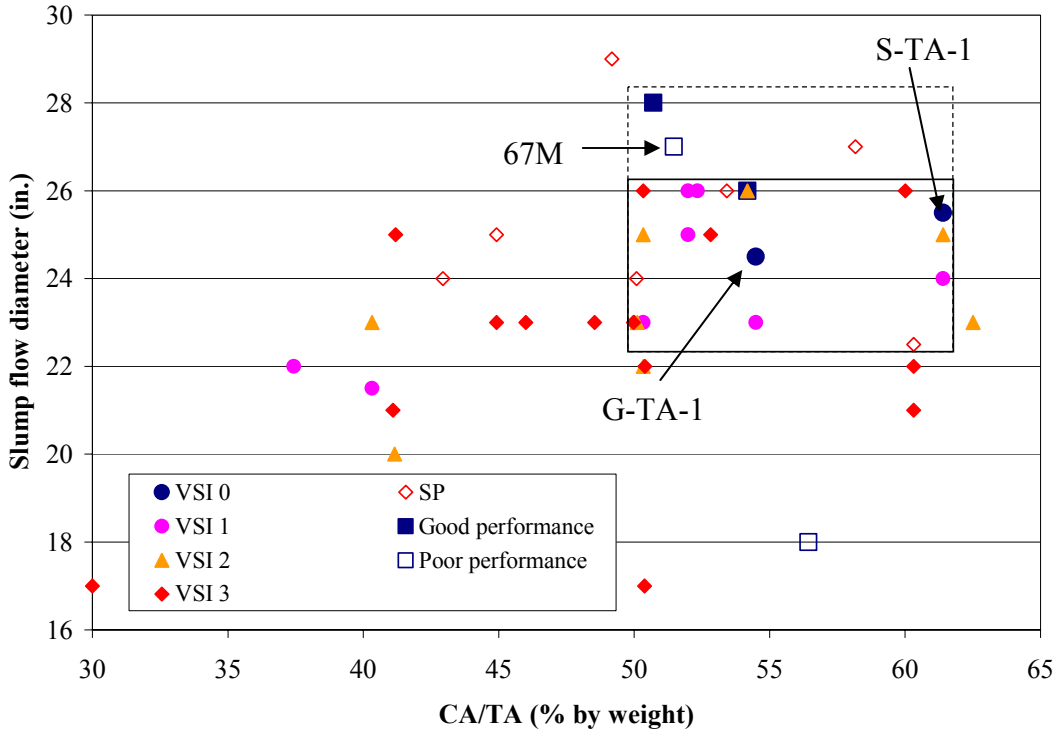

Figure 6-3. Workability boxes of field and laboratory mixes considering coarse aggregate content as it relates to the slump flow diameter

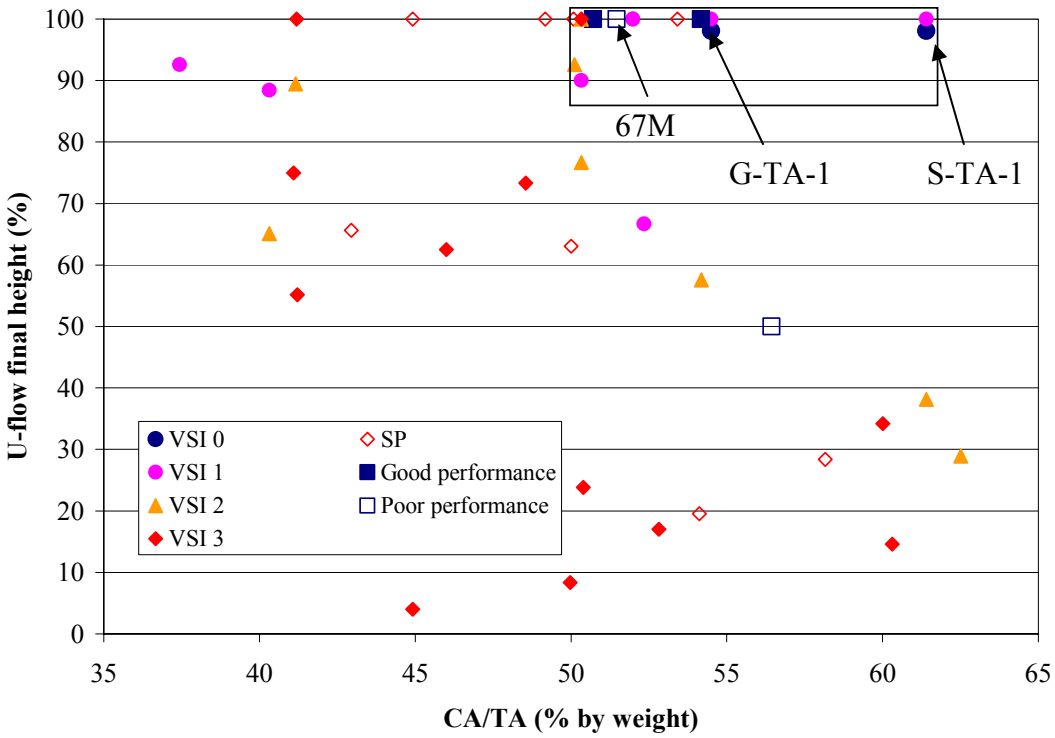

Figure 6-4. Workability box of field and laboratory mixes considering coarse aggregate content as it relates to U-flow final height

The workability box defined for the slump flow diameter in laboratory mixes fell short for the field mixes results. An expanded workability box that accounts for the good performance of the field mixes was proposed and is shown by the dashed line rectangle in the charts. The new workable range proposed for the slump flow diameter of stable mixes was from 22 to 28 in. (558 to 712 mm). These new limits corresponded well with previous research that recommends slump flow diameters greater than 26 in. for highly congested applications (Constantiner and Daczko, 2002). Field mixes with good performance fell inside the workability box defined for the U-flow test. Mixes with poor performance in the field fell outside the workable range, except mix 67M which achieved a 100% passing in the U-flow test; therefore, it fell within the workable range (Figure 6-4). The range of coarse aggregate-to-total aggregate ratio by weight between 50 and 62% proposed by the laboratory report to achieve workable SCC also accommodated the field mixes with good performances.

Figures 6-5 and 6-6 illustrate the relation between total aggregate-to-concrete ratio (TA/Concrete) by volume and the slump flow diameter and U-flow final height, respectively. The total aggregate-to-concrete ratio is an important parameter in the design of SCC mixes as the amount of aggregate may directly influence the flowability and workability of the concrete as described by Kennedy's (1940) excess paste theory. The total aggregate-to-concrete ratio by volume given by Ramage et al. as workable range for SCC mixes was between 58% and 65%.

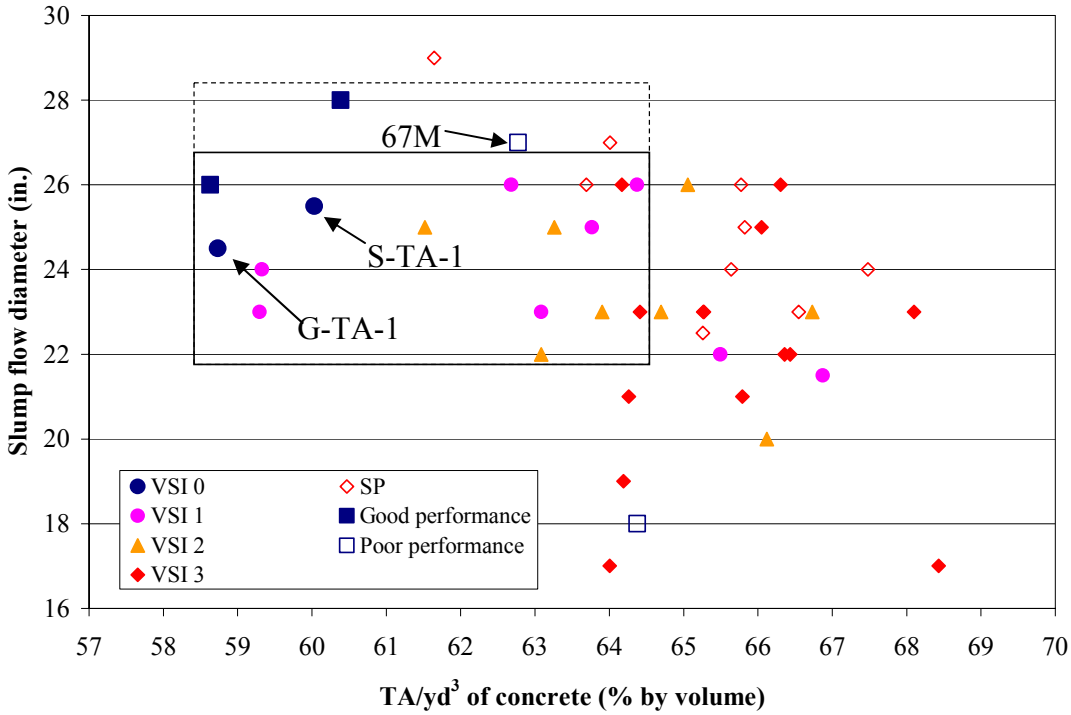

Figure 6-5. Workability boxes of field and laboratory mixes considering total aggregate content as it relates to the slump flow diameter

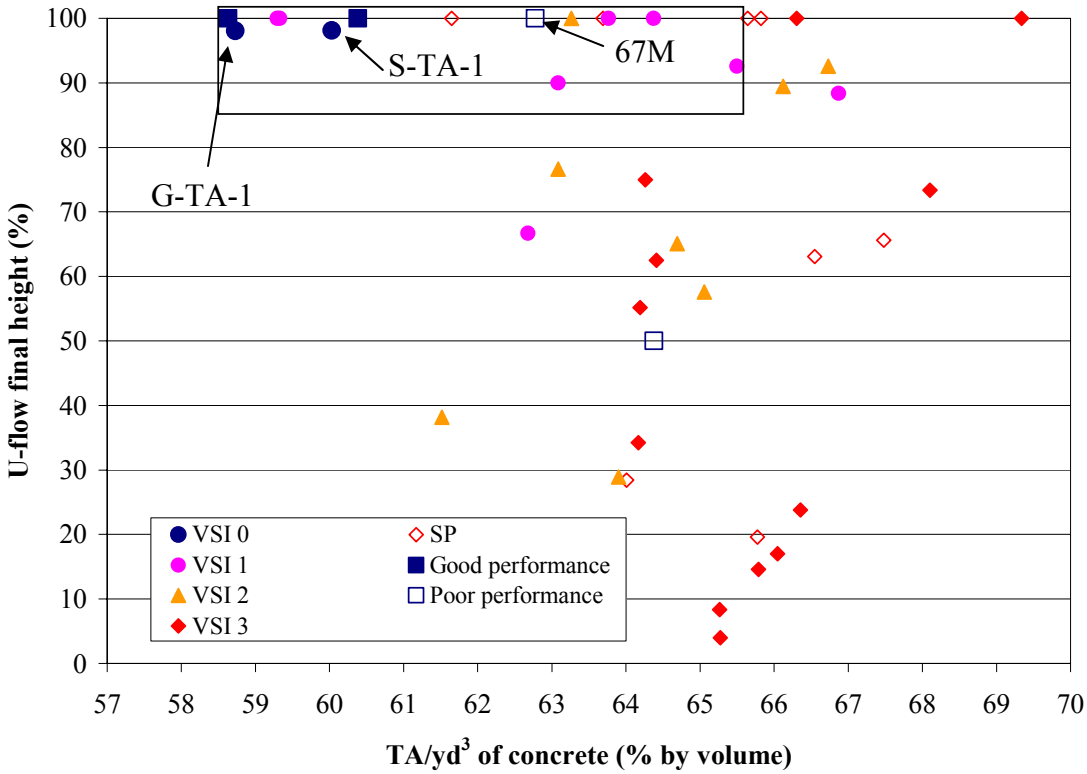

Figure 6-6. Workability box of field and laboratory mixes considering total aggregate content as it relates to U-flow final height

Field mixes with good performance fell within the workable range of TA/Concrete ratio proposed by Task 1 report. However, not all good performance mixes fell inside the workability box, as the upper limit of the slump flow diameter for workable was 27 in., and mix 7BLv showed a 28 in. slump flow. An extended workable range for the slump flow test was proposed, which ranged from 22 to 28 in. to account for the results of all field mixes with good performances (Figure 6-5). The poor performance mixes used in the field applications fell outside the workable range, except mix 67M, which in both the slump flow test and U-flow test showed results similar to those of mixes with good performance. Mix 67M results fell inside the range of workable mixes. Kosmatka et al.(2002) proposed typical SCC mixes to use 60% of total aggregate by volume; the workable range for TA/Concrete ratio from 58% to 65% established by the laboratory and field results of this research confirmed such findings.

Figures 6-7 and 6-8 showed the direct correlation between coarse aggregate-to-total aggregate and total aggregate-to-concrete ratios by weight and volume, respectively. Field mixes with good performance fell inside the workable range defined for the laboratory mixes. However, the fact that poor performance mixes also fell inside the workability boxes (Figure 6-8), illustrated the fact that the proposed values for workable CA/TA ratios and TA/Concrete ratios were not sufficient to assure proper workability of the mixes, and other parameters as the specific gradation and angularity of the aggregate may also influence the self-consolidating ability of a mix.

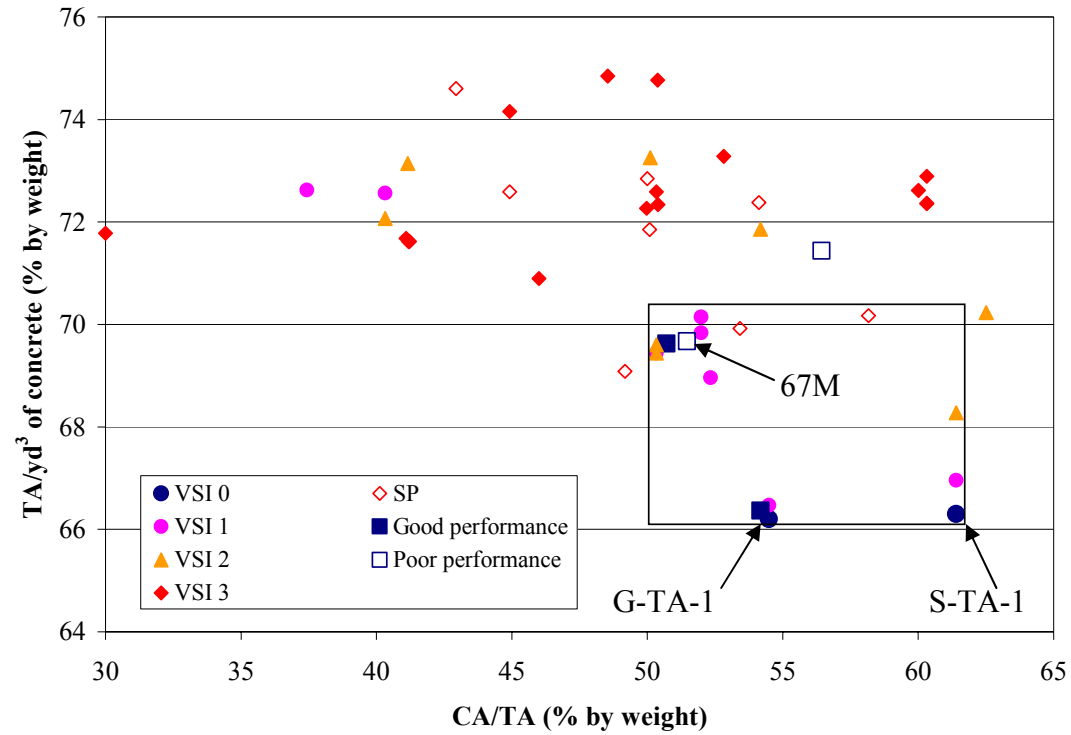

Figure 6-7. Workability box for field and laboratory mixes for the correlation between total aggregate content and coarse aggregate percentage by weight of concrete

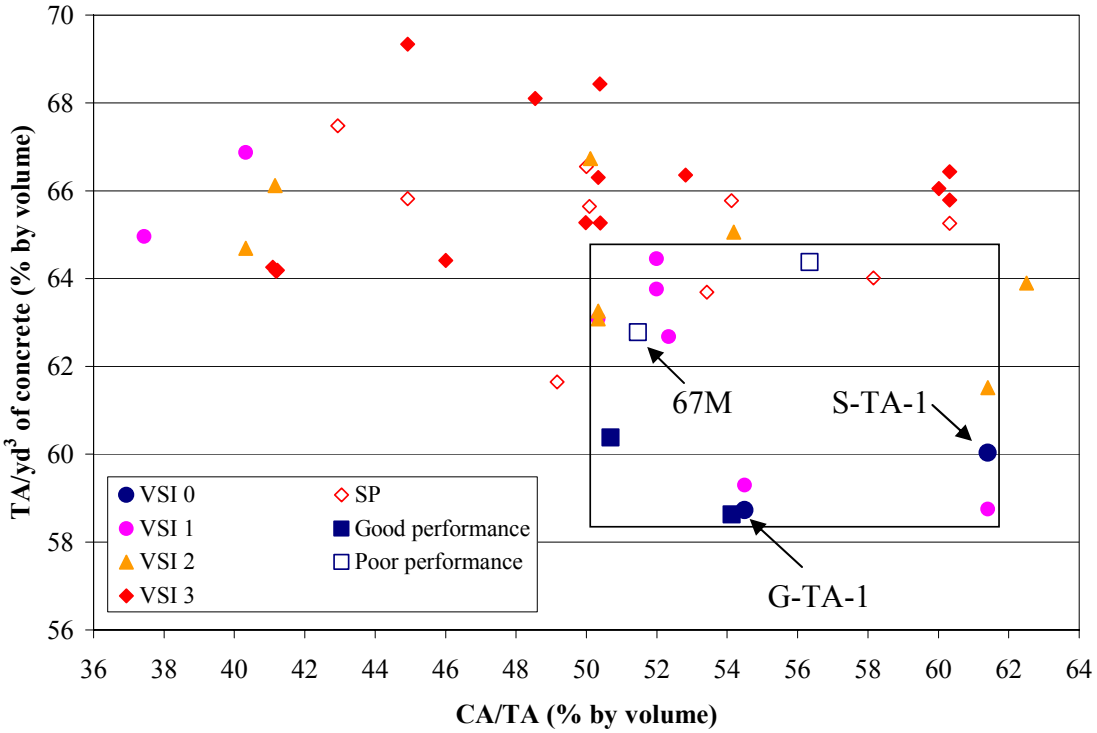

Figure 6-8. Workability box for field and laboratory mixes for the correlation between total aggregate content and coarse aggregate percentage by volume of concrete

The third parameter analyzed in this comparison between field and laboratory results was the percent replacement of SCMs in the SCC mixes. The laboratory investigation reported that workable mixes were achieved with used of binary and ternary binders with a total SCM replacement ranging from 27% to 45%. Based on these results, the field mixes with good performance fell outside the proposed workability range for both the slump flow test and U-flow test. This implied that lower percentages of SCM replacements were valid to produce workable SCC. An extended workability box ranging from 16% to 45% of SCM replacement was proposed. Use of pure cement mixes proved in the laboratory to produce poor-performance SCC. The Tindall mix, which used no SCMs replacement, confirmed the laboratory results showing poor flowing and passing abilities.

Although the findings of this field investigation allowed the incorporation of SCM percentages as low as 16% to achieved good quality SCC, use of high percentages of SCM replacements is recommended, if possible, in order to reduce the heat of hydration and porosity of the concrete, which improve the concrete's general durability. Higher percentages of SCM replacements in design of SCC mixes also have an economic impact, and lower the material cost of SCC.

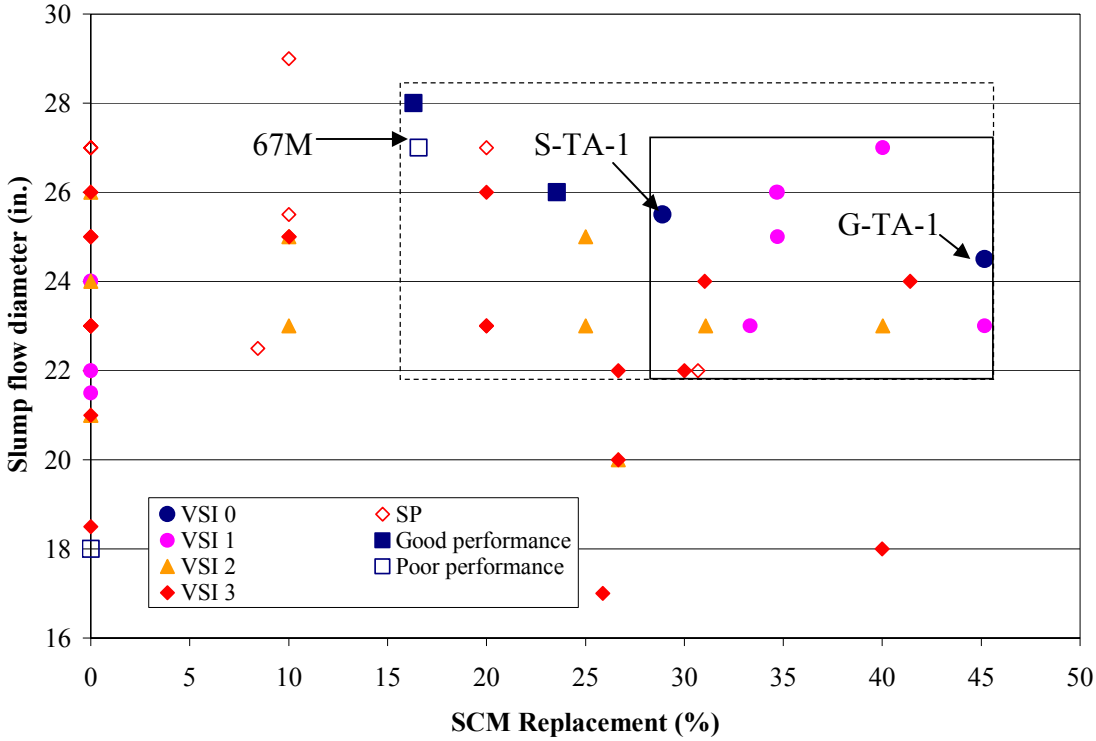

Figure 6-9. Workability boxes of field and laboratory mixes considering SCMs replacement as it relates to the slump flow diameter

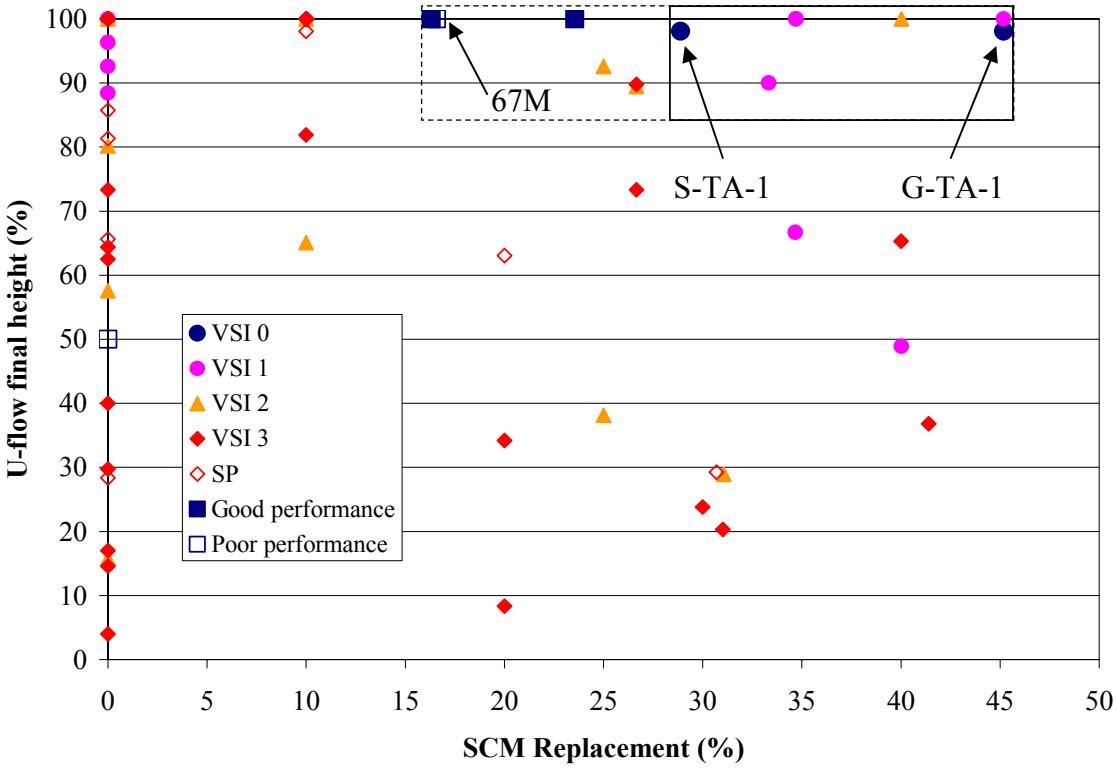

Figure 6-10. Workability boxes of field and laboratory mixes considering SCMs replacement as it relates to the U-flow final height

6.5 – Overall Acceptance Criteria of SCC Mixes

The self-consolidating abilities of a mix measured by slump flow test, U-box test and L-box test are not enough to assure good quality SCC in structural components. Other factors, like the shape of the section and its degree of reinforcement congestion must also be considered when assessing the adequacy of the performance of a given mix as found in this and other research (Constantiner and Daczko, 2002).

The selection of quality SCC mixes was based on final performance, including surface finish and homogeneity of concrete properties throughout the sections, and the selection was not based on the results obtained only in fresh state testing of the mixes. All mixes that displayed a good final performance also met the passing criteria in all the fresh state testing; however, the opposite of this statement was not always true. Mix 67M showed satisfactory results in all the fresh state testing, including slump flow test, U-box test and L-box test; yet, the final performance of this mix when used in casting of the BT-72 girders was considered poor.

Even though the fresh state tests of mix 67M proved it to have satisfactory self-consolidating abilities, the tests were not adequate for predicting the mix's performance in the congested BT-72 girder sections. Furthermore, at the trial-batch stage, the casting of concrete barriers with minimal reinforcement congestion using mix 67M produced excellent results and the surface finish, and the quality of the barriers was good (Section 4.3.2.3).

Difference in performance of SCC in congested and non-congested sections also was observed when using the Tindall mix in casting the wall panels. This mix did not meet any of the acceptable passing criteria of fresh state testing recommended by Task 1 report of this research (Ramage et al., 2004). Its performance in the wall panels was also inferior, characterized by large voids and honeycombing in the surface finish. However, the Tindall mix was used daily in production of jail cells for Tindall Corp. with excellent performance results.

The mixes presented here as "good quality" do not represent a universal formula for good quality SCC. These mixtures are recommended for applications with similar sections and degree of congestion. The acceptance criteria for SCC mixes are dependant on the specific application, and not on fixed parameters of mix proportions or levels of workability of the mix. Performance criteria of the structural component rather than mix design and fresh state testing criteria should be considered when assessing the quality of SCC mixes.

6.6 – Mechanical and Material Properties

The results obtained in hardened state testing, including compressive strength, modulus of elasticity and modulus of rupture of all the SCC mixes used in both the wall panels and girder sections are compared and discussed in this section. A discussion of how these properties compared with those of conventional concrete is also included.

6.6.1 – Compressive Strength

Over 900 lb/yd^3 (534 kg/m^3) of cementitious materials were used in the successful SCC mixes. Due to these high amounts, high compressive strengths were achieved at early ages and at 28 days. As for conventional concrete, the use of Type III cement in SCC mixes produced higher strength at early ages than those mixes with similar w/cm ratio using Type I cement. Variation in the moisture content of the aggregates produced significant changes in the w/cm of the mix, particularly when casting the BT-72 girder sections. The compressive strength of all mixes corresponded with their respective w/cm. However, the 6% increase in w/cm from the original design of 0.32 did not produced batches with a lower compressive strength than the specified target at 28 days (Figure 4-57). Air content in the mixes also influenced their respective compressive strength. Mixes with similar w/cm but higher percentage of air achieved lower strength values.

Based on the statistical analysis performed, the standard deviation of the SCC mixes was 550 psi. The mixes, therefore, resulted in a range of design strengths at 28 days, f_c', of 7,600 psi (52 MPa) to 10,180 psi (70 MPa). These values were greater than the objective 7,000 psi and 9,000 psi strengths.

6.6.2 – Modulus of Elasticity

The modulus of elasticity of SCC mixes ranged between 65% and 76% of what is predicted by the equation $33w^{1.5}\sqrt{f_c'}$ for conventional concrete mixes. The higher percentage of paste to concrete ratio seemed to be the cause of the lower modulus of elasticity observed in SCC mixes. Ramage et al. (2004) reported values of modulus of elasticity for SCC mixes of about 70% of those for conventional concrete, which agreed

with the findings from the field mixes. However, these findings are different than those reported by Persson (2001) who proposed an expression for modulus of elasticity of SCC mixes with values of about 80% of that of conventional concrete. It is recommended that Georgia DOT use a mean modulus of elasticity for SCC of $39{,}400\sqrt{f_c'}$ (psi).

6.6.3 – Modulus of Rupture

The SCC mixes used in both the wall panels and the girder sections reported a modulus of rupture 60% higher than that given by ACI 318 as $7.5\sqrt{f_c'}$. These results confirmed findings by Griffin et al. (2002), which also reported that the ACI equation for the modulus of rupture provided a conservative prediction based on the 28-day compressive strength of the SCC. An expression that better accommodates the experimental results for the SCC mixes tested is $11.0\sqrt{f_c'}$, but as the number of samples used was small further investigation is necessary to validate its accuracy.

CHAPTER 7

CONCLUSIONS AND RECOMMENDATIONS

7.1 – Introduction

The main objective of this research was to determine if good quality SCC could be produce for bridge structure applications, including precast prestressed girders and end-walls. The homogeneity of the concrete throughout the elements was studied to assess the performance of the different SCC mixes. Mechanical and material properties, as well as long-term creep and shrinkage and durability properties of SCC were also investigated.

7.2 – SCC in Field Applications

Good quality SCC mixes were produced for end-walls and BT-72 girder sections at precast concrete plants. The good mixes completely filled the 6-ft by 6-ft by 6-in thick wall sections and the 13-ft long BT-72 prestressed girder sections without the need of internal or external vibration, and the mixes exhibited a good surface finish. The 28-day strengths of the SCC mixes varied from 8,300 psi (57 MPa) to 13,700 psi (94 MPa).

7.3 – Mix Design Requirements

The acceptance criteria for SCC mixes are dependant on the specific application, and not on fixed parameters of mix proportions or levels of workability of the mix. Performance criteria of the structural component rather than mix design and fresh state testing criteria should be considered when assessing the quality of SCC mixes.

Indicators proposed by Task 1 report (Ramage et al., 2004) of good stability and self-consolidating abilities of SCC, including fresh VSI numbers between 0 and 1, slump flow spread between 22 and 28 in. (560 to 711 mm), and over 85% passing in the U-flow test, complied with the results of good quality SCC mixes in field applications; yet those measurements were not sufficient for predicting a mix's performance in congested sections.

As a example, trial batches at Standard Concrete Products (SCP) Atlanta plant of a mix with only #67 stone as coarse aggregate and manufactured sand as fine aggregate (Mix 5, mixes 67M and 67Mv), showed excellent results in fresh state testing. Nevertheless, casting of BT-72 girder sections using these mixes produced honeycombing and multiple air-voids in the surface finish of girders.

The size and gradation of the aggregates were considered the most important factors affecting the performance of SCC mixes. The combine gradation of both coarse and fine aggregates must be taken into account when designing a workable SCC mix. The maximum percentage by weight of stones retained in large size sieves, like ¾-in. (19 mm) and ½-in. (13 mm) for workable SCC mixes was 5%, and a more uniform gradation of the fine aggregate was requiered, with a maximum difference of 7% between the weight of aggregates retained on sieve No. 16 and that retained on sieve No. 50.

Good quality SCC mixes used a blend of coarse and fine aggregates, which created a more uniform aggregate gradation than those mixes using a single type of stone. The good mixes included a blend of #7 (1/2-in., 13 mm) stone and #89 (3/8-in., 9 mm) stone, and also a blend of fine aggregates including natural and manufactured sand.

The use of #67 (3/4-in., 19 mm) stone as the only coarse aggregate in the mix design was proven to be inappropriate when the clear distance between reinforcement was 1.5 in. (38 mm) or less. Aggregate segregation and honeycombing along the reinforcement was apparent when this type of mix was used in the end-wall panels and BT-72 girder sections.

SCC mixes that the Task 1 laboratory phase of this research labeled as with poor performance were produced at the SCP plant with good results in the fresh state testing. Different gradation between the manufactured sand and #67 stone used in the laboratory and the gradation of those used by the SCP plant appeared to be the main cause of differences among fresh state testing results.

7.4 –Homogeneity of the Concrete in Walls and BT-72 Girders

7.4.1 – Surface Finish

Use of self-consolidating concrete in casting of bridge elements including girders and congested end walls was shown to improve the quality of the surface finish of these elements. Surface inspection of specimens with good results showed minimal presence, less than 0.5 % of the total surface area, of air bubbles of up to ¼-inch (6 mm) diameter and total absence of air bubbles with diameters of ½ inch (13 mm) or larger.

No significant differences were obtained in surface finish quality between externally vibrated and non-vibrated structures. No concrete vibration was necessary to achieve a high quality surface finish in either the girders or walls. The bottom flange of the BT-72 girder sections did not exhibited as good of a quality of surface finish as the rest of the girders' regions. Nevertheless, its quality was superior to that in girders using regular concrete.

The use of ground granulated blast surface slag (GGBFS) as cement replacement provided a more consistent pattern of air-bubble sizes and distribution than the use of Class C fly ash. The performance obtained with SCC mixtures using Class C fly ash largely surpassed the surface finish appearance obtained using regular concrete with no supplementary cementitious materials.

7.4.2 – Concrete Strength Distribution

Compressive strengths of cores taken from the walls and the BT-72 girder sections were the same for cores from the top or bottom, start or end of the elements. None of the factors considered in an analysis of variance (ANOVA) of the core samples strength provided significant differences within a single element or within elements of the same mix. The analyzed factors were vibration method, horizontal location of the core sample relative to the point of casting, and vertical location of the cores samples.

No statistically significant differences were observed between compressive strength of cores samples from vibrated and non-vibrated structures with the same mixture. No gain in compressive strength was observed in those elements where vibration was provided during casting.

7.4.3 – Aggregate Distribution throughout Cross Sections

Aggregates were distributed uniformly from top to bottom and throughout the length of girders and walls for the SCC mixes with good performance, with no statistically significant differences. A Digital Image Analysis (DIA) of the cross sections of each specimen quantitatively corroborated the visual observation of a uniform distribution of coarse aggregate and helped to identify cross sections with apparent segregation of the coarse aggregate within the structural element. The use of DIA allowed quantifying the percentages of coarse aggregate by volume for each specimen. The error of these observations with respect to the theoretical value of coarse aggregate percentage was, at the most, 6%.

A DIA proved to be a suitable, although not exact technique for the study of aggregate segregation in a cross section. The scale used in this analysis allowed for the observation of coarse aggregate only, as at this level fine aggregate was impossible to differentiate from the concrete paste. The results obtained were consistent for every analyzed mixture, but the method was sensitive to the quality of the provided data. Differences in light exposure of the images tended to affect the results.

7.5 – Mechanical and Material Properties of SCC

The cementitious material used in the good quality SCC mixes was over 900 lb/yd^3 (534 kg/m^3). High compressive strengths were achieved by these mixes at early ages and at 28 days. Variation in the moisture content of the aggregates produced significant changes in the w/cm of the mix. The compressive strength of all mixes corresponded with their respective w/cm.

The mean compressive strengths of SCC mixtures produced in the laboratory were successfully reproduced in field-cast girders and end-wall specimens. Based on the statistical analysis performed, the standard deviation of the SCC mixes was 550 psi. The range of design strengths at 28 days, f_c', of the mixes was from 7,600 psi (52 MPa) to 10,180 psi (70 MPa). These values were greater than the objective 7,000 psi and 9,000 psi strengths.

The modulus of elasticity of SCC mixes ranged between 65% and 76% of what is predicted by the equation $33w^{1.5}\sqrt{f_c'}$ for conventional concrete mixes (AASHTO, 2002). It is recommended that Georgia DOT use a mean modulus of elasticity for SCC of $39{,}400\sqrt{f_c'}$ (psi).

The SCC mixes used in both the wall panels and the girder sections reported a modulus of rupture 60% higher than that given by the AASHTO Standard (2002) as $7.5\sqrt{f_c'}$. An expression that better accommodates the experimental results for the SCC mixes tested is$11.0\sqrt{f_c'}$.

7.6 – Long-term Properties and Permeability of SCC

Drying shrinkage values after 200 days varied among the SCC mixes used in the walls from 350 to 500 με. The SCC mixes used in the BT-72 girder sections showed drying shrinkages after 70 days between 157 to 245 με. Mixtures with higher percentage of water and paste content by volume displayed higher drying shrinkage values. The ACI 209 (1997) and AASHTO-LRFD (2004) models for drying shrinkage of conventional

concrete gave values between 50% and 100% greater than those measured in the SCC mixes.

Creep specimens were loaded 28 days after casting to 40% of the 28-day compressive strength of each mix, and they were kept at 50% RH and 73°F (23°C). The 200-day creep coefficient of the mixes used in the walls ranged from 1.02 to 1.28. The creep coefficient of the mixes used in the BT-72 girders after 70 days ranged from 1.10 to 1.21. All SCC mixes displayed creep coefficients proportional to their respective applied stresses. The ACI 209(1997) and AASHTO-LRFD (2004) expressions of creep coefficient for conventional concrete gave values about 50 to 95% of those measured in the SCC mixes. The ACI 209 model reported higher creep coefficient values than the model given by AASHTO-LRFD.

The specific creep of the SCC mixes used in the walls ranged from 0.32 to 0.38 με/psi (46 to 55 με/MPa) after 200 days. The 70-day specific creep of the mixes used in the BT-72 girder sections ranged between 0.28 and 0.32 (40 to 46 με/MPa). After 70 days all mixes showed similar specific creep about 0.30 με/psi, which seemed to be related to similar water-to-paste ratio by volume of the SCC mixes, about 0.51. The ACI 209 and AASHTO-LRFD models of specific creep for conventional concrete showed the same characteristics describe above for creep coefficient.

Both ACI 209 and AASHTO-LRFD models for creep coefficient and drying shrinkage can be use to calculate prestress losses in elements using SCC, and expect results no greater than those found for conventional concrete.

The chloride permeability of the mixes used in the BT-72 girder sections was tested according to ASTM 1202 specifications. The tests showed that all SCC mixes had chloride permeability in the Moderate level, between 2,000 and 4,000 Coulombs. Mixes with the lower w/cm showed the lower chloride permeability. Mix 67N with w/cm of 0.31 showed the lowest permeability value with 2,911 Coulombs; while mix 7BLv with w/cm of 0.34 showed the highest permeability value with 3,752 Coulombs. Excessive bleeding of the mixes and low percentage of SCMs replacements seemed to be the caused of these high permeability values.

7.7 – Recommendations for Future Research

Development of a unique test for quality control performance of SCC is needed. Although the current tests provide significant information, the need of several tests to completely assess performance quality control of SCC make them not suitable for production standards.

Development of a rapid and accurate method of quality assurance of moisture control of the aggregates is needed. A small variation in water content greatly modified the properties of SCC. Enforcement of quality assurance techniques are necessary in order to obtained a consistent performance of the concrete.

Testing for actual gradation of the specific aggregates used in a given mix is recommended to properly assess the compliance of the aggregates with the uniform gradation requirements presented in this report. Although, all quarries supply aggregates within the ASTM specifications, the specific aggregate gradation of a stone may vary from different suppliers.

The Digital Image Analysis method can be used in future research to investigate the effects of different reinforcement layouts in causing aggregate segregation. The method differentiates reinforcing bars and prestressing strands from the surrounding aggregate, making it possible to study the local area around a given rebar layout.

Casting techniques for SCC mixes in long sections requires further study. The single-point casting technique used in this research may not be applied for longer sections, and attention must be paid to possible segregation of the mixes.

Future research is needed on how the mica content in fine aggregates and SCMs affects the fresh and hardened properties of SCC mixes, and also the mica's influence in possible chemical reaction with water-reducer agents.

Inclusion of finer cementitious materials including silica fume or metacaolin is recommended in the design of SCC mixes, to help reducing the chloride permeability of SCC.

Because of the relatively high paste fraction in SCC, specific durability issues require further examination. Long-term alkali-silica reaction performance should be studied in SCC mixtures. Specific attention should be given to those mixes containing Class C fly ash as supplementary cementitious material. In addition, the propensity for delayed ettringite formation, particularly in precast section subjected to steam curing or cast during the summer months, should be evaluated.

APPENDIX A

DIGITAL IMAGE ANALYSIS OF CROSS-SECTIONS

A.1 – Description of Process

To determine in a quantitative fashion the aggregate distribution in the hardened concrete, a Digital Image Analysis (DIA) method was developed. A digital picture was taken of every cross-section and then processed for analysis. With the help of *ImageJ* v1.34 software (Wayne, 2003), the color images were transformed to 8-bit grayscale or simple black and white images. Then the threshold level of the picture was adjusted. By setting lower and upper threshold values, the image was segmented into features of interest and background. In this case the features of interest were the coarse aggregate and the background would constitute the paste. Pixels with brightness values greater than or equal to the lower threshold and less than or equal to the upper threshold were displayed in red. When the desired threshold level was achieved, the picture was then converted into a binary image where aggregates were represented in white and the paste in black. By choosing the Histogram option, in Analyze pull-down menu, the software would tabulate the amount of pixels for each color tablet. The percentage of aggregates is then calculated by finding the percentage of white pixels to the total pixels of the image. Figure 3-28 illustrates the DIA process.

(a)

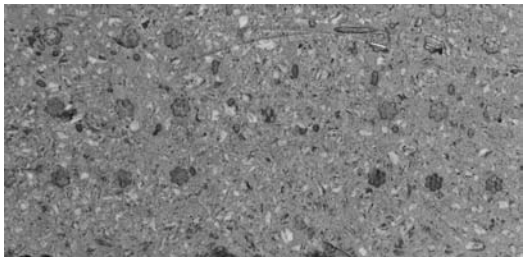

(b)

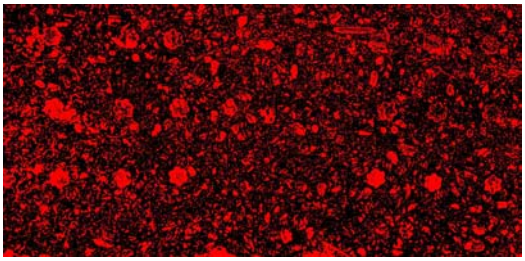

(c)

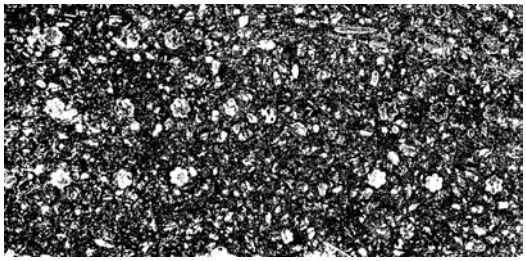

(d)

Figure A-1. Digital Image Analysis (a) cropping of color picture, (b) grayscale image, (c) threshold definition, and (d) final binary image

Defining the proper threshold for every picture was crucial in the analysis as it was up to the user to visually draw the limits between aggregate and paste. Only the coarse aggregate is possible to account for when using this method. Aggregate sizes equal to and less than No. 8 sieve (2.36 mm) were not possible to identify given the scale of the analyzed images.

A.2 – Sources of Error

The main source of errors associated with this method is the exposure of the picture to sunlight. A different sunlight exposure creates different shades of gray for both the paste and the aggregate which decreases or increases the color contrast between them. In order to obtain consistent results all pictures should be taken with the same light exposure. Other sources of error are introduced when defining the threshold level between aggregate and paste; the upper and lower limits are defined with integer numbers of grayscale, and 1 point variation of the threshold limits can produce changes of 1% in the final result. The scale used in the pictures and the presence of reinforcement in the picture are also sources of error in this method.

REFERENCES

ASTM, Annual Book of ASTM Standards, Vol. 04.02, American Society for Testing and Materials. West Conshohocken, Pennsylvania. 2002.

Attiogbe, E.; See, H.T.; and Dazkco, J.; "Engineering Properties of Self-Consolidating Concrete," <www.masterbuilders.com/eprise/main/MBT/Content/Products/Rheodynamic/ACBMpapers/EngineeringProperties.pdf>

Burgueño, R.and Haq, M.; "Strand Development Length in Prestressed, Self-Consolidating Concrete Beams," *Proceedings of the 2004 PCI National Bridge Conferece*; Atlanta, Georgia. CD-ROM, Oct. 2004.

Dietz, J. and Ma, J.; "Preliminary Examinations for the Production of Self-Compacting Concrete Using Lignite Fly Ash," April 2003.
<www.uni-leipzig.de/~massivb/institut/lacer/lacer05/l05_16.pdf>

EFNARC, "Specification and Guidelines for Self-Compacting Concrete," EFNARC. Hamphire, United Kingdon, Feb. 2002, 32 pp., <www.efnarc.org>

Euclid, "EUCO: Self-Consolidating Concrete, A History, Application, Testing and Admixture Guide," The Euclid Chemical Company. Cleveland, Ohio, 2003. <www.euclidchemical.com>

Ferraris, C.; Browner, L.; Ozyildirim, C.; and Daczko, J.; "Workability of Self-Compacting Concrete," *Proceedings of PCI/FHWA/FIB International Symposium on High-Performance Concrete: The Economical Solution for Durable Bridges and Transportation Structures;* Orlando, FL; Sept. 25-27, 2000; pp. 398-407.

Grace, "Admixtures for Self Consolidating Concrete: The Grace Solution," Grace Construction Production. Cambridge, Massachusetts. 2002. <www.graceconstruction.com>

Griffin, M.; Kahn, L.; and Kurtis, K.; "Preliminary Investigation of Self-Compacting Concrete," *Structural Engineering Mechanics and Material Special Research Problem Report*, Georgia Institute of Technology, Dec. 2002.

Hine, M. L.; "Special Provision for Self-Consolidating Concrete for Precast Products," Bureau of Materials and Physical Research, Illinois Department of Transportation. April, 2004. <http://dot.state.il.us/desenv/pdf/80132.pdf>

Hughes, D.G.; Knight, G.F.; and Manski, E.F.; "Self-Consolidating Concrete: Case Studies show benefits to Precast Concrete Producers" *First North American Conference on the Design and Use of Self-Consolidating Concrete*; Illinois; Ed. Hanley-Wood, LLC, 2002, pp.361-366.

Hughes, J.J.; "Evaluation of Self-Consolidating Concrete Summary Report" *First North American Conference on the Design and Use of Self-Consolidating Concrete*; Illinois; Ed. Hanley-Wood, LLC, 2002, pp.259-265.

Kahn, L; and Kurtis, K.; "Evaluation of Self-Compacting Concrete for Bridge Structure Applications," *Proposal to Georgia Department of Transportation, Georgia Institute of Technology,* Atlanta, Georgia, Dec. 2002.

Kennedy, C. T.; "The Design of Concrete Mixes," *Proceedings of the American Concrete Institute*, v.36, 1940, pp. 373-400.

Khayat, K. H.; "Workability, Testing and Performance of Self-Consolidating Concrete," *ACI Materials Journal*, v.96, No. 3, May-June 1999, pp. 346-353.

Khayat, K. H.; Bickley, J.; and Lessard, M.; "Performance of Self-Consolidating Concrete for Casting Basement and Foundation Walls," *ACI Materials Journal*, v.97, No. 3, May-June 2000, pp. 374-380.

Khayat, K. H.; Manai, K.; and Trudel, A.; "In Situ Mechanical Properties of Wall Elements Cast Using Self-Consolidating Concrete ," *ACI Materials Journal*, v.94, No. 6, Nov-Dec. 1997, pp. 491-500.

Khayat, K.H.; Hu, C.; and Monty, H.; "Stability of Self-Consolidating Concrete, Advantages,and Potential Applications," *Proceedings of the First International RILEM Symposium*; Cachan Cedex, France; Ed. RILEM Publications, 1999, pp. 143-152.

Kosmatka, S. H.; Kerkoff, B.; and Panarese, W. C.; "Design and Control of Concrete Mixtures," Portland Cement Association, Fourteenth Edition. Skokie, Illinois. 2002.

Lopez, M.; Kahn, L.; Kurtis, K.; and Lai, J. S.;"Creep, Shrinkage, and Prestress Losses of High-Performance Lightweight Concrete," *Structural Engineering Mechanics and Material Special Research Problem Report*, Georgia Institute of Technology, July 2003.

Marsh, D.; "Spreading The Word On Self-Consolidating Concrete," *Concrete Products,* Dec. 2002, <concreteproducts.com/ar/concrete_spreading_word_selfconsolidating>

Master Builders, "Rheodynamic Self-Consolidating Concrete," Master Building Concrete Solutions. Cleveland, Ohio. 2003. <www.masterbuilders.com>

Mehta, P.K.; and Monteiro, P.J.M.; "Concrete: Microstructure, Properties, and Materials," Second Edition, McGraw Hill, 1996.

Mindess, S.; Young, J.; and Darwin, D.; *Concrete*, Prentice Hall, Second Edition, New Jersey, 2003.

Neuwald, A.; "Self-Consolidating Concrete," *MC Magazine,* Jan-Feb. 2004, <www.precast.org/publications/mc/2004_janfeb/scc.htm>

Ouchi, M.; "Self-Compacting Concrete: Development, Applications, and Investigations," <www.itn.is/ncr/publications/doc-23-3.pdf >

Ouchi, M.; Nakamura, S.; Osterberg, T.; and Lwin, M.; "Applications of Self-compacting Concrete in Japan, Europe and the United States" U.S. Department of Transportation. Federal Highway Administration. 2003. <http://www.fhwa.dot.gov/bridge/scc.htm>

Ozyildirim, C.; and Lane, S.; "Evaluation of Self-Consolidating Concrete" *Final Report for the Virginia Transportation Research Council*, June 2003, <www.virginiadot.org/vtrc/main/online_reports/pdf/03-r13.pdf>

PCI; "Guidelines for Self-Consolidating Concrete in Precast/Prestressed Concrete Institute Member Plants," TR-6-03, April 2003.

Persson, B.; "A Comparison between mechanical properties of Self-Compacting concrete and the corresponding properties of normal concrete," *Cement and Concrete Research*, vol. 31, No.2, February 2001, pp. 193-198.

Petersson, O.; Gibbs, J.; and Bartos, P.; "Testing-SCC" *First North American Conference on the Design and Use of Self-Consolidating Concrete*; Illinois; Ed. Hanley-Wood, LLC, 2002, pp.229-233.

Poppe, A. M.; and De Schutter, G.; "Influence of the Nature and the Grading Curve of the Powder on the Rheology of Self-Compacting Concrete," *Proceedings for the Fifth CANMET/ACI International Conference on Recent Advances in Concrete Technology*, Singapore, Ed. V. M. Malhotra, 2001, pp.399-414.

Raghavan, K.P.; Sarma, B. Sarma; and Chattopadhyay, D.; "Creep, Shrinkage and Chloride Permeability Properties of Self-Consolidating Concrete" *First North American Conference on the Design and Use of Self-Consolidating Concrete*; Illinois; Ed. Hanley-Wood, LLC, 2002, pp.307-311.

Ramage, B..; Kahn, L.; and Kurtis, K.;"Evaluation of Self-Consolidating Concrete for Bridge Structure Applications: Task 1 Report," *Structural Engineering Mechanics and Material Special Research Problem Report*, Georgia Institute of Technology, June 2004.

Ramsburg, P.; "The SCC Test: Inverted or Upright?" *The Concrete Producer*, July 2003, <www.oldcastleprecast.com/Oldcastle_Precast/Locations/Location/locationspecialprojects.asp?LocationID=50&P=87>

Sika, "Self consolidating Concrete," Sika. <www.sikausa.com>

Skarendahl, A.; and Petersson, O.; *Self-Compacting Concrete*, RILEM Report 23, RILEM Publications, 2000.

Sonebi, M.; and Bartos, P. J. M.; "Performance of Reinforced Columns Cast with Self-Compacting Concrete," *Proceedings for the Fifth CANMET/ACI International Conference on Recent Advances in Concrete Technology,* SP-200, Singapore, Ed. V. M. Malhortra, 2001, pp.415-431.

Sonebi, M.; Tamimi, A.; and Bartos, P.; "Performance and Cracking Behavior of Reinforced Beams Cast with Self-Consolidating Concrete," *ACI Materials Journal*, v.100, No. 6, Nov-Dec. 2003, pp. 492-500.

Takenaka, H.; KAkizaki, M.; Abe, Y.; and Okada, M. "Effects of Specimen Preparation on the Properties of Fresh and Hardened High Fluidity Concretes," *Proceedings for the Fifth CANMET/ACI International Conference on Recent Advances in Concrete Technology*, Singapore, Ed. V. M. Malhotra, 2001, pp.605-616.

Turcry, P.; Loukili, A.; and Haidar, K.; "Mechanical Properties, Plastic Shrinkage and Free Deformations of Self-Consolidating Concrete," *First North American Conference on the Design and Use of Self-Consolidating Concrete*; Illinois; Ed. Hanley-Wood, LLC, 2002, pp.301-305.

Van, B. K.; Montgomery, D. G.; Hinczak, I.; and Turner, K.; "Rapid Testing Methods for Segregation Resistance and Filling Ability of Self-Compacting Concrete," *Proceedings for the Four CANMET/ACI/JCI International Conference on Advances in Concrete Technology;* Tokushima, Japan; Ed. V. M. Malhotra, 1998, pp. 85-102.

Walraven, J.; "Self-Compacting Concrete in the Netherlands" *First North American Conference on the Design and Use of Self-Consolidating Concrete*; Illinois; Ed. Hanley-Wood, LLC, 2002, pp.355-359.

Wayne, R.; "Documentation notes" ImageJ software v1.34. Research Service Brach of the National Institute of Mental Health. May 2005. <http://rsb.info.nih.gov/ij/docs/index.html>